UNIVERSITY OF CALIFORNIA,
IRVINE

Mechanochemical Regulation of Macrophage Inflammatory Activation by Fibrin(ogen)

DISSERTATION

submitted in partial satisfaction of the requirements
for the degree of

DOCTOR OF PHILOSOPHY

in Biomedical Engineering

by

Jessica Yi-Chia Hsieh

Dissertation Committee:
Associate Professor Wendy F. Liu, Chair
Professor Elliot L. Botvinick
Associate Professor Lisa A. Flanagan

2018

DEDICATION

To

My Family

who has always been and will always be my **number one**

"I am among those who think that science has great beauty."
-Marie Curie

TABLE OF CONTENTS

LIST OF FIGURES

LIST OF FIGURES (Continued)

LIST OF TABLES

ACKNOWLEDGMENTS

I would like to express the deepest appreciation and gratitude to my committee chair, Professor Wendy Liu. Over the past five years, Wendy has allowed me to take creative license with my research, providing me invaluable guidance and advice along the way. More importantly, Wendy's understanding and open-mindedness has enabled me to pursue many interests both in and outside the lab, ranging from research topics to professional development. Without her guidance, kindness, and support, I would not be the professional I am today.

I would also like to thank my committee members, Professor Elliot Botvinick and Professor Lisa Flanagan. I am thankful for Elliot's boundless enthusiasm and resourcefulness. Elliot never hesitated to help me locate resources for my projects and even found me a dermatologist for my thumb before BMES 2016. Dr. Flanagan has helped provide great insight into fibrin, the main extracellular matrix in question in this dissertation. I am grateful for her willingness to share her knowledge with me and provide great feedback. Last, I would also like to extend my gratitude to Dr. Christopher Hughes and Dr. Andrea Tenner for providing me with great experimental suggestions during my qualification exam.

I am also incredibly thankful to the wonderful scientists in my lab who have helped me on my Ph.D. journey—I could not have asked for a better team to work alongside with. My lab mates, past and present, have made an indelible mark on my life. To Drs. Frances McWhorter and Tim Smith—thank you for showing me the ropes of graduate school. I am especially grateful for Dr. Smith for being one of my biggest critics and teaching me practically everything I know about data analysis and visualization. I would also like to thank Drs. Vijaykumar Meli and Yoon Kim for their unending patience and willingness to share their wealth of knowledge. Finally, I am grateful to Dr. Thuy Luu; her strict training, incredibly steady hands, and dedication to protocol adherence inspire me to become a better scientist.

For the soon-to-be doctors of the Liu lab, I am delighted to thank Esther Chen for letting me eat her snacks at all times, be the embarrassing highlight of her lab related videos, and giving me the pleasure of hearing her sing and play the guitar. To future double doctor Raji Nagalla, I thank her being the best "cubicle" neighbor, giving me sound advice, and taking on my projects. I also would not have been able to survive graduate school without the dynamic trio of Hamza Atcha, Joe Hsu and Praveen Veerasubramanian. To Hamza Atcha, I thank him for tolerating my inability to understand him half the time, responding with witty comebacks that kept me laughing throughout graduate school, and introducing me to my inner Brit. To Joe Hsu, I thank him for constantly reminding me of our Triton connection, making me chuckle when we are both at our lab benches, and supplying me with NSII candy during dissertation writing. To Praveen Veerasubramanian, I am inspired by his quick wit and ability to solve any riddle, thankful for his introduction to his beautiful music, and grateful for his "bro hugs" and "fist pumps". Last, I would like to thank the undergraduates, the members of the party planning committee, Arian Cano, Sien Tam, and Kyle Brumm for quizzing me on endless riddles that I cannot solve, showing me magic tricks, and planning our lab excursions. To close, I would also like to acknowledge the new undergraduates, Jessica Chin, Kevin Jiang, and Felicia Tran for giving me the opportunity of getting to know them.

I am also in debt to Linda McCarthy for all her help with supply orders, general lab inquiries, and career advice over the past five years. Additionally, I am grateful for Ann Fain for running the CARE program and keeping the Edwards Lifesciences Center for Advanced Cardiovascular Technology in tip-top shape. In addition, I would like to thank all my friends in the BEAMS lab, the CML lab, and the Downing lab at the Edwards Lifesciences Center. I would like to highlight Dr. Abishek Kurup and Tim Tran for starting our BEAMS-Liu Lab collaboration. Notably, I would also like to acknowledge my great friends in the BEAMS lab—soon to be Drs. Mark Keating and Rachel Gurlin, Dr. Shreyas Ravindranath, and "on fleek"-style undergrad Micah Lim. In particular, I thank Mark Keating for being the best CARE-llaborator, awesome game night planner, and brilliant accent imitator.

To my graduate cohort, I could not have survived my Ph.D. (especially math and optics courses) without my dearest friends in my BME cohort—Jie Zheng, Rachel Qu, Jessica Kwong, and Shirley Zhang. I thank them for inducting me into the crew even though I was never part of the Competitive EDGE program and injecting me with doses of "backbone" when I most needed it. Moreover, I would like to thank Christian Crouzet for recruiting me and giving me the honor of playing intramural flag football (TWICE!) with him. In addition, for my graduate underclassmen, I am honored to have met so many of them while serving as the president of the Graduate Association of Biomedical Engineers (GABES). In particular, I would like to thank Jeff Lim, Tae Kim, and Hamsa Gowda for taking on the GABES torch. Moreover, I would like to acknowledge Hamsa Gowda for being the best co-TA, conference accomplice, and educational outreach coordinator for GABES (and thanks to Dr. Beth Lopour for advising GABES.)

Next, I would like to give a special shout-out to my great friends from UC San Diego: cheers to our unwavering friendships! Tiff: thanks for being the best bestie anyone could ever ask for—10 years and still going on strong! Coral and Viv: I am so very glad I sat next to both of you in C++ in freshman year and started something beautiful. Liu, Choy, and Chelsea: Forever PRIME-mates and Asia-Pac gangsters. ChaoChao, Wen, and Jenny: BTEC/BENGers for life.

Last, words cannot express how eternally grateful I am for my family. My parents and two older sisters have always been my safe harbor and anchor. My parents understood that the pursuit of a Ph.D. was not a trivial one and flooded me with unwavering love, support, encouragement, and understanding during the ups and downs of my Ph.D. career. Thank you, Daddy, for the words of wisdom. Thank you, Mommy, for my endless supply of bentos. To $(Jane)^2$ and $(Bi)^2$—thank you both for giving me the requisite reality punches, keeping me focused on what really matters, and allowing me to always be the big baby. Finally, Evie: you are forever my favorite tiny human. I love you all so very, very much. ♥

Financial support was provided by NIH T32-HL116270-02, NIH Director's Fund/NIDCR DP2DE023319, NIH R21AI128519, Edwards Lifesciences Fund, UCI Henry Samueli School of Engineering, and the Institute for Clinical and Translational Science. I thank Elsevier for granting me permission to use copyright material for this dissertation in Chapter 2; the journal is open access under the creative commons license.

CURRICULUM VITAE

Jessica Yi-Chia Hsieh

Education & Training

2013-2018	**Candidate for Ph.D. in Biomedical Engineering (BME)**
	The Henry Samueli School of Engineering, University of California, Irvine (UCI)
2011-2013	Research Associate, Sequenom Inc. (San Diego, CA)
2007-2011	**Bachelor of Science, Bioengineering: Biotechnology,** Magna Cum Laude
	Jacobs School of Engineering, University of California, San Diego (UCSD)
2010	**Summer International Exchange Student,** National Yang Ming University, Taipei, Taiwan
2008	**Summer Study Abroad Student,** Burgos, Spain

Positions Held

2017-2018	Invention Transfer Group Fellow, Technology Transfer Office & Applied Innovation, UCI
2016	Global Regulatory Affairs Intern, Allergan Inc.
2013-2018	Graduate Researcher, Department of Biomedical Engineering, UCI (Dr. Wendy Liu)
2011-2013	Research Associate I, Sequenom Inc.
2010-2011	Undergraduate Researcher, Department of Bioengineering, UCSD (Dr. Karen Christman)

Honors and Awards

2017	American Association of University Women (AAUW) Dissertation Fellowship Alternate
2017	UCI Tech & Entrepreneurship Competition Best Chief Technology Officer
2016	UC Irvine Grad Slam Third Place Winner
2014-2016	Cardiovascular Applied Research and Entrepreneurship Fellowship Trainee (NIH T32)
2015	Edwards Lifesciences Student Leader Scholarship for heart surgery volunteering in **China**
2014	STAR Honorable Mention for research excellence at Society of Biomaterials Annual Meeting
2014	Associated Graduate Students Award for travel to Society of Biomaterials Annual Meeting
2014, 2015	National Science Foundation Graduate Research Fellowship Honorable Mention
2007-2011	UCSD Alumni-Regents Leadership Scholarship for demonstrated leadership involvement
2007-2011	UCSD Regents Scholarship for academic accomplishments
2007-2011	Provost's Honors, Revelle College for maintaining a 3.5 GPA or higher every quarter
2010	Traditional Medicine, Culture, and Art Scholarship to study abroad in **Taiwan**
2009	Pacific Rims Research Experiences Scholarship to conduct research abroad in **Malaysia**
2008	Ernest C. Mort International Scholarship to study abroad in **Spain**

Publications

J5 **Hsieh J.Y.**, Keating M.T., Botvinick E.L., Liu W.F. Matrix Crosslinking Controls Macrophage Adhesion, Migration, and Inflammatory activation. In preparation for invited submission to Advanced Healthcare Materials.

J4 **Hsieh J.Y.**, Wilson R., Kennedy G., Tromberg B., Liu W.F. Non-invasive Monitoring of Biomaterial Implant-Induced Host Response Through Spatial Frequency Domain Imaging. In preparation for invited submission to APL Bioengineering.

J3 **Hsieh J.Y.**, Luu, T.U., Atcha, H., Liu W.F. (2017) Biophysical Regulation of Macrophages in Atherosclerosis. Invited book chapter forthcoming in Mechanomedicine.

J2 Kim Y.K., Chu, S.H., **Hsieh, J.Y.**, Kamoku, C.M., Tenner, A.J., Liu, W.F., Wang, S.W. (2017) Incorporation of a Ligand Peptide for Immune Inhibitory Receptor LAIR-1 on Biomaterial Surfaces Inhibits Macrophage Inflammatory Responses. Advanced Healthcare Materials. 1700707. doi:10.1002/adhm.201700707.

J1 **Hsieh J.Y.**, Smith T.D., Meli V., Tran T.N., Botvinick E.L., Liu W.F. (2017) Differential regulation of macrophage inflammatory activation by fibrin and fibrinogen. Acta Biomaterialia. 47:14-24. Doi:10.1016/j.actbio.2016.09.024

Conference Presentations

A7 Hsieh JY, Kim YK, Liu WF. Mechanochemical Regulation of Macrophage Inflammatory Activation by Fibrin(ogen). Biomedical Engineering Society Annual Meeting, Pheonix, AZ, 2017.

A6 Hsieh JY, Smith TD, Meli V, Tran TT, Botvinick EL, Liu WF. Differential Regulation of Macrophage Inflammatory Activation by Fibrin(ogen). Tissue Engineering & Regenerative Medicine International Society (TERMIS) Annual Meeting, San Diego, CA, 2016. (Podium)

A5 Hsieh JY, Smith TD, Meli V, Tran TT, Botvinick EL, Liu WF. Differential Regulation of Macrophage Inflammatory Activation by Fibrin and Fibrinogen. 14th Annual Immunology Fair, Irvine, CA, 2016. (Podium)

A4 Hsieh JY, Tran TN, Botvinick EL, Liu WF, Investigating the Effects of Fibrin/Collagen Composite Gels on Macrophage Phenotype Polarization. 13th Annual Immunology Fair, Irvine, CA, 2015.

A3 Hsieh JY, Wilson RH, Kennedy GT, Krishnan R, Lakey JR, Durkin AJ, Tromberg BJ, and Liu WF. Spatiotemporal Monitoring of Foreign Body Response Using Spatial Frequency Domain Imaging (SFDI). Biomedical Engineering Society Annual Meeting, Tampa, FL, 2015.

A2 Hsieh JY, Smith TD, Liu WF. Investigating the Migratory Behavior of Macrophage Subtypes. Society of Biomaterials Annual Meeting, Charlotte, NC, 2015. (Podium)

A1 Hsieh JY, Konstorum A, Kang DK. Quantification of in vitro tumor microenvironment interactions. Center for Complex Biological Systems Conference, Pasadena, CA, 2014 (Podium).

Professional Presentations

2. Hsieh JY, Angkachatchai V. Blood Fill and Ambient Storage Stability Study, Sequenom Research Associate Meeting, San Diego, CA 2013. (Podium)

1. Hsieh JY, Angkachatchai V. Evaluation of Alternative Homogenization Platforms, Sequenom Research Associate Meeting, San Diego, CA 2012. (Podium)

Undergraduate Presentations

3. Hsieh JY, Chan, C, Chou YC. Entry Prevention of Inflammatory Mediators into Lactiferous Ducts Annual Bioengineering Day, UC San Diego, 2011.

2. Hsieh JY, Singelyn JM, Christman KL. Tissue Decellularization, Degradation, and Analysis of Porcine Myocardial Matrix, Annual Faculty Mentor Undergraduate Research Symposium, UC San Diego, 2010. (Podium)

1. Hsieh JY, Wahab, H, Li, W. Optimizing the Design of SiRNAs Targeting the NP Protein, Fall Biomedical Engineering Senior Seminar, UC San Diego, 2009. (Podium)

Teaching Experience

Fall 2017	**Graduate Instructor,** Quantitative Physiology, Biomedical Engineering Department, UCI
2014, 2015	**Summer Graduate Instructor,** CardioStart Summer Cardiovascular Program, UCI
Winter 2011	**Teaching Assistant,** Introduction to Bioengineering, Bioengineering Department, UCSD
Winter 2010	**Textbook Editor,** Systems Biology and Bioengineering, Bioengineering Department, UCSD

Educational Outreach

2017-2018	**Mentor,** (1) Women and Minorities in STEM; (2) Biomedical Engineering Society, UCI
2013-2015	**Instructor,** Rocket Science Tutors, Willard and McFadden Intermediate Schools
2011-2013	**Head Volunteer,** San Diego Science Festival Planning Committee, Sequenom Inc.
2009-2011	**Volunteer,** ENSPIRE, Triton Engineering Student Council, UCSD

Leadership Experience

2017, 2018	**Graduate Program Ambassador,** Biomedical Engineering Department, UCI
2014-2017	**Founder & President,** Graduate Association of Biomedical Engineering Students, UCI
2013-2014	**Communications Chair**, IEEE-EMBS, UCI
2009-2011	**Events Coordinator & Community Liaison,** Slow Food Organization, UCSD

ABSTRACT OF THE DISSERTATION

Mechanochemical Regulation of Macrophage Inflammatory Activation by Fibrin(ogen)

By

Jessica Yi-Chia Hsieh

Doctor of Philosophy in Biomedical Engineering

University of California, Irvine, 2018

Associate Professor Wendy F. Liu, Chair

Proper wound healing still remains a clinical challenge. Fibrin is a major component of the provisional extracellular matrix that forms initially after injury, enabling cell infiltration and anchoring to the wound site. Fibrinogen, the precursor of fibrin and a blood plasma protein, is also important in inflammation, wound healing, angiogenesis, and other biological functions. Of the many cells present during the wound healing process, macrophages play a key role in modulating the immune response. The plasticity of macrophages permits them to adopt behaviors along a spectrum of phenotypes depending on signals in their microenvironment. While much is known about how chemokines, cytokines, and other soluble mediators influence macrophages, less is understood about the roles of the ECM and the physical properties of the surrounding tissue. In this study, we examined the interactions between fibrin(ogen) and macrophages to gain a better fundamental understanding of how physical and biochemical properties of the provisional matrix together influence immune cell behavior. We separately looked at the roles fibrinogen and fibrin on macrophage inflammatory or anti-inflammatory functions and explored how mechanical

properties of fibrin(ogen) such as substrate stiffness and tethering affect macrophage activation and behavior.

First, we investigated the differential regulation of macrophage activation by fibrinogen and fibrin. The presentation of fibrin(ogen), either presented in the soluble form or incorporated within an insoluble matrix, plays an important role in regulating macrophage phenotype. In particular, fibrin exerts a protective effect on macrophage inflammatory activation. Additionally, we altered mechanical properties of fibrin by controlling matrix stiffness and explored methods of adsorbing or tethering fibrinogen. Substrate rigidity alters the expression of integrins, proteins receptors that facilitate macrophage-ECM interactions. Adsorption of fibrinogen also inhibits inflammatory activation. Finally, we utilized a light-based crosslinking technique to stiffen fibrin matrices. Increased substrate rigidity enhances inflammatory macrophage behavior. Moreover, macrophages are more motile, both in terms of velocity and distance traveled, on stiffer fibrin matrices. Together, these findings contribute to our understanding of how the extracellular matrix regulates macrophages during wound healing and disease and offer new insight for designing biomaterials that can precisely control the host response and promote proper tissue regeneration.

Introduction

Overview and Significance

Proper wound healing in response to injury after surgery, trauma, or disease still remains a clinical challenge. Chronic inflammation can lead to the formation of scar tissue that may impair or destroy tissue function.[1] Moreover, for material implantation such as that of a medical device, prosthesis, or biomaterial, aberrant wound healing can lead to the foreign body response—a phagocytic response and encapsulation by the host body that ultimately compromises the safety, efficacy, and function of the implanted material.[2,3] The wound healing process not only involves numerous infiltrating immune cells and resident cells but also dynamic changes in the extracellular matrix (ECM) in order to orchestrate a series of events to promote inflammation followed by tissue regeneration.[4,5] In particular, in the very early process of wound healing, blood and material interactions develop a blood-based transient matrix.[2] Fibrin is a major component of this provisional extracellular matrix while its precursor, fibrinogen, also plays pivotal roles in inflammation, wound healing, angiogenesis, and other biological functions.[6,7]

Of the many cells present during the wound healing process, macrophages play a key role in modulating immune responses.[2] The plasticity of macrophages enables them to adopt behaviors along a spectrum of phenotypes.[8] While much is known about how chemokines, cytokines, and other soluble mediators regulate macrophage behavior, less is understood about the impact of the ECM.[9,10] Aside from a structural role, evidence is emerging that the ECM can provide both mechanical and adhesive cues to macrophages and influence their behaviors.[11] By examining the interactions between fibrin(ogen) and macrophages, we can gain a fundamental understanding of

how this provisional matrix influences immune cell behavior and engineer potential solutions for mitigating undesirable immune responses.

Chapter 1: Fibrin(ogen) and Macrophage Biology

1.1 Macrophages

1.1.1 Macrophage Origin and Activation

Macrophages are immune cells that are central to many biological processes such as development, metabolism, and tissue homeostasis.[12] There are two main types of macrophages in adult tissues—tissue-specific macrophages and macrophages derived from circulating blood monocytes, sometimes referred to as monocyte-derived macrophages (MDMs).[13] Tissue-specific macrophages, originating from the embryonic yolk sac, are permanent residents in adult tissues and capable of self-renewal by local proliferation.[14,15] It should be noted though that there is emerging evidence that macrophages in several tissues, such as the liver or microglia, were found to be different from yolk sac macrophages.[16] Contrastingly, MDMs mature in the bone marrow during hematopoiesis and can be recruited to a tissue in order to respond to a metabolic, immune, or pro-inflammatory stimulus.[14,17] Both resident and recruited macrophages have a proliferative capacity in tissue during inflammation.[14]

Macrophages are master regulators of the immune system and play critical roles in both innate and adaptive immune functions. Independently of immune-cell signaling, macrophages participate in "janitorial" processes that involve removal of apoptotic cells and cellular debris—macrophages in these instances are unstimulated and produce little to no immune mediators.[18] However, when macrophages phagocytose debris as a result of traumatic or stressful necrosis, the resulting detection of endogenous danger signals consequently alters their downstream behavior.[18] Additionally, macrophages also act as the first line of defense along with neutrophils against many common bacteria and microorganisms—they are also activated during these instances.[19] Finally,

along with dendritic cells, macrophages that have phagocytosed foreign contaminants can present antigens to T lymphocytes, or T cells, and play a part in the adaptive immune response.[19] Thus, whether participating in innate or adaptive immune processes, macrophages can assume a diverse range of phenotypes and thus are recognized for their remarkable plasticity.

The adoption of a variety of phenotypes by macrophages is dependent on their microenvironment.[20] These cells exhibit a spectrum of activation states—each with their own behaviors, functions, and unique transcriptional profiles.[21,22] Though it is widely accepted that macrophage phenotypes should be viewed as a continuum, macrophages can be classified into two extremes: classically-activated (M1) and alternatively-activated (M2) macrophages.[23] These names are reflective of the Th1—Th2 polarization of T-lymphocytes as well as the differential metabolism of arginine in these two phenotypes.[24]

Macrophages can undergo M1 activation upon stimulation by pathogen-associated molecular patterns (PAMPs), danger or damage-associated molecular patterns (DAMPs), microbial products, or the cytokine interferon-γ (IFN-γ).[25] Pattern recognition receptors, such as the Toll-like receptors (TLRs), bind to bacterial lipopolysaccharide (LPS), hypomethylated DNA, flagellin, and double-stranded RNA.[17] The term ‘‘classical’’ activation, which originally referred to macrophages stimulated with IFN-γ, is now interchangeably used to describe macrophages simulated with IFN-γ and/or TLR ligands.[24] M1 macrophages, dominated by NF-κβ (nuclear factor kappa-light-chain-enhancer of activated B cells) and STAT1 (signal transducer and activator of transcription 1) pathway activation, are characterized by their high expression levels of inflammatory cytokines such as tumor necrosis factor alpha (TNF-α), interleukin-1 (IL-1), interleukin-6 (IL-6), interleukin-12 (IL-12), and interleukin-23 (IL-23).[25,26] In addition, M1 macrophages also increase intracellular

production of reactive nitrogen and oxygen intermediates, thereby promoting a Th-1 response while enhancing its own microbicidal and tumoricidal activities.[25]

In a different manner, the term M2 macrophages was first coined after observing that macrophages upregulated their expression of mannose receptor (MR) or cluster of differentiation 206 (CD206) post interleukin-4 (IL-4) stimulation.[27] The mannose receptor, another pattern recognition receptor, binds to mannoyslated and polymannosylated compounds. M2 macrophages, typically associated with antiparasitic or tissue repair programs, release anti-inflammatory mediators such as interleukin-10 (IL-10), a chemokine known to directly inhibit the production of inflammatory cytokines via STAT-3 dependent pathways.[28,29] Aside from an increased expression of mannose and galactose receptors, murine M2 macrophages are also characterized by the production of the enzyme arginase, which hydrolyzes arginine to ornithine and urea. Ornithine is important for downstream polyamine and proline syntheses, amino acids critical for cellular proliferation, collagen synthesis, and tissue repair.[30] Interestingly, arginine is acted upon by either inducible nitric oxide synthase (iNOS) or arginase pathways: in mice, the former leads to M1 activation while the latter results in M2 polarization.[30] It should be noted though that while arginase and NOS enzymes can be used to ascertain murine macrophage activation, this same response is not observed in human macrophages.[31,32] Moreover, in mice, macrophages are phenotypically defined as F4/80^{hi} cells because F4/80 is a mature murine macrophage marker.[13]

Finally, there are more specific classifications of alternative activation: M2a, M2b, M2c, and M2d (Fig. 1.5).[26,33] Notably, M2a, elicited by IL-4 and interleukin-13 (IL-13) stimulation and M2b, induced by immune complexes and TLR agonists, are regarded as immunoregulatory macrophages.[26,28] Next, M2c macrophages, stimulated with IL-10, transforming growth factor beta

(TGFβ), or glucocorticoids are typically involved in the suppression of immune responses and tissue remodeling.[26,28] Last, M2d activation is elicited by IL-6 and adenosines; M2d macrophages function independently of interleukin-4 receptor alpha (IL-4Rα) signaling.[34,35]

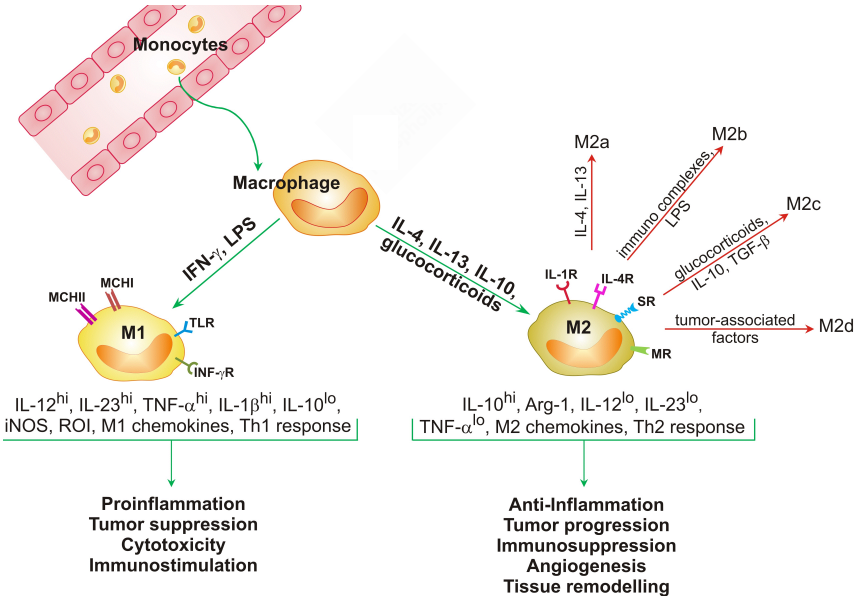

Figure 1.1. Schematic of macrophage phenotype polarization (adapted from [36]).

1.1.2 Macrophage Heterogeneity in Wound Healing

Macrophages are also dynamic regulators of the wound healing process, advancing and resolving inflammation in response to cues in their microenvironment.[37] These cells contribute to remodeling and repair in both homeostatic and damage conditions. It has demonstrated that animals that are depleted of macrophages at the wound site exhibited delayed re-epithelialization, reduced collagen deposition, impaired angiogenesis, and decreased cell proliferation in healing skin wounds; these results suggest that macrophages are essential to the healing process.[38,39]

Wound macrophages also have different phenotypes during the repair process (Fig. 1.6).[40] Though the wound healing process is complex, it has been observed that macrophages that arrive early to the wound site are of the M1 phenotype, typically secrete inflammatory cytokines such as

TNF-α, IL-1, and IL-6.[39,41] M1 macrophages need to prevent infections at the injury site. Consequently, M1 macrophages will also display a metabolic shift towards the anaerobic glycolytic pathway in order to trigger microbicidal activity as well as increase its survival in a hypoxic tissue microenvironment.[37,42] Over time, M2 macrophages arrive to resolve inflammation, organizing extracellular matrix deposition and tissue repair. M2 macrophages in contrast exhibit a metabolic shift to oxidative glucose metabolism because they require a sustained energy supply in order to carry out tissue remodeling and healing demands.[43]

A delicate balance between macrophage phenotypes is necessary to orchestrate proper wound healing. It has been shown that depletion of M1 macrophages early on during murine skin repair models resulted in the reduction of vascularized granulation tissue and impaired epithelialization.[44,45] Later on, the destruction of M2 macrophages during tissue formation resulted in severe hemorrhage in the wound tissue.[44] However, heightened M2 macrophage activity can also result in a pro-fibrotic response, leading to hypertrophic scarring if left unchecked.[46] Thus, it still remains unclear how much inflammatory versus anti-inflammatory activation of macrophages is necessary to achieve the optimal host response, since both functions are needed for proper wound healing.

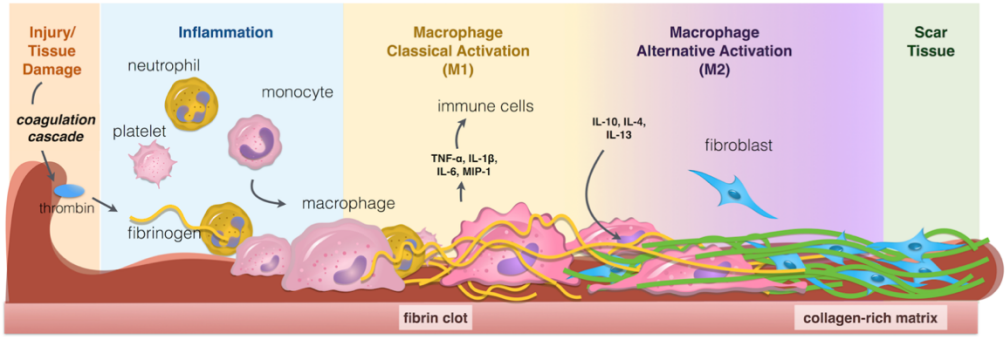

Figure 1.2. Macrophage phenotypes in wound healing. Macrophages arrive within a few hours after injury and become M1 activated. As the wound resolves, macrophages shift to a M2 phenotype, coordinating tissue repair over weeks to months. Figure courtesy of Esther Y. Chen

1.2 Fibrin(ogen)

1.2.1 The Extracellular Matrix (ECM) in Wound Healing

The extracellular matrix (ECM) not only provides structure, organization, and orientation to cells and tissues but also serves many other functions such as storing and delivering growth factors and cytokines or regulating cell activity and function via interactions with cell surface receptors.[47] In the first stage of wound healing, the provisional matrix, a term first coined in the early 1980s by R.A. Clark, is established.[48] The blood coagulation cascade is activated in response to vascular damage, resulting in a fibrin-rich matrix at the site of injury.[49] As the name implies, the early provisional ECM is temporary and eventually gets degraded and replaced by infiltrating immune cells to give way to a resident cell-derived matrix.

The resident cell-derived matrix is formed during the granulation tissue formation phase and is composed primarily of fibronectin and proteoglycans. Fibronectin helps to regulate cell adhesion dynamics, enabling subsequent collagen deposition during the later stages of wound healing.[50] Additionally, the fibronectin matrix also mediates wound contraction during wound resolution.[51] The granulation tissue formation phase is further characterized by cellular proliferation and migration of different cell types.[4] Notably, the migration of keratinocytes to the site of injury helps to restore the epithelium.[52,53] Ultimately, ECM remodeling occurs; this last stage of wound repair can last from weeks to months.[4] Remodeling, a process carried out by matrix metalloproteinases and deposition of new ECM, involves replacement of a matrix that is predominately type III collagen to one that consists mainly of type I collagen.[51,53]

1.2.2 Role of Fibrin(ogen) in the Early Provisional Matrix

Fibrinogen, a 340 kDa dimeric glycoprotein made primarily in the liver, is normally found at a concentration between 2.5 to 3.0 mg/ml in human blood plasma.[54] Upon injury, the fibrin network is generated by enzymatic cleavage and polymerization of soluble blood plasma fibrinogen—this process is facilitated by thrombin, an enzyme which becomes activated during tissue damage.[55] Concomitant activation of the coagulation cascade and aggregation of platelets generate the fibrin-rich clot that plugs severed blood vessels and temporarily fills discontinuities in the wounded tissue.[56] The blood clot, aside from maintaining hemostasis, also serves as the anchoring matrix for coming immune cells.[56,57]

Fibrin facilitates the influx of neutrophils and monocytes/macrophages as they home to the site of injury to clear infectious agents.[58,59] Moreover, the matrix also provides binding sites for fibroblasts that enter the wound site to help rebuild the tissue.[60] During the angiogenesis process, endothelial cells will degrade the fibrin matrix, migrate in, and proliferate to form new-capillary like tubes.[7] Without fibrin, local cell migration and proliferation to the wound site may be stunted. In fact, there are wound healing defects in mice lacking fibrinogen: (1) altered patterns of epithelial cell migration, (2) increased epithelial hyperplasia, and (3) failed closure of wound gap were all observed.[61] With respect to the immune cell in question in this dissertation, fibrin(ogen) has been observed to influence the activity of monocytes and macrophages and plays a role in modulating the transition rate between inflammation and tissue repair.[62]

1.2.3 Fibrin(ogen): Structure and Polymerization

Fibrinogen is composed of three pairs of polypeptide chains designated Aα, Bβ, and γ (Fig. 1.1).[63] The six chains are held together by 29 disulfide bonds.[57] Joined at the N-terminal of the E

region, the $(A\alpha B\beta\gamma)_2$ chains are interconnected by five disulfide bridges and further stabilized by disulfide rings along the coiled-coil regions in both the E and D regions, forming a 45 nm long molecule.[64] The C-termini of the α, β, and γ chains are often referred to as αC, βC, and γC domains.[57]

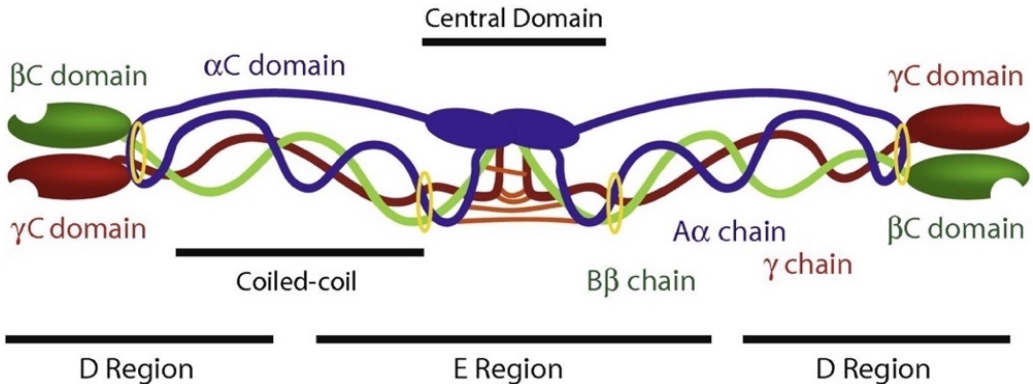

Figure 1.3. Schematic diagram of the three pairs of polypeptide chains of fibrinogen. Interchain symmetrical disulfide bridges are shown in orange. Stabilizing non-symmetrical disulfide rings are shown in yellow (adapted from [64]).

Fibrin polymerization involves the following sequential steps: (1) the conversion of fibrinogen into fibrin monomers, (2) the formation of insoluble fibrin polymers and eventually (3) the formation of a network of fibrin fibers.[7] Thrombin, generated from prothrombin, cleaves both fibrinopeptides A and B from the N-termini of the α and β chains, cutting at specific Arg-Gly residues.[65] Following the cleavage of the fibrinopeptides, peptide sequences, referred to as "knobs A and B", are exposed and available to interact respectively with "holes A and B" located at the end of the C termini on γ and β chains (Fig. 1.2).[57] Knob A on one fibrinogen molecule will form a non-covalent bond with hole A on an adjacent molecule, thereby forming half-staggered dimers.[57] The addition of other fibrinogen molecules will result in double-stranded protofibrils that can extend up to a length between 600-800 nm.[65] Knob B:hole B interactions, though still debatable, are also thought to contribute to protofibril formation.[66]

The network of fibrin is formed by lateral aggregation carried out by the αC domains.[67] 20 to 25 protofibril monomers aggregate to form fibrin oligomers.[66] The fibers are half-staggered, closely packed to result in 22.5 nm periodicity.[66] Branching of fibers ultimately leads to a complex fiber network (Fig. 1.3).[68] Fibrin matrices can be heterogenous in structure and variables such as thickness of the fibers, number of branch points, porosity, and permeability can be used to describe the resulting network.[68]

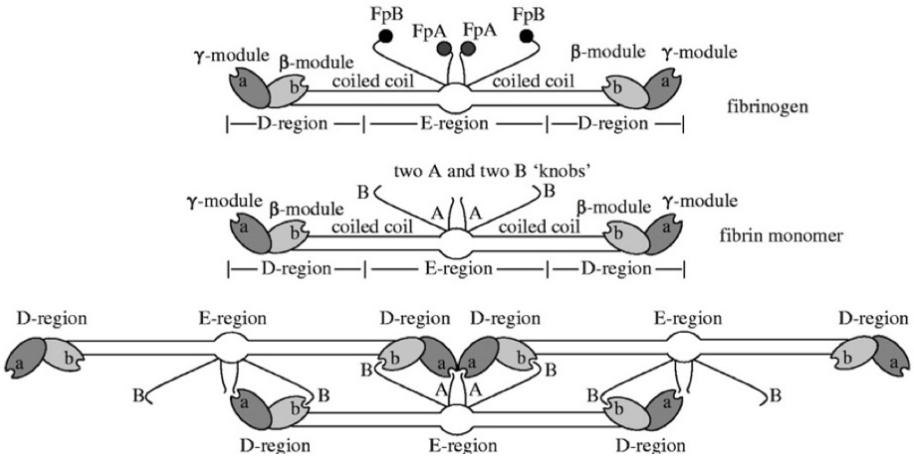

Figure 1.4. Schematic of fibrinogen's conversion to fibrin protofibrils (adapted from [65]).

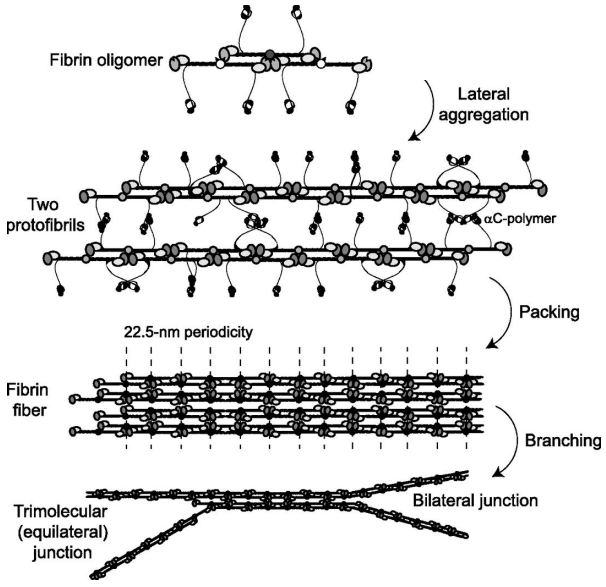

Figure 1.5. Schematic representation of the latter steps of fibrin polymerization (adapted from [66]).

1.2.4 Fibrinolysis

Infiltrating cells can degrade the provisional matrix by secreting proteolytic enzymes that degrade fibrin, which is eventually by fibronectin, collagen, and other ECM components to form new tissue. The fibrin degradation process, known as fibrinolysis, is mediated by the protease plasmin. Circulating plasminogen is bound by fibrin and activated to its active form, plasmin, by tissue-type plasminogen activator (tPA), which is synthesized by vascular endothelial cells and circulated in the blood.[68–70] Plasmin can cleave fibrinogen, fibrin, or crosslinked fibrin.[71] Since plasmin cleavage creates new lysine binding sites on fibrin that can further engage with plasmin, there is actually a positive feedback mechanism that accelerates plasmin lysis as it proceeds.[57,68] Interestingly, the presence of soluble fibrinogen causes little or no stimulatory effect on this positive feedback loop.[63,72] However, there are many antifibrinolytic compounds that can inhibit fibrinolysis. α2-macroglobulin, also known as α2-antiplasmin, is a primary physiological inhibitor of plasmin, blocking either the conversion of plasminogen to plasmin or the active binding sites of plasmin on fibrin.[57,68,73] Additionally, fibrinolysis can also be inhibited by plasminogen activator inhibitor type 1 or thrombin activable fibrinolysis inhibitor (TAFI).[57]

A variety of fibrin degradation products (FDP) can be generated post plasmin cleavage (Fig. 1.4). For fibrinogen cleavage, the αC domains are cut, resulting in fragment X, which can be further cleaved to fragments D and Y, the latter which is composed of both a D and a E fragment. Consequently, fibrinogen degradation by plasmin results in two fragments D and one fragment E molecule.[64] In a different manner, for fibrin, plasmin cleavage, in addition to fragments Y, D, and E, produces larger intermediates: (1) X-oligomer (cleavage of C domains) and (2) D-dimer (cleavage of coiled-coil region between D and E domains).[64]

There is growing evidence that fibrin fragments can play an important role in modulating inflammation in wound healing and disease progression.[74–76] Robson et al. demonstrated in *in vitro* experiments that D-dimer induces the synthesis and release of IL-1β and IL-6.[77] Fragment E has also been shown to upregulate IL-6 and IL-1β expression and downstream protein production in rat peritoneal and human THP-1 macrophages respectively.[78,79] Moreover, in atherosclerosis, D-dimer and fragment E have also been implicated to contribute to the development of atheromatous plaques and further progress atherosclerosis.[80,81] Yet, fragment E has been also been demonstrated to promote angiogenic activity.[82] Consequently, fibrinolysis is important to consider during wound healing because of the potential immunomodulatory effects of the degradation products.

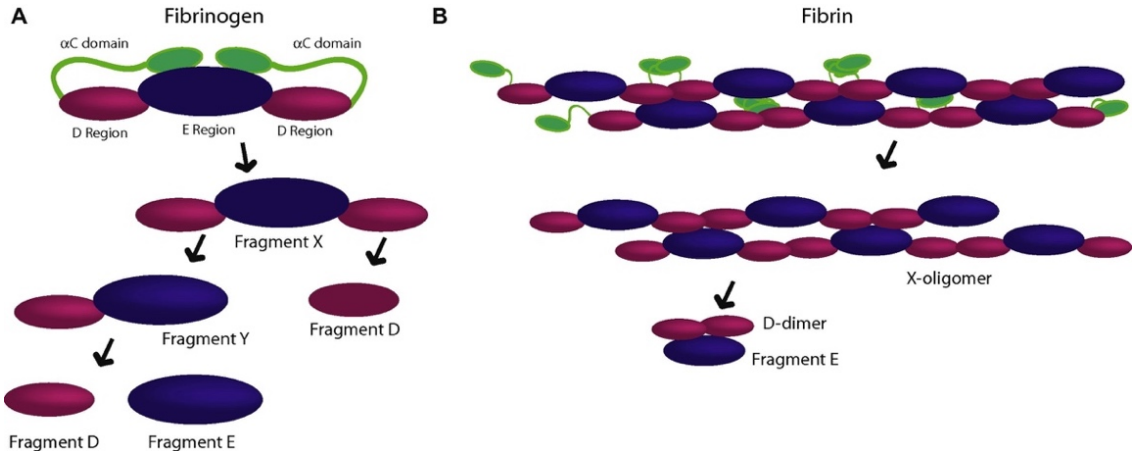

Figure 1.6. FDP generated after plasmin cleavage of (A) fibrinogen and (B) crosslinked fibrin (adapted from [64]).

1.2.5 Biological Relevance of Fibrin(ogen)

Aside from its role as the primary component of the provisional matrix during wound healing, fibrin is also essential—among other biological functions—for hemostasis and blood clot contraction.[83] First, it has been demonstrated that in transgenic mice possessing a fibrinogen that cannot be cleaved by thrombin, the animals demonstrated a strong propensity for bleeding,

indicating that cleavable fibrinogen may be necessary for hemostasis.[84] Second, fibrin plays a key role in blood clot contraction—this platelet-driven, fibrin-mediated shrinkage of the clot is necessary to prevent blood loss, reduce clot volume, and restore blood flow past an obstructive thrombus.[85,86] If blood clot contraction does not properly occur, this can lead to pathogenesis of both arterial and venous thrombosis.[83]

Moreover, aside from playing an important biological role in wound healing, fibrin is also necessary for protection against immunopathology.[87,88] It has been demonstrated that fibrin(ogen) can serve as an early line of host protection by mediating bacterial killing, limiting bacterial growth, and suppressing dissemination of the bacterial microbes.[89] In instances in which transgenic mice carry normal levels of circulating fibrinogen that lack the capacity for polymerization, the animals exhibited a compromised capacity for antimicrobial host defense.[84]

1.2.6 Clinical Applications of Fibrin(ogen)

Fibrin(ogen) has been used in the clinic as both a therapy and a biomaterial. In situations of severe bleeding such as during trauma or surgery, fibrinogen replacement, or the administration of fibrinogen concentrates, is emerging as a treatment method.[90] In a porcine model study in which animals received standardized bone injury, it was demonstrated the administration of fibrinogen was able to reverse dilutional coagulopathy and restore blood clot firmness.[90] Moreover, in another study, fibrinogen concentrates also helped to reduce bleeding and increase clot firmness in Syrian golden hamsters after shock and resuscitation.[91] Finally, fibrinogen supplement therapy has also been demonstrated to be beneficial in rescuing fibrin clot firmness *in vitro* and reversing coagulopathy in human patients during cases of severe trauma.[92,93]

Given its natural role in wound healing as well as its ease of being purified from blood, fibrin has been developed and successfully used in the clinic as an effective, safe, and easy tissue sealant or wound dressing.[94–98] Clinicians and engineers have also explored the use of fibrin as a matrix for cell culture, scaffold for tissue engineering and carrier for targeted delivery of drugs and growth factors.[99–101] Using fibrin as a matrix for cell culture or tissue engineering applications is advantageous because on top of guiding cell growth, fibrin has been shown to promote angiogenesis.[102] As a carrier, fibrin has also demonstrated promise because impregnation or tethering of drug molecules and factors to fibrin via covalent linkages have resulted in efficient and precise deliveries to desired locations.[100]

Aside from these clinical uses, fibrinogen is also often used as an inflammatory marker. Up-regulation of circulating fibrinogen is utilized as a marker of inflammation in a number of diseases including cardiovascular and vascular wall diseases, neuroinflammatory diseases, and cancer, among others.[103] First, in cardiovascular disease, an increased level of plasma fibrinogen has been associated with an enhanced risk of coronary artery disease (CAD).[104] Moreover, with respect to atherosclerosis, fibrin and FDP have been found within disease lesions but not in normal healthy vessels.[105] In particular, the D-dimer has been implicated to play a pro-atherosclerotic role, enhancing the inflammatory response during macrophage-derived foam cell formation.[80] The presence of D-dimer fragments in human plasma has also been strongly correlated to the occurrence of future venous thrombosis events for patients who suffer from acute deep vein thrombosis.[106] Nonetheless, fibrinogen may have some protective effect because deletion of fibrinogen exacerbates atherosclerosis in low-density lipoprotein receptor and apolipoprotein B-

edisome complex deficient mice.[107] In addition, there is also growing evidence that the fibrin-derived peptide $B\beta_{15-42}$ protects the myocardium against ischemia-reperfusion injury.[108–110]

Second, in cancer, most solid tumors in animals and humans contain a substantial amount of fibrin because fibrin gels can trap plasma proteins and water, providing a provisional matrix for tumor cells.[111] Tumor-associated fibrin deposition has been studied to examine how microvascular permeability, extravascular coagulation, and fibrinolysis each play a role in tumor development.[111] Moreover, since fibrin matrices also promote neovascularization, fibrin has also been implicated to facilitate tumor stroma formation.[112] Finally, it has also been proposed that fibrin can help a tumor evade the immune system.[113,114]

Last, in neuroinflammatory diseases, fibrinogen is thought to act as an initial trigger, stimulating innate immune responses that lead to axonal damage; accumulation of fibrin further promotes inflammation.[115,116] Additionally, elevated fibrinogen levels have also been linked with the future occurrence of ischemic stroke, Alzheimer's disease, and vascular dementia.[117,118] However, the role of fibrinogen in neuropathological diseases still needs to be elucidated because just like in cardiovascular diseases, fibrin(ogen) can also be beneficial. Schachtrup et al. suggested that fibrinogen is a regulator of TGF-β mediated signaling within the central nervous system tissues after vascular damage.[119] Furthermore, Adams et al. demonstrated that the fibrin-derived peptide $\gamma^{377-395}$ inhibited both microglial activation and relapse paralysis in central nervous system autoimmune diseases.[120] Thus, unraveling fibrin(ogen)'s role in injury repair and numerous clinical diseases will help build new understanding of how fibrin(ogen) regulates either anti- inflammatory or inflammatory responses.

1.3 Fibrin(ogen) & Macrophage Interactions

1.3.1 Role of Integrins

Macrophages interact with its extracellular environment primarily via heterodimeric transmembrane protein receptors known as integrins.[121,122] Integrins transduce signals via activation of signaling cascades or modulation of cytoskeletal elements—integrins not only regulate cellular adhesion but also mediate phagocytosis, morphology, and migration.[122] Along with soluble signals from growth factor receptors, cytokine receptors, and chemokine receptors, integrin-mediated intracellular signaling regulate numerous behaviors of anchorage-dependent cells.[121] In particular, monocytes and macrophages express integrins of the β1, β2, and β5 families (Table 1.1). β1 associates with α1, α2, α3, α4, α5, and α6 while β2 and β5 with αL or αM and αV respectively. Human macrophages also express αxβ2, also known as CD11c/CD18; however, in mouse, this integrin is not highly expressed in monocyte-derived macrophages.

Table 1.1. Monocyte and macrophage integrins[121,122]

β chain family	Associated α	Other names	Ligands
β1	α1		Collagen
	α2		Collagen, Laminin
	α3		Laminin
	α4	CD49d/CD29, VLA-4	Fibronectin, VCAM-1 (CD106)
	α5	CD49e/CD29, VLA-5	Fibronectin
	α6	CD49f/CD29, VLA-6	Laminin
β2	αM	CD11b/CD18, CR3, Mac-1	ICAM-1, ICAM-2, C3bi, fibrinogen, Factor X
	αL	CD11a/CD18, LFA-1	ICAM-1, ICAM-2, ICAM-3
	αx	CD11c/CD18, p150/95	RGD-containing proteins, Fibrinogen, Lipopolysaccharide, C3bi
β3	αV	CD51/CD61	Vitronectin, Entactin, RGD-containing proteins

1.3.2 Fibrin(ogen) as an Integrin Ligand

Fibrin(ogen) as either a soluble protein or an insoluble scaffold provides binding sites for integrins by interacting with CD11b (αM) and CD11c (αx).[123–126] Specifically, αMβ2, also known as CD11b/CD18, Mac-1, or CR3 binds to fragment D while αxβ2, also known as CD11c/CD18 or p150/95, binds to fragment E.[125,127] Notably, the integrin αMβ2 is also most commonly known for mediating phagocytosis.[121] Interestingly, there has also been recent evidence that a distinct population of pro-inflammatory macrophages can also interact with extravascular fibrin via C-C chemokine receptor type 2 (CCR2), specifically for the purpose of fibrin removal.[128] Ultimately, fibrin(ogen) provides molecular signals to direct macrophage function because it contains not only binding sites for integrins but also interaction sites for growth factors and other ECM components such as fibronectin.[56,129–131]

1.3.3 Fibrin(ogen)-Macrophage Interactions

There is growing evidence suggesting direct interactions between macrophages and fibrin(ogen). In the context of biomaterials, the adsorption of fibrinogen to biomaterial surfaces is thought to be important for the recruitment of macrophages. *In vitro* experiments have demonstrated that fibrinogen can promote both inflammatory and anti-inflammatory activation. Fan et al. showed that when human peripheral blood mononuclear cells (PMBCs) were seeded onto fibrinogen coated surfaces, both TNF-α mRNA expression and protein secretion were enhanced.[132] Similarly, when PMBCs were exposed concomitantly to fibrin gels that were forming in situ, mRNA expression of the proinflammatory cytokine, interleukin 1β (IL-1β) was induced.[133] Contrastingly, there has also been evidence suggesting that fibrinogen may also promote the alternative activation of macrophages. When human monocyte-derived macrophages were exposed

to fibrinogen coated surfaces, Wang et al. observed an upregulation of IL-10 and regulators A20, ABIN3, and SOCS3 via the tyrosine kinase Syk pathway—the cytokine and suppressors in turn indirectly inhibited Toll-like receptor 4 (TLR4) and type I interferon signaling.[134]

In animals, Tang et al. demonstrated that when polyester terephthalate film (PET) was implanted intraperitoneally in mice post coating with human plasma, PET that was pre-incubated with hypofibrinogenemic plasma recruited fewer phagocytes than the number of cells recruited by the control.[135] In a separate study, Tang et al. precoated implants with purified fragments of fibrinogen and consequently determined that the primary pro-inflammatory sequence in fibrinogen lies within the fibrinogen D30 domain.[136] In particular, it has been implicated that a peptide sequence, P1 (residues 190-202 of the γ chain of fibrinogen) within D30 interacts with CD11b/CD18.[137] Additionally, it was observed in CD11b/CD18 knockout mice that although phagocytes were recruited to the sites of implants, the phagocytes failed to adhere and accumulate on the implant surfaces.[138] Moreover, in murine disease models, CD11b/CD18 has also been implicated to play a role: (1) in murine tumor models, lack of CD11b engagement enhanced antitumor response to radiation in cell carcinoma xenografts and (2) in rabbit stent-induced injury models, blocking CD11b/CD18 reduced restenosis after vascular injury.[139,140] Overall, these data implicates a potential immunomodulatory role for integrins in mediating macrophage-fibrin(ogen) interactions.

1.4 Overview of Dissertation

1.4.1 Chapter Overviews

First, in **Chapter 2,** differential regulation of macrophage activation by fibrin and fibrinogen will be described. Furthermore, macrophage differentiation on collagen and fibrin

ECMs will also be briefly touched upon. We also examine macrophage differentiation, morphology, motility on fibrin matrices in this section. Next, in **Chapter 3**, studies involving altering mechanical properties of both fibrin and fibrinogen will be elaborated upon. Macrophage differentiation on ECM and synthetic matrices will also be discussed. Moreover, modulating the stiffness of fibrin gels via biological and chemical agents were examined. In addition, mechanical tethering of fibrinogen onto synthetic matrices were also investigated. Then, in **Chapter 4**, a light-based crosslinking technique of fibrin will be introduced. The effects of the crosslinked matrix on macrophage behavior and function will be detailed. Finally, in **Chapter 5**, research summaries will be presented and future directions will be provided.

Chapter 2: Differential Regulation of Macrophages by Fibrin(ogen)

2.1 Background

2.1.1 Reconstituted Type I Collagen or Fibrin Matrices

The three-dimensional ECM governs how cells sense and respond to its environment and is a subject of great interest in the field of mechanobiology—a field that studies how physical forces and changes in the mechanical properties of the substrate contribute to cell differentiation, development, and function as well as disease pathogenesis and progression.[141] ECM in interstitial tissues exhibit three-dimensional cell-scale microarchitecture.[142] However, matrices like those found in tissues that can orchestrate complex functions are not easily recreated *in vitro*. Single-component natural or synthetic matrices are typically utilized to provide structural integrity and mediate cellular adhesion. Among the natural matrices, reconstituted fibrin or type I collagen gels are the most common.[143] Fibrin, like previously mentioned, is a primary component of a healing wound; it is usually reconstituted to a protein density of 1.5 to 2.2 mg/ml.[144]

Unlike fibrin, type I collagen is the most abundant fibrous protein found in interstitial tissue such as the skin, lung, etc.[145] Reconstituted collagen gels are typically made in the range of 0.3 to 30 mg/ml from typically rat tail tendon or bovine sources.[146,147] Specifically, collagen gel polymerization is initiated by raising an acidic solution of collagen to neutral pH. It is important to note that reconstituted collagen gels are mechanically weaker and more hydrated than those found in natural tissues.[143] Unlike fibrin, individual collagen monomers condense upon the pH switch and are linked laterally to form large fibers—however, these fibers are merely entangled instead of being covalently bounded to each other.[143,148] Consequently, collagen fibers can slip and slide with respect to each other.[143]

2.1.2 Matrix Architecture of Collagen and Fibrin Gels

Matrix microarchitecture is physically-instructive because cellular behavior on a scaffold can be dependent on the physical and mechanical cues.[142] A number of properties, such as porosity, mesh size, fiber density and diameter, can all contribute to building the microarchitecture in a cell's microenvironment. For collagen gels, pore size and fiber diameter can be tuned by modulating the concentration of the protein or the pH during gelation. However, only moderate ranges for both properties are achievable because large changes in pH will inhibit gelation.[149]

Fiber density in collagen gels, impacted by the rate of fibril self-assembly, can be influenced by factors such as temperature, PH, and ionic strength.[142] It has been observed that with rapid fibril assembly—induced by low or very high ionic strength, high pH, or high temperature condition—results in gels with small pores and high fiber density.[150–152] For example, increasing the pH in the range between 6.0 and 9.0 results in decreased average fiber diameter (from 500 to 392 nm).[149] Conversely, obtaining gels with relatively larger pores and sparser, yet larger fibers requires slower fibril assembly, which can be achieved under moderate ionic strength, low pH, or low temperature conditions.[142] Finally, it has been shown that although increases in collagen concentration increases fiber density, fiber diameter is not influenced.[149]

Contrarily, the network architecture of fibrin can be tuned to a greater extent by varying its composition. Modulating fibrinogen, thrombin, and/or ion concentration(s) as well as having active factor XIII present can all have an effect on fibrin structure.[143] Unlike collagen gels, fibrin matrices exhibit enhanced fiber and branchpoint densities when fibrinogen concentration increases.[144] Interestingly, it has been reported that increasing thrombin concentrations result in

tight networks with finer and thinner fibers as opposed to more porous gels with decreasing thrombin concentrations.[153]

With respect to changing the ionic strength, fibrin polymerization is enhanced by the presence of calcium ions, resulting in a higher fibrin fiber mass to length ratio compared to that observed in the control gel.[154] Another example is when fibrin gels are polymerized in the presence of zinc, scanning electron microscopic analysis indicated that there was a two-fold increase in fiber diameter compared to that of gels fabricated without zinc.[155] Finally, there is also evidence indicating that fibrin polymerization in the presence of chlorine prevents the growth of thicker and stiffer fibers.[156]

A broad range of values for fiber diameter and mesh size have both been reported for collagen and fibrin gels. Collagen fibers range anywhere from 30 to 800 nm, averaging around 350 nm.[148,149,157,158] Contrarily, fibrin fibers range anywhere from 4 nm to 500 nm, averaging around 160 nm.[144,159–161] For pore sizes, collagen can have pores from 1-10 μm in diameter while fibrin can have 0.1-10 μm in diameter.[159,162]

In this chapter, we first sought to characterize various reconstituted ECM gels and examine their abilities to modulate macrophage inflammatory activation. In particular, we found that fibrin matrices were capable of regulating macrophage inflammatory behavior and thus further investigated the differential roles played by fibrinogen and fibrin in immunomodulation. Additionally, we also explored how a fibrin matrix influences macrophage differentiation, morphology, and migration.

2.2 Materials & Methods

2.2.1 Macrophage Cell Isolation & Culture

Femurs from 6 to 12 weeks old female C57BL/6J mice (Jackson Laboratory) were harvested. Bone marrow was flushed with Dulbecco's Modified Eagle's medium (DMEM) supplemented with 10% heat-inactivated FBS. Cells were treated with ACK lysis buffer (Thermo Fisher) to lyse red blood cells, centrifuged, resuspended, and cultured in D-10 media. D-10 media is composed of high-glucose DMEM supplemented with 10% heat-inactivated FBS, 2 mM L-glutamine, 100 U/ml penicillin, 100 μg/ml streptomycin (Thermo Fisher), and 10% conditioned media from CMG 14–12 cell expressing recombinant mouse macrophage colony stimulating factor (M-CSF) to induce differentiation to bone marrow derived macrophages (BMDMs).

After culture for 7 or 8 days on non-treated polystyrene Petri dishes, BMDMs were dissociated using cell dissociation buffer (Thermo Fisher) and seeded onto 96 or 24 well tissue culture polystyrene (TCPS), round 18 mm diameter No. 1 glass coverslips, or gels fabricated on TCPS and glass coverslips in D-10 media. For studies examining the effects of collagen, fibrin, and fibrinogen, cells were seeded at 50,000 cells/cm^2. For studies examining the effects of cytokines in conjunction with fibrin and fibrinogen or cytoskeletal staining, cells were seeded at 100,000 cells/cm^2, a density that we have previously used to examine the effect of cytokines on macrophages.[163] For cytokine or fibrinogen stimulation, macrophages were stimulated at 6 hours post seeding with a combination of 1.0 ng/ml of E. coli-derived LPS (Sigma-Aldrich), 1.0 ng/ml of recombinant murine IFN-γ (R&D Systems), 10 ng/ml of IL-4 (BioLegend), 10 ng/ml IL-13 (BioLegend), or 2.0 and 4.0 mg/ml soluble fibrinogen. Polymyxin B (PMB, InvivoGen) was added at a concentration of 20 μg/ml.

2.2.2 Gel Fabrication

Pure collagen gels containing 2.0 mg/ml protein were fabricated using rat tail Type I collagen (Corning) according to the manufacturer's suggested protocol. Briefly, collagen was mixed with appropriate amounts of 10X PBS (Lonza), 1 N NaOH, and Millipore water. Pure fibrin gels were fabricated at 2.0 mg/ml using bovine plasma Type IS fibrinogen (Sigma). The lyophilized protein was reconstituted in PBS containing calcium and magnesium (Sigma). 0.4 U of thrombin was used per milligram of fibrinogen to initiate the polymerization reaction. Collagen-fibrin mixture constructs were formed using rat tail collagen I and bovine fibrinogen such that the final protein content remained 2 mg/ml. To form 3D gels, TCPS or glass coverslips were coated with ECM solutions and incubated in a humidified 37 °C incubator overnight.

2.2.3 Laser Scanning Confocal Microscopy

For imaging purposes, composite gels were fabricated on 35 mm glass bottom dishes. Laser scanning confocal back reflection microscopy (backscatter) was performed with an Olympus IX81 microscope. Samples were illuminated with a 488 nm laser light (NTT Electronics Optiλ) with a 40X objective (Olympus). Images were captured using the Olympus Fluoview software. The backscattered light signal was detected with a photomultiplier tube. Fibers differing in refractive indices from their surroundings enabled 3D structure details to be recognized as reflection images were taken along the z-axis at sequential focal lengths.

2.2.4 Assessment of Cytokine Secretion via Enzyme-linked Immunosorbent Assay

Supernatants of BMDMs cultured on collagen/fibrin composites or fibrin, with and without fibrinogen stimulation, were collected at 36 hours after stimulation. Tumor necrosis factor alpha (TNF-α) and interleukin-10 (IL-10) secretion levels were assessed by enzyme-linked

immunosorbent assay (ELISA) following manufacturer's protocol (BioLegend). For samples analyzed with a Luminex 32-plex mouse cytokine array and TGF-β Array 3-plex (Eve Technologies), BMDMs were seeded on 2 mg/ml fibrin gels and further stimulated with 4 mg/ml of fibrinogen or external cytokines mentioned in 2.2.1. Supernatants were collected 4 and 18 hours after stimulation. Hierarchical clustering was performed in R utilizing a complete linkage method and presented with the gplots package. Z-scores were calculated for each sample relative to the column-wise mean for presentation.

2.2.5 Quantitative Reverse Transcriptase-Polymerase Chain Reaction (qRT-PCR)

BMDMs were harvested by scraping for conditions on TCPS; BMDMs on fibrin gels were extracted with a mortar and pestle. Cells were pelleted and stored at -80 °C until RNA was extracted with the Qiagen RNeasy Mini kit. RT was performed with the Qiagen Quantitect Reverse Transcriptase kit, which includes a DNase treatment step before RT and uses random hexamer primers. The resulting cDNAs were diluted tenfold in water before qPCR. qPCR was performed with Bio-Rad Ssofast Evagreen master mix on a Bio-Rad CFX96 instrument using the manufacturer's recommended cycling protocol, i.e. a 30 s incubation at 95 °C followed by 40 cycles of 5 s at 95 °C and 5 s at 55 °C.

Samples were ran in duplicate with primers found in Table 2.1. Forward and reverse primers were both used at 400 nM except for *Tnfa*—the primer concentration was 200 nM. NTCs for all templates showed no amplification. cDNAs were verified to be free of genomic DNA contamination by the ValidPrime assay.[164] C_qs were called by a threshold method. Results were analyzed in R; transcript abundance was determined relative to *Gapdh* using the $2^{-\Delta C_q}$ method. Data and the analysis script are available at https://github.com/WendyLiuLab/Hsieh2016PCR.

Table 2.1 Primers used for qRT-PCR[164,165]

Gene	Direction	Sequence	Amplicon Length (bp)
Arg 1	F	CTCTGTCTTTTAGGGTTACGG	152
	R	CTCGAGGCTGTCCTTTTGAG	
Chi3l3	F	AGTGCTGATCTCAATGTGGATTC	142
	R	TAGGGGCACCAATTCCAGTC	
Gapdh	F	GTCAAGCTCATTTCCTGGTATGAC	131
	R	TCTCTTGCTCAGTGTCCTTGC	
Il10	F	CCCACTTCCCAGTCGGCCAG	300
	R	GGAGAAATCGATGACAGCGCCTC	
Kdm6b	F	GGTTCACTTCGGCTCAACTTAG	75
	R	CTCCACCGTATGTTCACCGC	
Mrc1	F	TGTTTTGGTTGGGACTGACC	269
	R	TGCAGTAACTGGTGGATTGTC	
mVPA1	F	GGAGCCCAGTGTAGAAGAGCA	87
	R	AGCCAGCGAACCATATCCTGA	
Nos2	F	TTGGGTCTTGTTCACTCCAC	211
	R	TGTATTGTTGGGCTGAGAACAG	
Retnla (Fizz-1)	F	GCCAATCCAGCTAACTATCCC	187
	R	AGTCAACGAGTAAGCACAGG	
Tnfa	F	CCCACGTCGTAGCAAACCACCA	172
	R	TCGGGGCAGCCTTGTCCCTT	

2.2.6 Fluorescence Staining & Imaging

For arginase-1 (Arg-1) and inducible nitric oxide synthase (iNOS) staining, BMDMs were seeded on plain or fibrin gel-coated glass coverslips and stimulated with fibrinogen at 6 hours after adhesion. Control BMDMs were stimulated with LPS and IFN-γ, IL-4 and IL-13, and LPS with IL-4 and IL-13 at concentrations described in 2.2.1. After 18 hours, cells were fixed with 100% cold methanol on ice for 15 minutes. Samples were blocked with both 5% normal donkey and goat serum in PBS (both from Jackson ImmunoResearch). Samples were then incubated with goat anti-Arg-1 and` rabbit anti-iNOS (both from Santa Cruz Biotechnology) primary antibodies, followed by Alexa Fluor-594 donkey anti-goat and Alexa Fluor-488 goat anti-rabbit secondary antibodies (both from Jackson ImmunoResearch), and counterstained with Hoechst 33342 (Thermo Fisher).

For detection of the actin cytoskeleton, BMDMs were seeded on plain or fibrin gel-coated glass coverslips and further stimulated with fibrinogen. After 4 or 18 hours, cells were fixed with 4% paraformaldehyde (Electron Microscopy Sciences) and washed with PBS (Lonza), and permeabilized with 0.1% Triton X-100 (Sigma) in PBS. Samples were incubated with Alexa Fluor-488 conjugated phalloidin and counterstained with Hoechst 33342 (both from Thermo Fisher). Images of fixed samples were acquired in epifluorescence with an Olympus IX83 inverted microscope with a 40X oil immersion lens and Micro-Manager microscope control software.[166] In particular, contrast of F-actin images was normalized using ImageMagick; intensity values were stretched to cover the entire range of possible values.

2.2.7 Statistical Analysis

Data presented are from three independent biological experiments and values are represented as mean ± SEM unless otherwise indicated. Statistical analysis was performed considering $p < 0.05$ to be statistically significant. Data were analyzed using an one-way ANOVA followed by Tukey's HSD post-hoc test or a Student's two-sided *t*-test assuming equal variance followed by false discovery rate correction for multiple comparisons.

2.3 Results

2.3.1 Composition of Fibrin and Collagen Gels Influences Fiber Architecture

Using laser scanning confocal microscopy, also known as back reflection microscopy, we observed distinct fiber architectures in gels of different composition (Fig. 2.1) In a pure collagen gel, fibers were long, thick and branching. Contrarily, a pure fibrin gel exhibited short, thin, and non-branching fibers. Last, gels containing a mixture of fibrin and collagen displayed both thin and thick fibers. It is also apparent from these images that a pure collagen gel had bigger pore sizes

than those observed in a pure fibrin gel. In a mixed gel, pores were intermediate in size. Finally, it was not obvious if fiber density was necessarily enhanced with increasing collagen concentration because the fibers may have been just more bundled together.

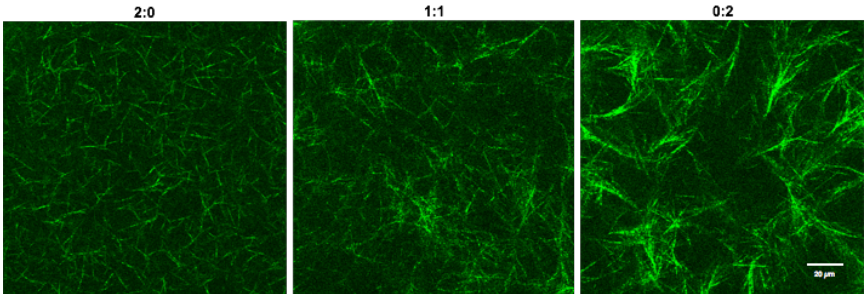

Figure 2.1 Composition of fibrin-collagen gels affects fiber architecture. Representative backscatter images of composite fibrin-collagen gels with indicated mg/ml fibrin: mg/ml collagen concentrations. Total protein content was maintained at 2 mg/ml. Scale bar: 20 μm.

2.3.2 Thrombin Alone Induces Moderate Inflammatory Activation

Previous work has suggested that fibrin may function as an inflammatory mediator. Thrombin induces several cellular responses involved in inflammation—specifically, it activates macrophages and promotes the production of IL-1.[167] Moreover, thrombin also acts as a chemotactic agent for neutrophils, one of the immune cell types that appear very early on during the onset of injury.[168,169] *In vivo* evidence has demonstrated that thrombin injections in rat models induce edema via activation of the thrombin receptor.[170] However, it has also been implicated that thrombin plays a role in potentiating wound healing and scar tissue formation by increasing fibroblast proliferation and collagen secretion.[171–173] With respect to macrophages specifically, *in vitro* evidence suggests that thrombin biases macrophages towards an M2a phenotype.[174] M2a macrophages are known to secret IL-4 and IL-3, cytokines known to promote fibrocyte differentiation and potentiate collagen secretion by fibroblasts.[175,176]

To specifically explore the effect of bovine thrombin on murine macrophages, we adsorbed thrombin overnight or spiked it in the culturing media solution with varying dosages (Fig. 2.2). We

found that increasing concentrations of soluble thrombin enhanced the secretion of TNF-α. As little as 0.0075 unit of thrombin was sufficient to stimulate TNF-α while higher units brought about TNF-α levels averaging around a little over 200 pg/ml. Interestingly, adsorbed thrombin did not seem to have as strong of an effect on TNF-α secretion, eliciting low values of TNF-α throughout the different dosages of thrombin. Contrastingly, IL-10 secretions were also influenced by thrombin. Notably, adsorbed thrombin had more of an effect than that of soluble thrombin. IL-10 secretions gradually increased with more units of thrombin; TNF-α secretions began to saturate at around 80 pg/ml beginning with 0.04 units of thrombin. Together, these results suggest that thrombin alone can mediate the inflammatory and anti-inflammatory activities of macrophages.

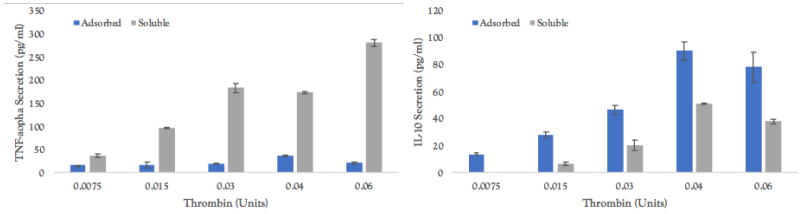

Figure 2.2 Presentation of thrombin modulates macrophage cytokine secretion. Graph of TNF-α secretion by macrophages cultured with indicated units of thrombin, either adsorbed or delivered in culture media. Values are averages ± SD of n = 1.

2.3.3 Presentation of Fibrin(ogen) Modulates Macrophage Cytokine Secretion

As previously mentioned, it has been suggested that fibrinogen, the soluble precursor of fibrin, simulates macrophage inflammatory activation.[132,133,177] In particular, it has been suggested that fibrinogen-induced chemokine secretion requires the presence and expression of functional TLR4.[177] To specifically examine the effect of fibrinogen vs. fibrin, we cultured BMDMs on TCPS surfaces or fibrin gels. We stimulated BMDMs with varying concentrations of soluble fibrinogen at 6 hours post seeding and investigated the cytokine secretion 36 hours after stimulation.

We found that increasing concentrations of soluble fibrinogen significantly enhanced the secretion of TNF-α, confirming observations previously reported by others (Fig. 2.3B) .[177] As little

as 0.02 mg/ml of fibrinogen was sufficient to stimulate moderate TNF-α secretion and higher fibrinogen stimulation concentrations of 0.2–4 mg/ml saturated TNF-α levels at approximately 1000 pg/ml. IL-10 secretion also saturated with 0.2–4 mg/ml fibrinogen stimulation, but reached a more moderate level of 200 pg/ml. In contrast, cells cultured on fibrin gels secreted much higher levels of IL-10 and little TNF-α. Macrophages exposed to gels with a concentration between 1 and 4 mg/ml of fibrin secreted significantly more IL-10 than cells exposed to 1–4 mg/ml of soluble fibrinogen. Moreover, TNF-α remained relatively low and was less than 200 pg/ml across all gel conditions of varying concentrations, although there was still a moderate increase with increasing fibrin concentration. Together, these results demonstrate that fibrin and fibrinogen activate opposing macrophage functions: fibrin is anti-inflammatory while fibrinogen is inflammatory. These data suggest that the molecular presentation of fibrinogen—either presented in the soluble form or incorporated within fibrin networks—may play an important role in modulating macrophage inflammatory activation.

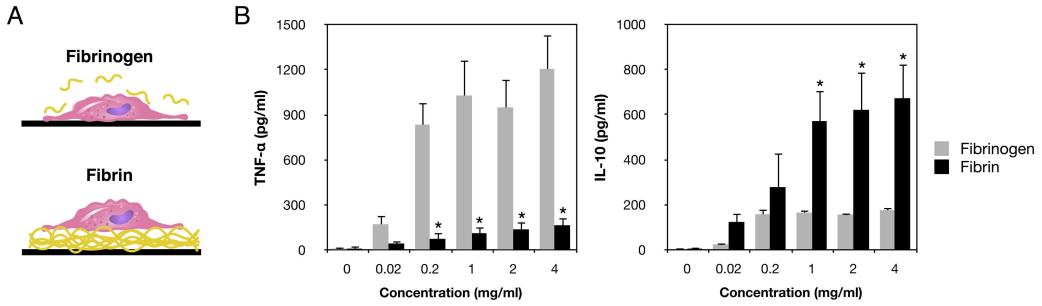

Figure 2.3 Presentation of fibrin(ogen) modulates cytokine secretion. (A) Schematic of experimental conditions examining the individual effects of fibrin or fibrinogen. (B) Graph of TNF-α (left) and IL-10 (right) secretion by macrophages cultured on different concentrations of fibrin or stimulated with different doses of soluble fibrinogen for 36 hours. Values are mean ± SEM of n = 3 biological replicates and asterisks denote $p < 0.05$ by Student's t-test followed by false discovery rate correction for multiple comparisons for comparisons within each concentration group.

2.3.4 Adhesion to Fibrin Inhibits Macrophage Inflammatory Activation

In the native wound healing environment, it is likely that macrophages are simultaneously exposed to fibrinogen and fibrin, as the precursor fibrinogen molecule is cleaved and incorporated

into the fibrin gel network. To examine the combinatorial effect of fibrinogen and fibrin, we seeded macrophages on 2 mg/ml fibrin gels or TCPS surfaces, further stimulated with different doses of soluble fibrinogen 6 hours after seeding. We then analyzed for cytokines secreted into the supernatant at 36 hours post stimulation (Fig. 2.4). We found that cells cultured on fibrin matrices maintained high IL-10 secretion levels, independent of the presence of fibrinogen. The levels of IL-10 secretion by cells cultured on fibrin and stimulated with fibrinogen were significantly higher, by approximately two-fold, than the levels secreted by macrophages stimulated with fibrinogen alone. Interestingly, culture of macrophages on fibrin completely abrogated the TNF-α activated by soluble fibrinogen.

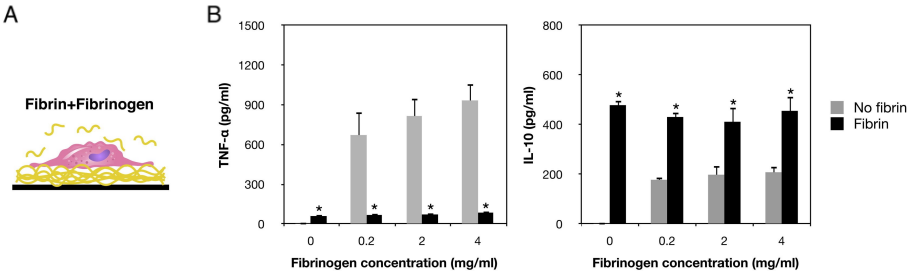

Figure 2.4 Adhesion to fibrin inhibits inflammatory activation. (A) Schematic of experimental conditions to examine the combined effect of fibrin and fibrinogen. (B) Graph of TNF-α (left) and IL-10 (right) secretion by macrophages cultured on 2 mg/ml fibrin or TCP surface, and stimulated with different doses of soluble fibrinogen for 36 hours. Values are mean ± SEM of n = 3 biological replicates and asterisks denote $p < 0.05$ by Student's t-test followed by false discovery rate correction for multiple comparisons for comparisons within each concentration group.

2.3.5 Fibrin Inhibits Fibrinogen-Induced Inflammatory Signaling

To more comprehensively assess macrophage cytokine secretion profiles elicited by fibrinogen and fibrin, we performed a multiplex analysis of a panel of 35 secreted proteins. BMDMs were seeded on fibrin gels or 24 well TCPS wells, further stimulated with soluble fibrinogen, and supernatants were collected at 4 and 18 hours after simulation. Here, the time points were shortened in order to better capture the temporal dynamics of the secreted proteins. In addition, we compared the cytokine levels of cells cultured on fibrin and/or stimulated with

fibrinogen to levels from cells stimulated with LPS and IFN-γ, IL-4 and IL-13, and LPS with IL-4 and IL-13, molecules known to induce macrophage activation.

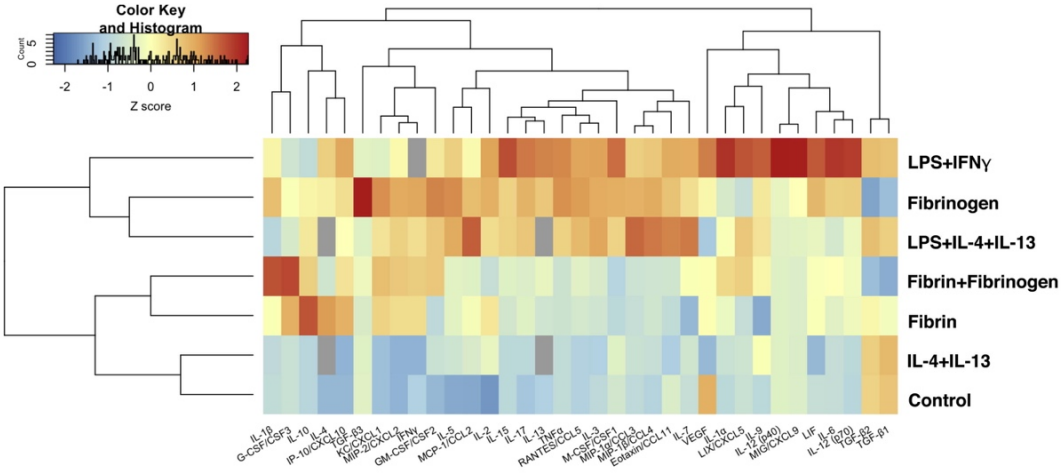

Figure 2.5 Fibrin inhibits multiple inflammatory cytokines. Column-wise mean normalized Z-score heat map of cytokines secreted by macrophages after culture on 2 mg/ml fibrin gels with or without 4 mg/ml fibrinogen or cultured on tissue culture plastic and stimulated with 4 mg/ml fibrinogen, 1 ng/ml LPS/IFN-γ, 10 ng/ml IL-4/IL-13, or 1 ng/ml of LPS and 10 ng/ml IL-4/IL-13 for 18 hours

Hierarchical cluster analysis of the Z-score, the number of standard deviations away from the mean across all conditions, suggested that the cells cultured on fibrin and stimulated with fibrinogen were more similar to cells cultured on fibrin alone as opposed to cells stimulated with fibrinogen alone (Fig. 2.5). We found that the concentrations of inflammatory cytokines elicited by cells stimulated with fibrinogen were mostly comparable to cells stimulated with LPS and IFN-γ, although there were some cytokines that were more highly elicited by LPS and IFN-γ, including IL-6, IL-12, and monokine induced by gamma interferon (MIG). Interestingly, IL-10 and granulocyte-colony stimulating factor (G-CSF) levels were higher in cells cultured on fibrin compared to cells stimulated with conditions containing IL-4 and IL-13, suggesting that adhesion to a fibrin matrix may in fact promote anti-inflammatory activities more effectively than soluble cytokines. Cluster analysis of the entire cytokine panel suggested that cells stimulated with fibrinogen were more closely related to cells stimulated with LPS, in combination with IL-4 and IL-13 or IFNγ, whereas

cells cultured on fibrin were more closely related to cells stimulated with IL-4 and IL-13 or control, unstimulated cells.

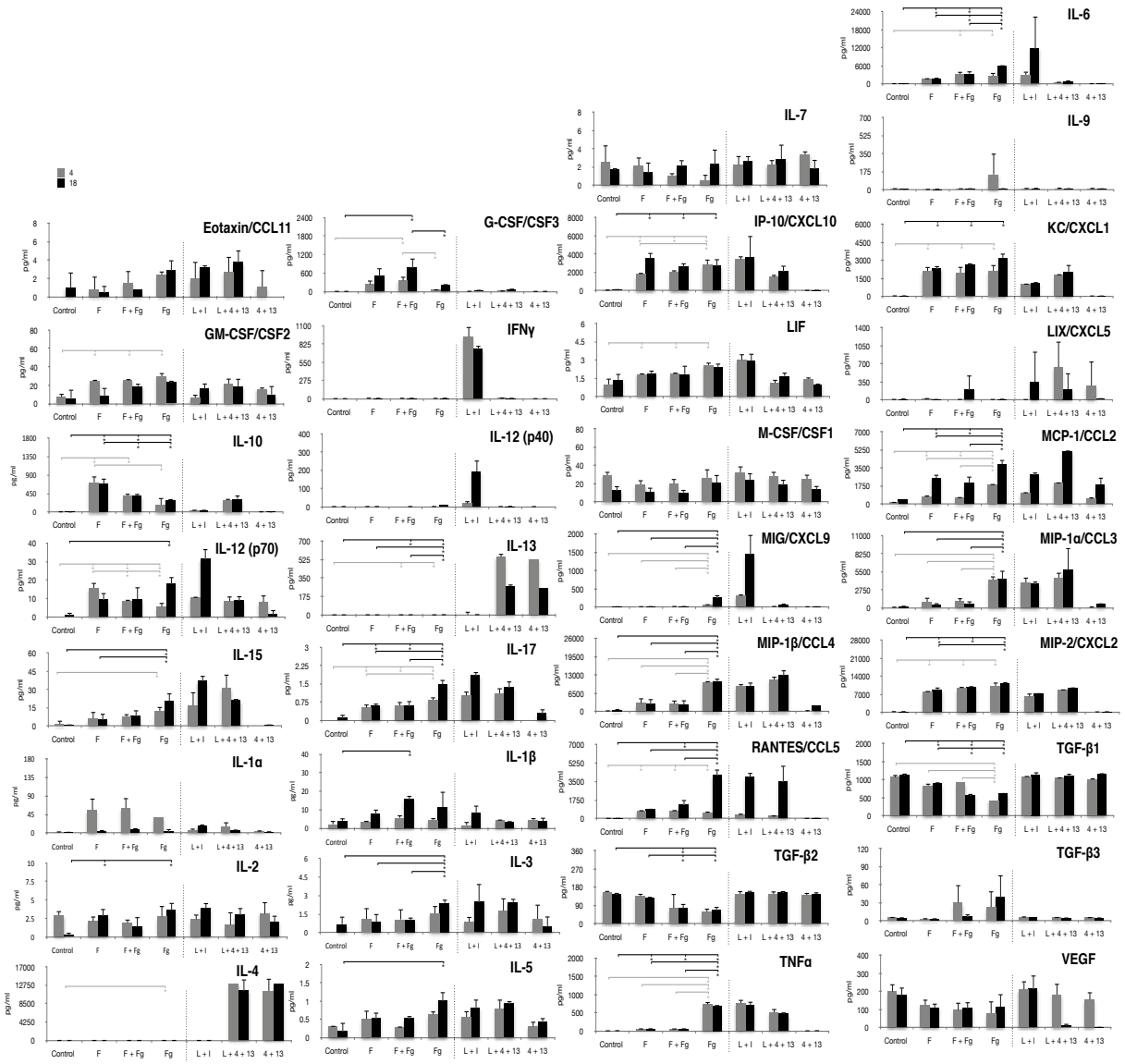

Figure 2.6 Macrophage cytokine secretion as determined by multiplex ELISA. Macrophages were cultured on 2 mg/ml fibrin gels with 4 mg/ml of fibrinogen (F+Fg) or without 4 mg/ml fibrinogen (F). They were also cultured on TCPS without (control), or with 4 mg/ml fibrinogen (Fg). Finally, controls included BMDMs stimulated with 1 ng/ml LPS/IFN-γ (L+I), 10 ng/ml IL-4/IL-13 (4+13), or 1 ng/ml of LPS with 10 ng/ml IL-4/IL-13 (L+4+13). All were further cultured after stimulation for 4 or 18 hours. Asterisks denote $p < 0.05$ by one way ANOVA followed by Tukey's HSD post-hoc test. Error bars indicate standard deviation of n=3 biological replicates except for the following: IL-1α (Fg, 4 hours and 18 hours), IL-7 (Fg, 4 hours), KC (Fg, 4 hours), IL-9 (Fg, 4 hours and 18 hours), VEGF (Fg, 4 hours), TGF-β1 (Fg, 18 hours), which each had n=2, and TGF-β2 (Fg and F+Fg, 4 hours), which each had n=1. In these cases, the viscosity of the sample interfered with the assay beads and data could not be recovered.

Further examination of cytokines that were secreted at the highest absolute levels revealed that many inflammatory cytokines shared a similar trend with that of TNF-α, including in particular, IL-6, MIG, monocyte chemoattract protein-1 (MCP-1), macrophage inflammatory protein-1α (MIP-1α), macrophage inflammatory protein-1β (MIP-1β) and RANTES (regulated on activation, normal T cell expressed and secreted) (Fig. 2.6). These cytokines were induced by fibrinogen and their secretion levels decreased when cells were cultured on a fibrin gel, with or without fibrinogen. A few cytokines such as interferon gamma-induced protein 10 (IP-10), macrophage inflammatory protein-2 (MIP-2), and neutrophil-activating protein 3 (NAP-3 or KC) were upregulated by fibrinogen and not affected by or only moderately diminished (in the case of MIP-2) in the presence of fibrin.

Concordant with IL-10, concentrations of cytokines involved in wound healing, including G-CSF and TGF-β1, were higher in cells cultured on fibrin when compared to cells stimulated with fibrinogen, although TGF-β1 was moderately reduced with the addition of fibrinogen while G-CSF was not. Unstimulated macrophages had the highest concentration of TGF-β1, which may suggest that the basal activation state in M-CSF-containing media is polarized towards an alternatively activated phenotype.[21] Many of the cytokines examined were upregulated by 4 hours and the levels were maintained at 18 hours, although IL-6, RANTES, MCP-1, MIG, and G-CSF did not appear at maximal concentrations until the longer time point.

Overall, the majority of the cytokines are consistent with TNF-α and IL-10—this suggests that fibrin promotes anti-inflammatory signaling and inhibits inflammatory signaling induced by fibrinogen. Some inflammatory cytokines were induced by both fibrinogen and fibrin, implicating the potential involvement of multiple pathways. However, despite the range of results, the cytokine

secretion levels from cells cultured on fibrin and further stimulated with soluble fibrinogen were overall more similar to those cultured on fibrin alone as opposed to those stimulated with fibrinogen alone, suggesting that the effects of adhesion to fibrin matrices dominate the response.

2.3.6 *Fibrin(ogen) Modulates Gene Expression of Polarization Markers*

To more broadly examine whether fibrinogen and fibrin lead to changes in macrophage phenotype polarization, we assessed the expression of a panel of gene markers by RT-PCR. Cells were cultured on fibrin or TCPS for 6 hours, and then soluble stimuli including fibrinogen, LPS, and/or cytokines were added for an additional 4 hours. Cluster analysis of the entire panel showed that cells cultured on fibrin, with or without fibrinogen, were more similar to control or LPS with IL-4 and IL-13 stimulated cells, whereas cells stimulated with fibrinogen were more similar to cells stimulated with LPS and IFN-γ (Fig. 2.7A)

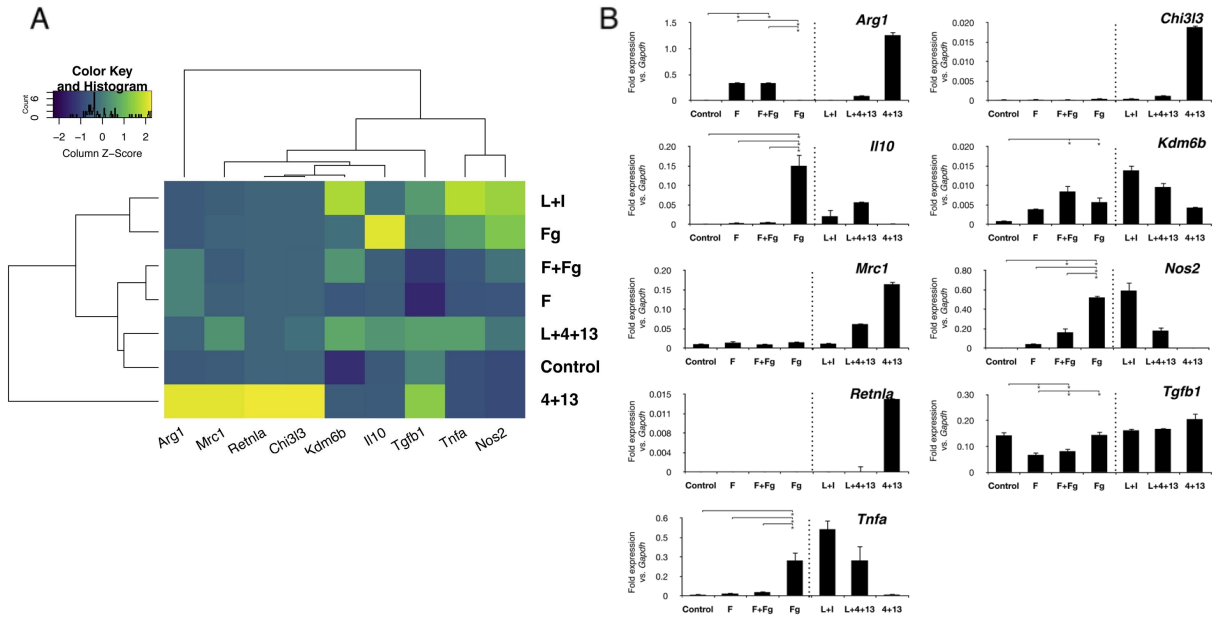

Figure 2.7. Macrophage gene expression determined by qRT-PCR. (A) Column-wise Z-score normalized heat map of mean gene expression by macrophages after culture on 2 mg/ml fibrin gels with or without 2 mg/ml fibrinogen, or cultured on TCPS and stimulated with 2 mg/ml fibrinogen, 1 ng/ml LPS/IFN-γ (L + I), 10 ng/ml IL-4/IL-13 (4 + 13), or 1 ng/ml of LPS and 10 ng/ml IL-4/IL-13 (L + 4 + 13) for 4 hours. (B) Graphs of expression levels relative to Gapdh of indicated gene expressed by macrophages. Values are mean ± SEM of n=3 biological replicates. Asterisks denote $p < 0.05$ by one way ANOVA followed by Tukey's HSD post-hoc test.

Expression of *Arg1* was consistent with IL-10 secretion and higher in cells cultured on fibrin, with or without additional fibrinogen, when compared to control or fibrinogen only stimulated cells (Fig 2.7B). However, amounts of *Nos2* (gene encoding for nitric oxide synthase), *Tnfa*, and *Il10* were all upregulated in cells stimulated with fibrinogen and reduced when cells were cultured on fibrin gels. Notably, *Il10* gene expression was not correlated with secreted cytokine levels, perhaps because of the time point used for evaluation. In addition, expression of some genes including *Retnla*, *Chi3l3*, *Kdm6b*, and *Mrc1* did not appear to be affected by fibrin or fibrinogen (Fig. 2.7B)

2.3.7 Fibrin(ogen) Influences Macrophage Polarization Marker Expression

We next examined whether adhesion to fibrin or exposure to soluble fibrinogen induced changes in the protein expression of Arg-1 and inducible nitric oxide synthase (iNOS), established pro-healing and pro-inflammatory macrophage phenotype markers respectively (Fig. 2.8). BMDMs were seeded on 2 mg/ml fibrin gels or glass coverslips, stimulated with 2 mg/ml soluble fibrinogen, and then fixed and stained for Arg-1 and iNOS expression at 18 h after stimulation. Expression levels were compared against control cells that were polarized by treatment with LPS and IFN-γ, IL-4 and IL-13, and LPS with IL-4 and IL-13. As expected, control cells stimulated with LPS and IFN-γ expressed iNOS and minimal levels of Arg-1 while those stimulated with IL-4 and IL-13 and LPS with IL-4 and IL-13 expressed Arg-1 but not iNOS. We found that macrophages seeded on glass and exposed to fibrinogen expressed moderate levels of Arg-1 and high levels of iNOS when compared to the unstimulated condition or cells seeded on fibrin gels, with or without fibrinogen. However, macrophages seeded on fibrin gels, with or without fibrinogen,

expressed Arg-1 and little iNOS. Together, these data suggest that adhesion to fibrin promotes Arg-1 and inhibits iNOS induced by fibrinogen.

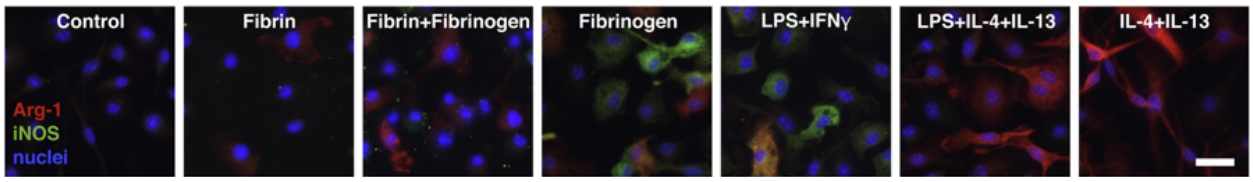

Figure 2.8 Fibrin(ogen) modulates expression of markers associated with polarization. Representative fluorescence images of macrophages cultured in the indicated conditions for 18 h and stained for arginase-1 (red), iNOS (green) or nuclei (blue). Scale bar: 25 μm.

2.3.8 Fibrin(ogen) Elicits Changes in Cytoskeletal Organization and Cell Shape

Our previous work suggested that cell shape plays a role in the modulation of macrophage phenotype and that cell elongation is associated with an alternatively activated or anti-inflammatory phenotype.[178] To determine if there was an association between cell shape and changes in macrophage function in the context of fibrinogen and fibrin, we evaluated the actin cytoskeleton by phalloidin staining. BMDMs were seeded on 2 mg/ml fibrin gels or glass coverslips, stimulated with 4 mg/ml soluble fibrinogen, and then fixed and stained at 4 hours and 18 hours after stimulation (Fig. 2.9).

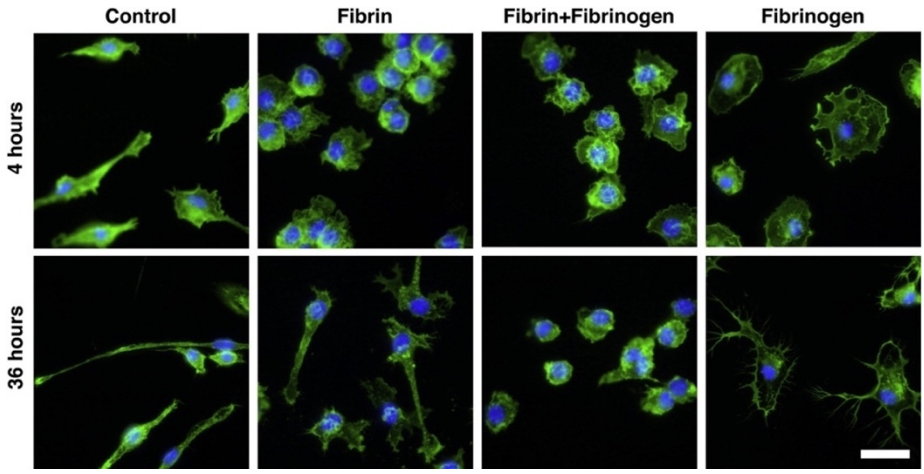

Figure 2.9 Actin distribution and cell shape are modulated by fibrin(ogen). Representative fluorescent images of phalloidin (green) and Hoechst (blue)-stained macrophages cultured on glass or 2 mg/ml fibrin and stimulated with 4 mg/ml fibrinogen for 4 hours or 18 hours. Scale bar: 25 μm.

At 4 hours post stimulation, macrophages cultured on glass and stimulated with fibrinogen appeared to be the most well spread, with considerable lamellipodia formation, when compared to the unstimulated condition or cells seeded on fibrin gels with or without fibrinogen. Cells seeded on fibrin tended to cluster with each other. At 18 hours, macrophages stimulated with fibrinogen exhibited most of their actin towards the periphery of the cells with dramatic filopodial extensions. Macrophages cultured on fibrin appeared to also have more extensions by 18 hours and were in some cases quite elongated and well spread. Interestingly, the cells cultured on fibrin and further stimulated with fibrinogen were very round, suggesting that fibrin inhibits filopodial extensions induced by fibrinogen observed on glass or, conversely, that fibrinogen inhibits the protrusions formed on fibrin gels. In all cases where cells were cultured on fibrin, phalloidin staining appeared to be more intense when compared to cells cultured on glass and stimulated with fibrinogen.

2.3.9 Fibrin Offers Protection from Inflammatory Activation by LPS and IFN-γ

Given that macrophages are also likely to be exposed to cytokines in the native wound healing environment, we also studied the combined effect of fibrin(ogen) and soluble stimuli known to activate inflammatory or anti-inflammatory pathways. Macrophages were cultured on fibrin gels or TCPS surfaces, stimulated with fibrinogen, with or without further stimulation with LPS and IFN-γ, IL-4 and L-13, or a combination of LPS with IL-4 and IL-13, and analyzed for TNF-α and IL-10 production levels at 36 hours after stimulation (Fig. 2.10).

As expected, macrophages seeded on TCPS surfaces and stimulated with LPS and IFN-γ or LPS with IL-4 and IL-13 had higher levels of TNF-α and IL-10 when compared to unstimulated cells, with the highest level of TNF-α observed with LPS and IFN-γ stimulation and highest level of IL-10 observed with LPS with IL-4 and IL-13 stimulation. Consistent with our previous

experiment, fibrinogen stimulated both TNF-α and IL-10 and, in this case, the levels of IL-10 were higher, most likely due to the increased number of cells seeded in this experiment. Interestingly, IL-10 secretion stimulated by fibrinogen was inhibited by the co-addition of LPS and IFN-γ, whereas TNF-α level was somewhat enhanced. Neither TNF-α nor IL-10 level was affected by the co-addition of IL-4 and IL-13 or LPS with IL-4 and IL-13. Most strikingly, all conditions in which macrophages were cultured on fibrin exhibited similarly high levels of IL-10 and low levels of TNF-α regardless of further stimulation. The abrogation of TNF-α secretion even in conditions containing LPS and IFN-γ suggests that fibrin is able to exert a protective effect on macrophage inflammatory activation.

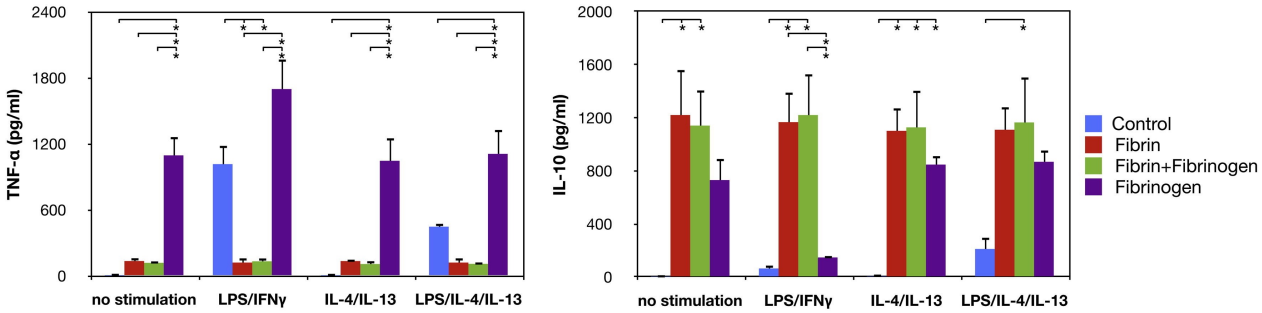

Figure 2.10 Effect of fibrinogen and fibrin on macrophage activation by LPS and cytokines. Graph of TNF-α (left) and IL-10 (right) secretion of macrophages seeded on TCPS surface or 2 mg/ml fibrin gels, with and without 2 mg/ml fibrinogen, and further stimulated with 1 ng/ml LPS/IFN-γ, 10 ng/ml IL-4/IL-13 or 1 ng/ml of LPS and 10 ng/ml IL-4/IL-13 (LPS/IL-4/IL-13). Values are mean ± SEM of n = 3 biological replicates; asterisk groups denote $p < 0.05$ by one way ANOVA followed by Tukey's HSD test for comparisons within each stimulation group.

2.3.10 Fibrin's Inhibitory Effect is not Hampered by the Presence of Endotoxins

In the midst of our studies, we became aware that there may be endotoxin contamination in fibrinogen because it has been reported that significant levels of endotoxin have been detected in a number of commercial-grade plasma and/or serum-derived proteins.[179] Endotoxins are part of the outer cell membrane of gram-negative bacteria—the lipid A component of endotoxin is mainly responsible for its biological activity.[180] Moreover, these contaminants are highly heat-stable,

requiring a temperature of over 180°C for inactivation.[180] Typically, endotoxins are measured in endotoxin units per milliliter (EU/ml) with 1 EU being approximately 0.1 to 0.2 ng of endotoxin per ml solution. The U.S. Food and Drug Administration (FDA) currently limits medical device eluates to have less than 0.5 EU/ml; if the device is to come in contact with cerebrospinal fluid, the limit is even lower, at less than 0.06 EU/ml.[181] We proceeded to test the fibrinogen utilized in this study along with those from other vendors with a limulus amoebocyte lysate (LAL) assay, a FDA accepted method for endotoxin detection and measurement (Table 2.2). In particular, we found that the fibrinogen used for this study contained approximately 50 EU/mg, as measured by ToxinSensor™ Chromogenic LAL Endotoxin Assay kit (Genescript).

Table 2.2. Endotoxin values of bovine fibrinogen from various vendors

Vendor	EU/ml	EU/mg	EU/mg reported by vendor
EMD (Calbiochem)	0.07	0.036	Not reported
MP Biomedicals	10.24	5.12	Not reported
RMBio	3.10	1.55	0.8 EU/mg
Sigma	50.0	25	Not reported

By utilizing the endotoxin inhibitor polymyxin B (PMB), we found that the previously reported effects were likely to be independent of the presence of endotoxin in the fibrinogen because no statistical differences were found when comparing with and without PMB using pairwise Student's t-test within each condition group (Fig. 2.11).

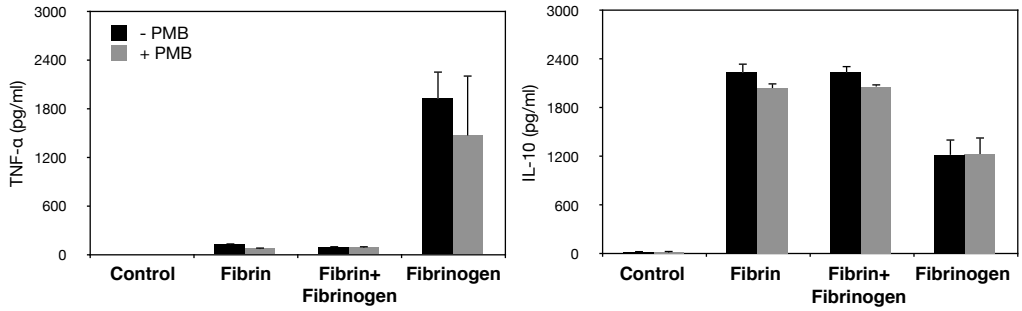

Figure 2.11 Effects of fibrin(ogen) are independent of endotoxin. Graph of TNF-α (left) and IL-10 (right) secretion by macrophages cultured on 2 mg/ml fibrin or TCPS and stimulated with 4 mg/ml soluble fibrinogen for 18 hours, with and without polymixin B (PMB). Values are mean ± SEM of n=3 biological replicates.

Next, we further proceeded to examine if fibrin's ability to inhibit TNF-α still held when using bovine fibrinogen from different vendors (Fig. 2.12). We were able to find that across the various vendors, culture of BMDMs on a fibrin matrix always lowered TNF-α secretion. However, in light of both the LAL assay and the TNF-α secretion results, we decided to switch over to bovine fibrinogen from EMD (Calbiochem) due to its low endotoxin content.

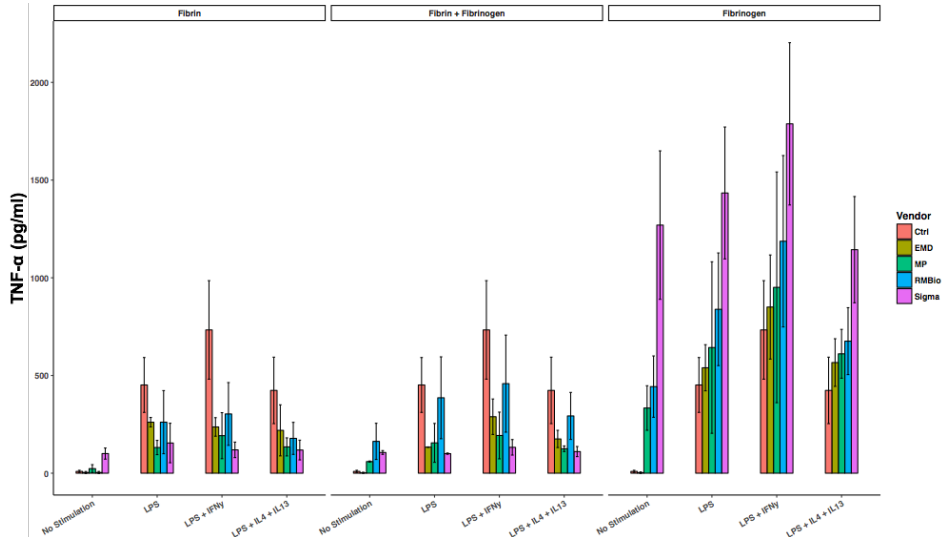

Figure 2.12 Effect of fibrin(ogen) from various vendors. Graph of TNF-α secretion of macrophages seeded of TCPS surface (Ctrl) or 2 mg/ml fibrin gels, with and without 2 mg/ml fibrinogen, and further stimulated with 1 ng/ml LPS/IFN-γ, 10 ng/ml IL-4/IL-13 or 1 ng/ml of LPS and 10 ng/ml IL-4/IL-13 (LPS/IL-4/IL-13). Values are mean ± SD of n = 2 biological replicates. Ctrl values are the same across the three groups. Day 7 or 8 BMDMs were used.

2.3.11 Fibrinogen's Ability to Elicit IL-10 Appears to be Influenced by Endotoxins

After the switch, we decided to further characterize the effect of endotoxins on IL-10 secretion. We fabricated fibrin gels using PBS++ with or without LPS spiked in. Three types of gels were fabricated: (1) gels that contained no additional LPS, (2) gels that contained 1.0 ng/ml of LPS, and (3) gels that contained 10 ng/ml of LPS. According to Genscript (manufacturer of the ToxinSensor™ kit), 1.0 ng/ml of LPS is equivalent to 10 EU/ml. Consequently, we chose to test

both 1.0 ng/ml of LPS and 100 ng/ml of LPS since Sigma bovine fibrinogen had an endotoxin of 50 EU/ml.

We found that IL-10 secretion was enhanced with increasing amounts of LPS regardless of the stimulation conditions. In fact, although the LPS was presumably embedded within the gel, its presence was sufficient to bring up the IL-10 secretion, even in the case of no stimulation. Moreover, when BMDMs were further stimulated by IL-4 and IL-13, the presence of LPS clearly induced IL-10 because very minimal secretion was observed in both the control TCPS or non-LPS-laden gel conditions.

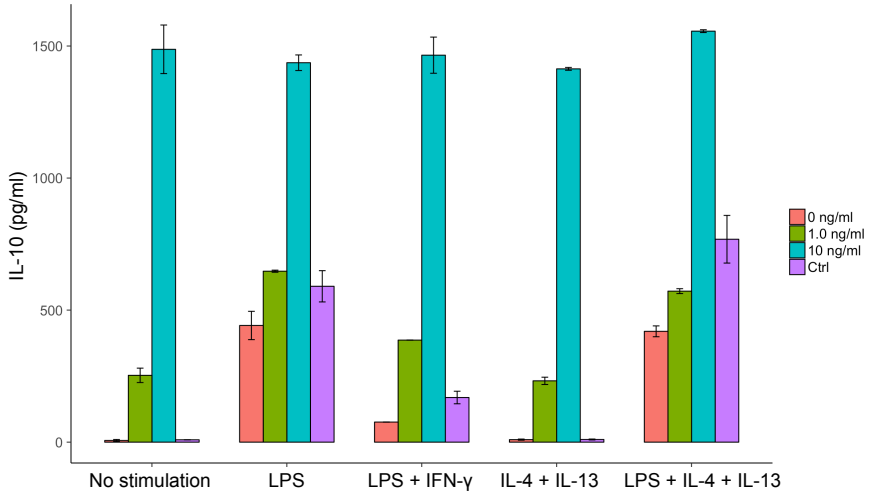

Figure 2.13 Effect of LPS-laden fibrin gels on IL-10 secretion. Graph of IL-10 secretion of macrophages seeded of TCPS surface (Ctrl) or 2 mg/ml fibrin gels containing indicated doses of LPS. Cells were further stimulated with 1 ng/ml LPS/IFN-γ, 10 ng/ml IL-4/IL-13 or 1 ng/ml of LPS and 10 ng/ml IL-4/IL-13 (LPS/IL-4/IL-13). Values are mean ± SD of n = 1 biological replicate (two technical replicates). Day 8 BMDMs were used.

2.4 Discussion

2.4.1 Discussion

Fibrin is the dominant extracellular matrix component during wound healing after tissue damage or injury. Yet, its effect on macrophage function has not been clearly elucidated. Here, we demonstrated that the addition of fibrin into collagen matrices reduced fibril size. Other groups

have done scanning electron microscopy work to reveal distinct matrix architectures as well—namely, pure fibrin matrices had smaller fibers and appeared to be more densely packed than pure collagen gels.[182] Additionally, we also demonstrated that thrombin alone has an effect on macrophage activation. Thrombin is a key enzyme in hemostasis and thus, it is not surprising that it can affect immune cell function and be involved in regulating inflammatory reactions. For example, it has been demonstrated that monocytes exposed to thrombin exhibit an enhanced expression of MCP-1.[183] However, it should be noted that the Sigma bovine thrombin used in the studies had an endotoxin content of about 9.2 EU/ml based on the LAL assay. Consequently, further examinations are required to understand how thrombin itself influences macrophage activation.

In addition, we have shown that culturing cells on pure fibrin gels or treating them with soluble fibrinogen revealed that the presentation of fibrin(ogen), either immobilized within a fibrin network or as a soluble molecule, modulates macrophage inflammatory versus anti-inflammatory function. Our results suggest that culture of macrophages on fibrin elicits a protective effect, preventing inflammatory activation by fibrinogen as well as LPS and IFN-γ, known inducers of classical macrophage activation. Many of the inflammatory cytokines that were released after treatment with fibrinogen, including TNF-α, IL-6, MCP-1, MIG, MIP-1α, MIP-1β, and RANTES were inhibited when macrophages were cultured on fibrin. Culture of macrophages on fibrin alone stimulated secretion of IL-10, G-CSF, and TGF-β1 and expression of Arg-1, which are all associated with inflammation resolution and tissue repair.[184]

Similarly, we observed that TNF-α secretion elicited by treatment with LPS and IFN-γ or LPS with IL-4 and IL-13 was also inhibited when macrophages were cultured on fibrin. Since fibrin

networks typically form at sites of tissue damage where inflammation is presumably high, it is possible that the matrix itself plays a key role in dampening local inflammation in order to promote the wound healing processes that follow. These data suggest that signals from the extracellular matrix may in fact be more potent than cytokines that are recognized as regulators of macrophage function—specifically, the mechanical role of the extracellular matrix will be further dissected in Chapter 3 of this dissertation.

Contrastingly, stimulating macrophages with fibrinogen led to inflammatory activation, as indicated by secretion of TNF-α and other inflammatory cytokines including IL-6, MCP-1, MIG, MIP-1α, MIP-1β, and RANTES, as well as expression of *Tnfa* and *Nos2* genes associated with inflammatory activation. Other research groups have suggested that fibrinogen is thought to activate macrophage inflammatory signaling primarily through its interactions with TLR4.[177] Interestingly, CD11b, an integrin mentioned previously that binds to fibrin(ogen), has been shown to negatively regulate TLR4 signaling—macrophages lacking CD11b have an enhanced response to LPS, a major TLR4 agonist.[185] Thus, it may be that CD11b engagement is different on fibrin versus that with fibrinogen.

There is evidence suggesting that the incorporation of fibrinogen into fibrin or adsorption of fibrinogen onto TCPS may expose otherwise cryptic CD11b-binding sites that enhance this inhibitory pathway.[186–188] In addition, adsorbed fibrinogen has been shown to inhibit TLR4 signaling through its interaction with CD11b.[134] Moreover, adsorption of fibrinogen or polymerization of the protein into fibrin may modulate its binding to TLR4 and/or CD11b. Supporting this idea, stimulation of macrophages with mechanically dissociated fibrin clots has been shown to elicit an inflammatory response.[189] Further work will be necessary to explore how

varying bimolecular and mechanical contexts regulate the differential binding interactions between macrophages and fibrin(ogen) and whether these changes in receptor binding modulate downstream pathways that regulate inflammatory versus anti-inflammatory signaling.

The switch between inflammatory and anti-inflammatory behavior through the presentation of a single molecule may suggest a simple yet potentially powerful approach to modulating macrophage function. Leveraging this strategy does however, require consideration about the effect of endotoxins. Although we have demonstrated that fibrin is able to inhibit an inflammatory assault despite the presence of endotoxins, it appears that we cannot fully discount the effect on endotoxins on IL-10 secretion. In particular, it has been suggested that murine BMDMs induce the expression of IL-10 after the activation of TLR4 by LPS. This is then followed by sequential induction of type I interferons (IFNs) and ultimately, signaling via interleukin-27 (IL-27).[190]

2.4.2 Concluding Remarks

Together, our results show that the presentation of a single molecule, either presented in the soluble form or tethered within an insoluble matrix, plays an important role in the regulation of macrophage phenotype. These findings contribute to our understanding of how the extracellular matrix regulates macrophages during wound healing and disease and offers a new strategy for designing biomaterials that can more precisely control the host response, minimize fibrosis, and promote proper tissue regeneration.

Chapter 3: Effect of Mechanical Properties of Fibrin(ogen) on Macrophage Function

3.1 Background

3.1.1 Matrix Rigidity as a Cue for Macrophage Activation

There are adhesive, physical, and mechanical cues that can regulate cellular behaviors. In a process known as mechanotransduction, cells sense mechanical signals via their cytoskeleton and membrane mechanosensitive proteins and convert them into biochemical signals, influencing their own proliferation, migration, differentiation, and activation, among others.[191] Macrophages are no exception—these cells have been shown to respond to physical cues such as substrate topography, applied forces like active stretching, or mechanical cues such as substrate stiffness.[11] In particular, matrix rigidity has been demonstrated to be important for adhesion and contractility, migration, and differentiation for many cell types.[192–194]

For macrophages, the effects of substrate stiffness have recently been explored. For murine macrophages, Nemir et al. tuned the moduli of poly(-ethylene glycol) diacrylate (PEGDA) hydrogels by varying polymer chain length and using photolithographic techniques—they demonstrated that RAW 264.7 macrophages preferentially adhered to the stiffer parts of the hydrogel but no further characterization was performed.[195] In another work by Blakney et al., poly(-ethylene glycol) or PEG hydrogels were modified with Arg-Gly-Asp (RGD) to examine the effect of substrate stiffness on macrophage phenotype. The group showed that without changing the amount of adhesive RGD ligands, the degree of classical activation was greater for BMDMs seeded on stiffer substrates when stimulated with LPS.[196] Moreover, *in vivo* results showed that subcutaneous implantation of stiff hydrogels in mice elicited more macrophages to the implant

surface after 28 days, further supporting the idea that hydrogels with lower stiffness may lead to reduced macrophage activation.[196] Meanwhile, Anselmo et al. also demonstrated that J774 murine macrophages uptook significantly less soft PEG-based nanoparticles (10 kPa) than hard nanoparticles (3000 kPa).[197] Finally, in Previtera et al., researchers also demonstrated that BMDMs cultured on soft polyacrylamide substrates produced less pro-inflammatory cytokines. Notably, the group suggested that the stiffness-regulated proinflammation was likely to be mediated by the TLR4 signaling pathway.[198]

For human macrophages, there has also been work investigating the role of substrate stiffness. First, Irwin et al. fabricated PEG-coated polyacrylamide gels ranging from 1.4 kPa to 378 kPa and demonstrated that human promonocytic THP-1 cells preferentially adhered to stiffer substrates. While the global amount of TNF-α secreted did not vary greatly across the different stiffness, interleukin-8 was shown to have a biphasic response—namely, the secretion profile was low on 1.4kPa and 348 kPa but high on 10 kPa.[199] Next, Okamto et al. employed agarose gels and found that M1-related marker expression and phagocytic activity of THP-1 cells was attenuated on a soft substrate (1%, 4%, or 10% agarose gels) compared to cells cultured a stiff substrate (TCP).[200] However, in another study where both activation of murine (RAW 264.7) and primary human alveolar macrophages were investigated on polyacrylamide gels with elastic moduli ranging from 0.3 kPa to 76.8 kPa, TNF-α secretion, in the presence of LPS stimulation, decreased with increasing substrate rigidity. Moreover, the researchers also found that for both cell types, phagocytosis of both non-opsonized or IgG opsonized latex beads was enhanced for cells cultured on softer substrates.[201]

Exploring the role of matrix rigidity is even more important in light of evidence that demonstrate that the response of macrophages to matrix rigidity can influence other cell types. Recently, He et al. demonstrated that although bone marrow-derived mesenchymal stem cells (BMMSCs) differentiated down the osteogenic lineage when cultured on high stiffness transglutaminase crosslinked gelatin gels, this was not the case when co-cultured with RAW 264.7 macrophages.[202] In fact, macrophages encapsulated in a low stiffness matrix actually exerted a positive effect on the osteogenesis of co-cultured BMMSCs.[202] In another study, Wu et al. cultured murine peritoneal macrophages on alginate gels of storage moduli 30 Pa (low), 100 Pa (medium), and 300 Pa (high) and found that when cultured alone, macrophage activation, measured by secretions of IL-6, IL-12p70, and IL-10 were most significant on the gel of medium stiffness. However, when cultured in the presence of 4T1 murine breast cancer cells, the expression of M1 type cytokines was increased significantly for cells cultured on gels of low stiffness. Thus, the influence of substrate rigidity on macrophage adhesion and activation still needs to be further explored and we intend to do so by using fibrin and collagen matrices as well as synthetic matrices to elucidate the effects.

3.1.2 Mechanical Properties of Fibrin and Collagen

3.1.2.1 Mechanical Properties of Fibrin and Collagen in Tissues

Mechanical properties of fibrous tissues can depend on both the organization and architecture of the fibers that make up the tissue as well as the strength of the fibers—fiber organization governs low strain response while fiber strength takes over in higher strain response until failure is reached.[143] In particular, fibrin matrices are generally known to be viscoelastic: fibrin's elastic component can be characterized by a stiffness or storage modulus while its inelastic

properties can be represented by a creep compliance or loss modulus.[203] Moreover, fibrin is known to display nonlinear elasticity and exhibit strain hardening, enabling fibrin clots to be stiffer at higher strains to prevent damage while still remaining compliant at lower strains.[204] Though creep can occur in fibrin over time, recovery of original stiffness is often observed after complete removal of the initial stress.[205]

Similarly, collagen matrices are also considered viscoelastic; in particular, these matrices are biphasic, containing both a solid phase represented by the collagen network and an interstitial fluid phase consisting mainly of water.[206] The water can be either tightly bound with the collagen molecules or "free" and bulk-like.[207] Collagen has elastic strength due to the tightly bound water; the water stabilizes the collagen structure by forming hydrogen bonds between the collagen molecules.[208] Moreover, the water molecules are free to move around, enabling collagen to deform yet retain viscoelastic responses.[208] Notably, though collagen can effectively resist shear and tension, it has little compressive strength.[209]

3.1.2.2 Natural Crosslinking of Fibrin by Transglutaminase Factor XIII

Thrombin, in addition to cleaving fibrinogen, also activates factor XIII (FXIII) to factor XIIIa (FXIIIa). FXIII is a protransglutaminase that is present in human plasma at a concentration of 14-29 μg/ml.[64] The latter, FXIIIa, is a transglutaminase responsible for introducing covalent bonds between the γ-γ, α-α, and α-γ chains of fibrin monomers.[210] In the presence of calcium, the tetrameric FXIII can dissociate to FXIIIa and induce crosslinking that can further stabilize fibrin clots, leading to fibrin's resistance to mechanical deformations.[211] Specifically, the crosslinking occurs between a ε-lysine (donor) and a γ-glutamine (acceptor) residue, resulting in intermolecular

ε(γ-glutamyl)lysyl bonds.[66,212] The resulting fibers, though still under debate, are able to arrange via either end-end longitudinal bonds or crossing transverse bonds.[213,214]

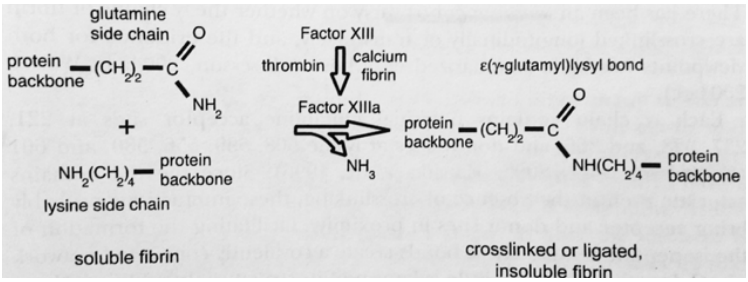

Figure 3.1 Formation of intermolecular ε(γ-glutamyl)lysyl bond catalyzed by factor XIIIa in the presence of calcium and fibrin. (Adapted from [57])

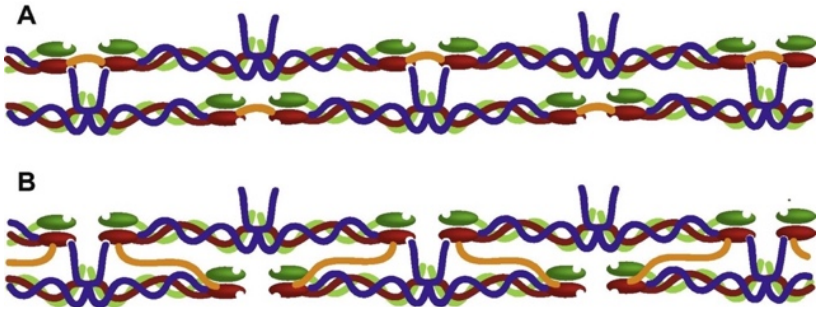

Figure 3.2 (A) Longitudinal or (B) Transverse factor XIII-mediated γ-γ crosslinks. Crosslinks are denoted in orange. (Adapted from [64])

Thus, unlike collagen gels, in which entangled fibers are held by weak hydrogen bonds, fibrin gels can be further crosslinked and hence, exhibit changes in its properties. First, it was observed that lateral bonds tightened between fibrin monomers within each fibrin fiber in a FXIII crosslinked gel, leading to slight decreases in overall fiber diameter.[144] This fiber compaction can influence pore sizes, which can in turn influence both the rates of molecular diffusion through the fibrin gel as well as fibrinolysis.[210] Second, these clots tend to have higher stiffness and a lower inelastic component of deformation compared to their non-crosslinked counterparts.[215] Crosslinked clots have been reported to exhibit five times greater mechanical stiffnesses compared to those of their non-crosslinked counterparts.[216,217]

3.1.2.3 Mechanical Properties of Reconstituted Fibrin and Collagen Matrices

In reconstituted collagen and fibrin matrices, the bulk mechanical properties are generally independent of fiber strength because the solid fraction of fibers is very low in these reconstituted gels.[143] Consequently, the matrix architecture—fiber density, organization, crosslink density—determines the pore size and porosity of the matrix, two properties that govern the ease of fluid movement into or out of these gels.[143] When the gels are subjected to shear or tension, the fiber network supports all of the load.[209] However, though the hydraulic conductivity enables these gels to deform, it also leads to weak resistance to compression. This is because compressive loads are borne by the fluid phase—once the fluid exits the gels, the fiber networks can collapse.[143,209]

3.1.3 Adsorption or Mechanical Tethering of Fibrinogen

The idea of adsorbing or tethering different ECM proteins onto biomaterials for tissue engineering or wound healing applications has been explored in recent years. In particular, for fibrinogen, researchers have adsorbed or conjugated the protein onto both natural and synthetic surfaces. For skin wounds, Venzin et al. demonstrated that a PEG-fibrinogen hydrogel is an attractive solution as a dressing matrix because it is biocompatible as well as resorbable and provides initial moisture to the wound bed on top of being biocompatible and resorbable.[218] For bone repair, Santos et al. showed that the incorporation of fibrinogen into chitosan scaffolds promoted new bone formation while stimulating angiogenesis in rats.[219] Moreover, the same group also demonstrated that PEG conjugated to fibrinogen facilitated healing of bone defects by inducing bone regeneration in rats with tibial defects.[220]

In this chapter, we explored the effects of altering mechanical stiffnesses using both natural and synthetic matrices. Here, we used fibrin as the natural matrix and introduced a variety of

biological and chemical agents to alter fibrin substrate rigidity. Moreover, we also investigated the mechanical effects of synthetic surfaces and document attempts to either adsorb or tether fibrinogen onto these surfaces of varying stiffnesses.

3.2 Materials & Methods

3.2.1 Differentiation on Collagen or Fibrin Matrices

Murine cells for differentiation experiments seeded on either collagen or fibrin were similarly isolated according to 2.2.1. 3D gels were formed onto standard 100 mm^2 Petri dishes. For the control conditions, after 7 days of culture on non-treated polystyrene Petri dishes, BMDMs were retrieved using cell dissociation buffer. Ultimately, BMDMs on collagen and fibrin matrices were retrieved after excision of the gels using a razor blade and extraction of cells utilizing a mortar and a pestle. Live cells were held on ice throughout the staining process.

3.2.1.1 Characterization by Flow Cytometry

First, cells were blocked with anti-CD16/32 antibody (clone 2.4G2, Tonbo Biosciences). Then, cells were then stained with anti-CD11b (clone M1/70, APC conjugate; BioLegend), anti-CD18 (clone M18/2, FITC conjugate; BioLegend), anti- F4/80 (clone BM8, PE conjugate; BioLegend), anti-CD14 (clone Sa14-2, APC or PerCP conjugate; BioLegend), and anti-CD284 (clone SA15-21, PE or PE-Cy7 conjugate; BioLegend). Isotype controls were stained with the corresponding isotype antibodies with the appropriate fluorophore conjugates: (1) Rat IgG2b, κ was used for CD11b while (2) Rat IgG2a, κ was used for CD18, F4/80, CD14, and CD284. Thorough washing was performed to remove excess, unbound antibodies.

Flow cytometry was performed on a BD LSRII flow cytometer using BD FACSDiva software (BD Biosciences). Post-processing was performed in FlowJo (Treestar) and further data

analysis and quantification was done in R. Cell populations were gated on forward and side scatter to select for intact, single cells. Acquisition was performed until at least 10,000 events were collected using a preliminary analysis gate or until the sample was exhausted. Statistical analysis was performed considering $p < 0.05$ to be statistically significant. Data were analyzed using an one-way ANOVA followed by Tukey's HSD post-hoc test.

3.2.2 Altering Mechanical Properties of Fibrin Gels with Biological Agents

3.2.2.1 Plasmin Degradation of Fibrin Gels

Fibrin gels at 2 mg/ml were fabricated according to 2.2.2 in 96 wells at 100 µl with the exception that gels were fabricated with water. The solvent was changed to water because there is evidence indicating that calcium can protect fibrin from degradation by plasmin.[221] After gels were fabricated, they were held for 3 hours or overnight in a humidified, 37°C incubator. Bovine plasmin (Roche), purchased at 5 U/ml, was diluted to varying units in water. 10 µl of plasmin was added directly to the fibrin gels and incubated at 37°C for 3 hours. Then, approximately 100,000 BMDMs/cm^2 were seeded directly onto the gels and stimulated at 6 hours post culture with 1.0 ng/ml of E. coli-derived LPS (Sigma-Aldrich) and 1.0 ng/ml of recombinant murine IFN-γ (R&D Systems). Supernatants were collected 12 hours later (culminating in 18 hours of total culture) and assessed for TNF-α secretion via ELISA (BioLegend).

3.2.2.2 Factor XIII Crosslinking of Fibrin Gels

100 µl fibrin gels were fabricated at 2 mg/ml according to 2.2.2 in 96 wells. After gels were fabricated, they were held for 3 hours in a humidified, 37°C incubator. Human FXIIIa (Enzyme Research Laboratories), purchased at 1.26 mg/ml with an activity of 2778 Loewy units/mg, was diluted 100 fold in PBS++. 80 µl of FXIIIa was added (in the presence of calcium ions) to crosslink

the gels, resulting in either 10 µg of FXIII per ml of fibrin or 22 Lowey units per ml of fibrin. This was selected based on literature that suggested up to 20 µg FXIII per millimeter of fibrin is appropriate; studies have also used units of FXIII in increments of 50 Lowey units per millimeter of fibrin. Crosslinking was performed for 6 hours; then, gels were washed once with 200 µl of PBS++ prior to BMDM seeding. Approximately 100,000 BMDMs/cm^2 were seeded directly onto the gels and stimulated at 6 hours post culture with 5.0 ng/ml of E. coli-derived UltraPure LPS (Invivogen) and 1.0 ng/ml of recombinant murine IFN-γ (R&D Systems). Downstream ELISA assessment was performed as described in 3.2.2.1.

3.2.2.3 Ancrod Polymerization of Fibrin Gels

Ancrod, a member of a subclass of snake venom thrombinlike enzymes (SVTLEs), was used to alter the mechanical properties of fibrin because ancrod selectively only cleaves fibrinopeptide A during polymerization (Fig. 3.3).[222] STA®-Reptilase® (Diagnostica Stago), purchased at 20 Batroxobin unit (BU), was reconstituted in 2 ml of distilled water. Gels were fabricated with either 0.4 U of thrombin or Reptilase. The resulting gels were held for 3 hours in a humidified, 37°C incubator prior to use for BMDM culture. Seeding and downstream methods were the same as those indicated in 3.2.2.1.

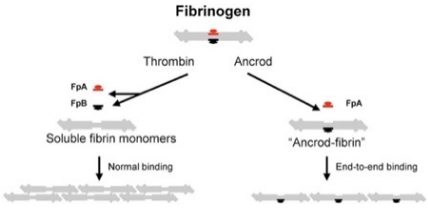

Figure 3.3 Schematic of fibrinogen molecule and its interactions with thrombin and ancrod. (Adapted from [222,223])

3.2.3 Bulk Rheology Using a Parallel Plate Rheometer

To determine bulk viscoelastic properties of the fibrin gels, bulk rheology was performed using a stress-controlled rheometer (Anton Paar MCR 301, Graz, Austria). The rheometer has a 25

mm parallel plate geometry and the Peltier temperature control system. Samples containing fibrinogen and thrombin were prepared as described in 2.2.2 at a volume of approximately 150 µl; samples were immediately loaded onto the rheometer upon fabrication. A solvent trap filled with water, PBS++, or D10 media was utilized to provide a humidified environment and prevent evaporation of liquid from the gel. Oscillatory measurements were performed at a strain of γ = 1% and frequency of f = 1 Hz with a gap height of 200 µm at 37°C. Storage (G') and loss (G'') moduli were recorded until G' showed no change over several hours.

3.2.4 Crosslinking Fibrin Gels with Chemical Agents

3.2.4.1 Glutaraldehyde Crosslinking of Fibrin Gels

100 µl fibrin gels were fabricated and held for 3 hours as described in 3.2.2.2 prior to incubation with glutaraldehyde. A homobifunctional crosslinker, glutaraldehyde, reacts to form polymers of pyridine in the presence of primary amines (Fig. 3.4).[224] Glutaraldehyde (Electron Microscopy Sciences) was purchased in 10 ml ampoule as 8% aqueous solutions. The stock solution was diluted to 1% in PBS. Gels were incubated for 5-10 minutes with 100 µl of the 1% solution after which gels were thoroughly washed with four times, each time with 200 µl of PBS with shaking. Seeding and downstream methods were the same as those indicated in 3.2.2.1. Images were taken with an EVOS XL Core Cell Imaging System (Thermo Fisher) with a 20X objective.

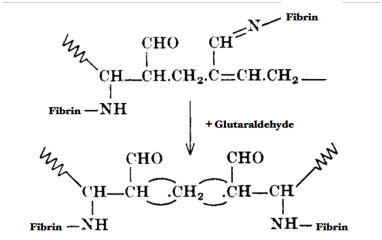

Figure 3.4 Schematic of crosslinking of primary amines by glutaraldehyde. (Adapted and modified from [225])

3.2.4.2 EDC Crosslinking of Fibrin Gels

Carboxyl groups are modified by EDC to create a o-acylisourea ester intermediate; in the presence of NHS, a NH_2-reactive intermediate that results ultimately enables conjugation of other biomolecules with a primary amine (Fig. 3.5).[226] 100 µl fibrin gels were fabricated and held for 30 minutes in a humidified, 37°C incubator. 1-Ethyl-3-(3-dimethylaminopropyl)carbodiimide (EDC) was used in combination with *N*-hydroxysuccinimide (NHS) to bind NH_2 to COOH groups. Gels were incubated with 50 µl of 4mM EDC (Sigma) reconstituted in 2-(N-morpholino)ethanesulfonic acid (MES) buffer (Sigma) for 5-10 minutes. Then, 50 µl of 10mM NHS (Sigma) in MES buffer was introduced. After 30 more minutes, the solutions were removed and the gels were washed twice with MES buffer for 15 minutes each wash. Seeding and downstream methods were the same as those indicated in 3.2.2.1. Images were also acquired with the EVOS system.

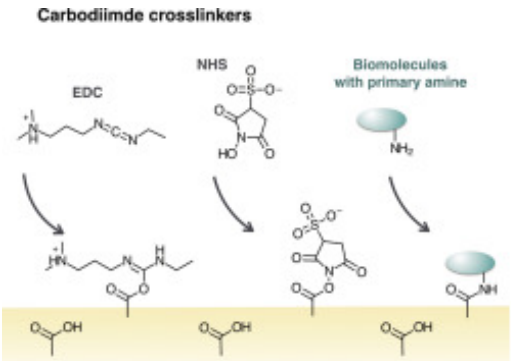

Figure 3.5 Covalent conjugation of biomolecules using EDC. (Adapted from [225])

3.2.5 Adsorption of Fibrinogen

Fibrinogen (EMD Millipore) solutions were prepared at varying concentrations (3-200 µg/ml) in a 0.05M Tris buffer, with 0.1 mM NaCl and 2.5 mM $CaCl_2$ at pH 7.4.[227] TCPS was incubated with 100 µl of fibrinogen solution at varying concentrations overnight at 4°C. Non-adsorbed fibrinogen was removed with 2 subsequent Tris buffer washes at 15 minutes each. Experiments using biotinylated fibrinogen confirmed adsorption of fibrinogen onto TCPS.

Seeding of BMDMs as well as downstream stimulation and ELISA assessment were the same as those indicated in 3.2.2.1. Statistical analysis was performed using Student's t-test.

3.2.6 Tethering of Fibrinogen onto Synthetic Matrices

3.2.6.1 Modulating Substrate Rigidity with Polyacrylamide Gels

18 mm diameter No. 1 glass coverslips were cleaned in 100% ethanol, dried, and UVO treated for 10 minutes. Coverslips were then incubated with bind-silane solution (95% of 100% ethanol, 0.3% of 3-(trimethoxysilyl) propylmethacrylate, and 5% of 10% acetic acid) for 5 minutes at room temperature (RT). Excess bind-silane solution was washed off with ethanol; coverslips were baked in the oven at 70°C for 1 hour to allow chemical reactions to occur. Meanwhile, glass slides were placed into dishes, covered with salinization solution (Sigma), and incubated for 5 minutes at RT in a vacuum desiccator. The hydrophobic slides were rinsed with water. For polyacrylamide gels, 1 kPa and 40 kPa gels were prepared according to specified proportions of 40% acrylamide (Sigma), 2% bis-acrylamide (Sigma), and PBS (Table 3.1). 1 ml samples in 1.5 ml Epi-tubes were degassed to remove dissolved oxygen prior to the addition of TEMED and APS.

Table 3.1. Volumes needed to make 1 ml of polyacrylamide gel [228]

Stiffness	***Acrylamide***	***Bis-acrylamide***	***PBS***	***TEMED***	***APS***
1 kPa	125 µl	15 µl	860 µl	1 µl	10 µl
40 kPa	200 µl	240 µl	560 µl	1 µl	10 µl

Approximately 35 µl of the polymerizing solution was pipetted onto the silanated glass slides. Then, coverslips were placed on top of the gels. Gels were allowed to polymerize for 30 minutes at RT. Coverslips were removed and immersed, gel side up, in PBS and stored overnight at 4°C in 12 well plates. 50 mM HEPES buffer solution was used to wash the gels prior to use. Gels were covered with 500 µl of 50 µM sulfo-SANPAH (50 mM HEPES, DMSO, sulfo-SANPAH) and subjected to UV light for 15 minutes. Thorough washing was performed with HEPES buffer.

Varying concentrations of fibrinogen (Sigma) solution were diluted in HEPES buffer. Gels were incubated at 4°C with the fibrinogen solutions and gels were thoroughly washed the next day with PBS. BMDMs were seeded at 45,000 cells/cm^2 and supernatants were collected 18 hours later and assessed for TNF-α.

3.2.6.2 Altering Substrate Rigidity with Polydimethylsiloxane (PDMS)

PDMS elastomer and curing agent (SYLGARD® 184 silicone elastomer kit, Sigma) were manually mixed in a 10 (base):1 (curing agent), 40:1, or 80:1 ratio by weight. Mixtures were degassed for 30 minutes to 2 hours. Then, 100 µl of each mixture was pipetted into 96 wells; the 96 well plate containing gels was baked for 2 hours at 65°C. The plate was removed and gels were cooled overnight at RT. Gels were ethanol washed once for sterilization and further washed three times with PBS to remove residual ethanol. After drying, gels were either used directly for seeding or adsorbed with varying concentrations of fibrinogen using the Tris buffer mentioned in 3.2.5 or PBS. If adsorbed with fibrinogen, gels were washed for with PBS to remove non-adsorbed fibrinogen. BMDMs were seeded and downstream analysis was performed according to 3.2.2.2.

3.2.6.3 Conjugation of Fibrinogen onto Poly(-ethylene glycol) Diacryalte (PEGDA)

In the early experiments, a mixture of 10% or 5% PEGDA (MW 3,400, Glycosan) was combined with 0.1% curing agent (Irgacure 2959, BASF), sterile filtered, and polymerized by UV irradiation for 10 minutes at room temperature. BMDMs were seeded and downstream analysis was performed according to 3.2.2.2. In another round of experiments, 5% or 10% PEGDA gels with varying molecular weights (MW 4,000, Polysciences; MW 10,000, Sigma) were separately fabricated with either 0.025% or 1% curing agent. Again, BMDMs were also seeded and downstream analysis was performed. Finally, in experiments attempting to conjugate fibrinogen,

PEGDA and acrylate-PEG-NHS (MW 3,400 or MW 10,000 Creative PEGWorks) were combined 100:1 and polymerized by UV irradiation to form 10% PEG-NHS linker surfaces. Resulting gels were incubated with either 0.5 or 50 μg/ml of fibrinogen in PBS at RT for 1 hour. Gels were washed three times with PBS to remove unbound fibrinogen. Seeding of BMDMs and downstream analysis were similarly performed as those previously mentioned.

3.2.7 Flow Cytometry for Cells Cultured on PDMS of Varying Stiffnesses

PDMS surfaces were fabricated according to 3.2.6.2 except in standard 100 mm^2 Petri dishes. Murine cells for differentiation experiments seeded on PDMS were also similarly isolated according to 2.2.1. BMDMs on all conditions were retrieved using cell dissociation buffer and cell scrapers. Downstream flow cytometry methods and processing were detailed previously in 3.2.1.1.

3.3 Results

3.3.1 Differentiation on Collagen or Fibrin Matrices Leads to Lowered CD11b and CD14

In Chapter 2, we focused on analyzing the inflammatory behavior of mature macrophages on fibrin. Here, we detail how fibrin can impact macrophage differentiation. We performed flow cytometry to examine integrin and surface receptor expression of murine bone marrow cells differentiated on type I collagen, fibrin, or non-treated Polystyrene Petri dishes. We examined CD11b, CD18, CD14, CD284 (TLR4), and F4/80. CD14 is commonly described as a marker for macrophage differentiation; however, it can play a critical role as a receptor for LPS.[229] On the cell surface, CD14 associates with TLR4. Binding of LPS and a plasma protein known as LPS-binding protein (LBP) induces downstream TLR4 signaling, resulting in the release of proinflammatory chemokines and cytokines.[230]

We found that differentiation of BMDMs on ECM matrices, regardless of fibrin or collagen, generally lowered expression of both integrins and surface receptors (Fig. 3.2). Interestingly, although we examined integrin or receptor pairs—CD11b/CD18 as well as CD14/CD284, their surface expression on macrophages did not match completely. First, culture on collagen or fibrin demonstrated almost a two-fold reduction in CD11b expression ($p \leq 0.001$) whereas CD18 expression saw only around a 25% decrease. Second, whereas differentiation on collagen or fibrin resulted in around 80% or more decrease for CD14 ($p \leq 2.2e^{-6}$), the ECM matrices had a more moderate effect on CD284, which only saw around a 50% reduction. Interestingly, F4/80 expression was actually enhanced on the ECM matrices. These results demonstrated that the adhesive substrate not only has an effect on downstream macrophage function but also macrophage differentiation.

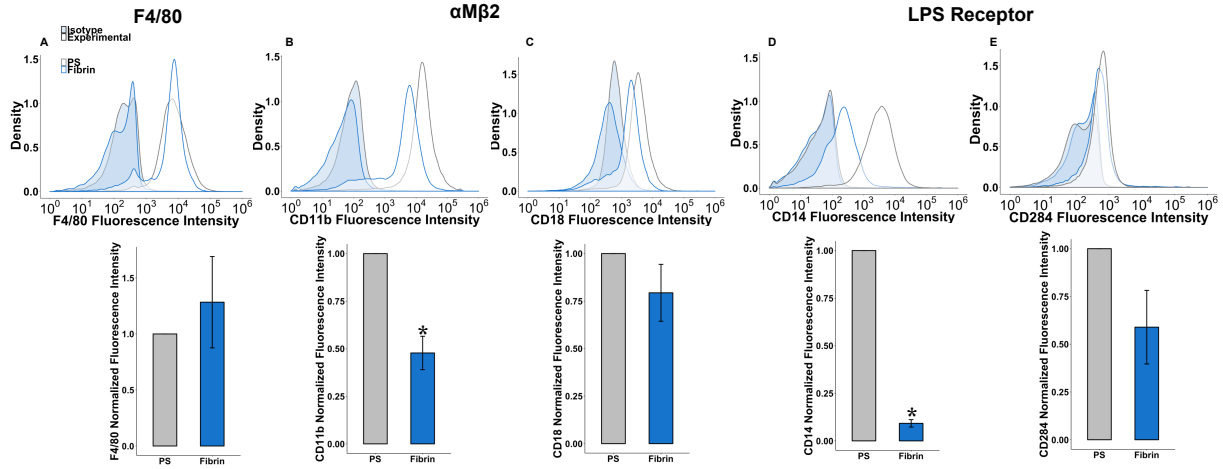

Figure 3.6 Differentiation of BMDMs on ECM matrices leads to lower integrin and surface receptor expression. Representative flow cytometry histograms with isotype controls indicated using shaded curves and average fluorescence intensity normalized to non-treated polystyrene bar plots are shown for F4/80, CD11b/CD18, and CD14/CD284. Normalized values were averaged across seven experiments except for F4/80, which was averaged across 3 normalized experiments. Asterisk indicates $p < 0.05$ compared to cells cultured on non-treated Polystyrene using one-way ANOVA followed by Tukey's post-hoc test.

3.3.2 *Plasmin Degradation Influences Fibrin's Ability to Inhibit Activation*

After seeing that culture of BMDMS on both collagen and fibrin matrices lower the integrin or surface receptor expression on BMDMs, we wondered if this observation could be related to substrate stiffness. We consequently explored the use of biological agents to alter the matrix rigidity of fibrin—the first biological agent was bovine plasmin. Prior to using the enzyme to degrade the gels, we first verified that it alone did not elicit a response from BMDMs (it would not be feasible to wash plasmin out post gel degradation). Unlike thrombin, plasmin adsorbed or spiked in solution did not elicit TNF-α secretion from the BMDMs. Thus, we proceeded to use plasmin to modulate the mechanical stiffness of fibrin and culture BMDMs in its presence.

We found that plasmin degradation only had moderate effects on impacting fibrin's ability to inhibit TNF-α secretion. After incubating gels with plasmin of varying units for 3 hours at 37°C, we could macroscopically observe disintegration of the gels, especially with the higher dosage at 0.005 units. Gels treated with 0.001 unit of plasmin was still able to similarly lower TNF-α secretion as that observed on the non-treated gel. We did observe a slight increase for the 0.005 unit plasmin treated gel (Fig. 3.7).

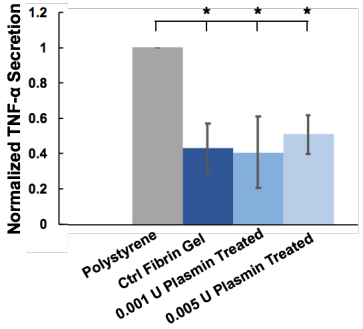

Figure 3.7 Plasmin moderately effects fibrin's ability to modulate inflammation. Graph of normalized TNF-α secretion by macrophages cultured on non-treated or plasmin-treated 2 mg/ml fibrin gels or TCPS. BMDMs were further stimulated with LPS and IFN-γ at 6 hours post seeding and cultured for a total of 18 hours. Values are mean ± SEM of n=3 biological replicates. Asterisk indicates $p < 0.05$ compared with TCPS using Student's T-test followed by false discovery rate correction for multiple comparisons.

3.3.3 *FXIII Crosslinking Elicits More TNF-α Secretion than No Crosslinking*

Unlike plasmin, the biological crosslinker of fibrin, FXIII, had an impact on fibrin's ability to inhibit inflammatory activation. After treating fibrin gels for 6 hours at 37°C followed by subsequent seeding of BMDMs, we observed that BMDMs cultured on FXIII and further stimulated with LPS and IFN-γ still secreted TNF-α abundantly (Fig. 3.8). Although the non-treated gel secreted more TNF-α than usual (relative to the PS ctrl), this experiment supports the idea that substrate rigidity may play a role in influencing macrophage phenotype behavior.

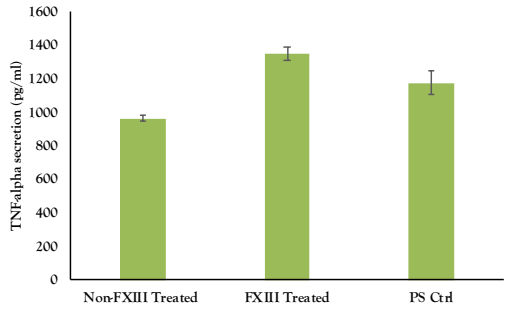

Figure 3.8 FXIII crosslinking undermines fibrin's ability to inhibit inflammation. Graph of TNF-α secretion by macrophages cultured on non-treated and FXIII-treated 2 mg/ml fibrin gels or TCPS. BMDMs were further stimulated with LPS and IFN-γ at 6 hours post seeding and cultured for a total of 18 hours. Values are mean ± SD of n=1 (two technical replicates).

3.3.4 *Ancrod Polymerization does not Impact Fibrin's Protective Effect*

Similar to degradation by plasmin, polymerization of fibrin gels with Reptilase did not alter the response of BMDMs. Although according to literature, ancrod polymerized gels can be as much as five times softer in stiffness, this potential change in rigidity did not seem to influence the TNF-α secretion greatly (Fig. 3.9). When the secretions were normalized to the polystyrene control, we saw that thrombin polymerized gels had around a 50% reduction in TNF-α level. Similarly, a decrease in TNF-α, also around 50%, was observed with the Reptilase polymerized fibrin gels. Although the error bar was slightly larger, overall, the data suggest that ancrod polymerized gels, with presumably softer stiffnesses, do not alter the behavior of activated macrophages.

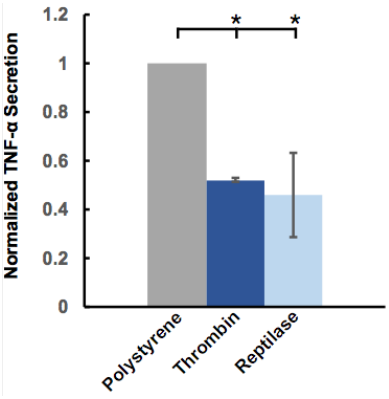

Figure 3.9 Ancrod polymerization for altering fibrin gel mechanics did not influence fibrin's ability to exert a protective effect. Plot of normalized TNF-α secretion by BMDM cultured on thrombin or Reptilase polymerized fibrin gels or TCPS. Error bars depict SEM of n = 2, and asterisks denote $p < 0.05$ by Student's T-test compared to polystyrene control.

3.3.5 *Ancrod Gels are Mechanically Softer than Thrombin Gels*

Since we were interested in examining the effects of substrate rigidity on BMDM activation and function, we decided to perform bulk rheology to get a sense of the stiffness range that we were experimenting with. Unfortunately, we could not perform parallel plate rheometry on neither plasmin degraded nor FXIII crosslinked gels since *in situ* gelation is required—lifting the parallel plate head to further degrade or crosslink a gel was not feasible.

Here, prior to comparing thrombin and ancrod polymerized gels, we did several runs of thrombin polymerized gels to obtain baseline storage modulus values. We demonstrated that over the course of 3 hours, G' moduli stabilize for thrombin polymerized gels (Fig. 3.10). Initially, samples show a more viscous than elastic behavior at the onset of polymerization—G'' (loss modulus) is greater than G' (data not shown). However, while G'' values continue to remain below 10 Pa, over time, the gels become more solid-like and G' eventually increases such that G' becomes greater than G''. The data demonstrates that the gels begin to exhibit stabilization of storage modulus values at around t = 140 minutes. Moreover, G' values plateaued near 100 Pa, resulting in an averaged value of 102.07 ± 16.26 Pa by the end of the 180 minutes monitoring period.

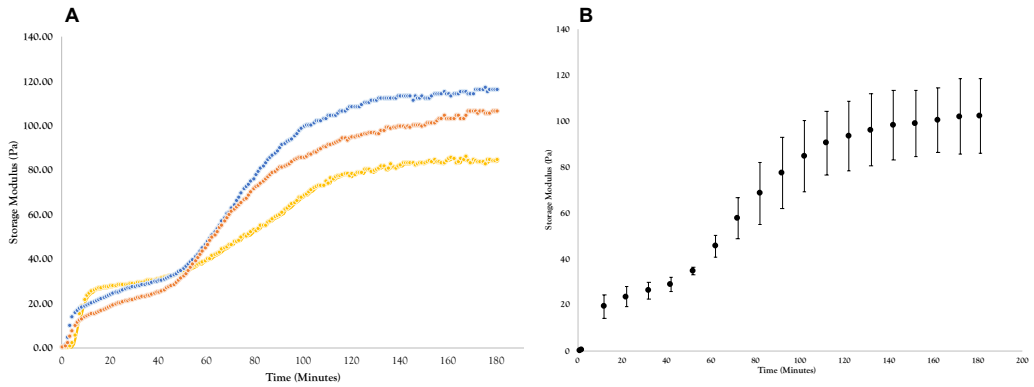

Figure 3.10 Thrombin polymerized gels have storage modulus values around 100 Pa. (A) Representative oscillatory shear measurements of storage (elastic) moduli. Each curve is an individual thrombin polymerized fibrin gel monitored over the course of 3 hours, starting from in situ gelation at 37°C at t = 0 minutes. (B) Averaged storage moduli values. Error bars indicate standard deviation (n = 3).

Then, we proceeded to verify if the ancrod polymerized gels were indeed softer by bulk rheology. Bulk rheology demonstrated that Reptilase polymerized gels did actually exhibit lower storage modulus values (Fig. 3.11). On average, G' values for Reptilase gels hovered between 20-30 Pa. Using the values shown in Fig. 3.10, we can see that thrombin polymerized gels can be anywhere from 3 to 5 times stiffer than ancrod polymerized gels. Interestingly, despite this difference in stiffnesses, TNF-α secretion levels remained similar between these two types of gels as shown in 3.3.4. It may be that the stiffness difference range we are operating in may be too narrow to detect a difference in macrophage inflammatory activation.

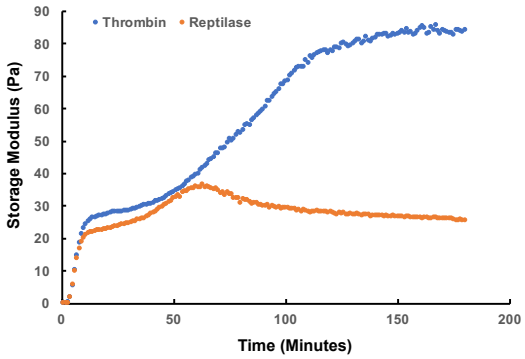

Figure 3.11 Ancrod polymerized gels have lower storage moduli than those of thrombin polymerized gels. Representative oscillatory shear measurements of storage (elastic) moduli made of either thrombin or ancrod polymerized fibrin gels over the course of 3 hours, starting from in situ gelation at 37°C at t = 0 minutes.

3.3.6 *Glutaraldehyde Crosslinking is Cytotoxic*

After examining the use of biological agents to alter the mechanical properties of fibrin, we proceeded to explore chemical agents. First, we utilized glutaraldehyde, a fairly inexpensive reagent that is one of the most extensively used crosslinking agent to fix collagenous tissues in the clinic.[231] Glutaraldehyde has been utilized to crosslink collagen although it is known that glutaraldehyde elicits cytotoxicity and often causes calcification in treated collagen.[232] We found that glutaraldehyde treated gels resulted in very low TNF-α secretion by BMDMs (Fig. 3.12A). However, 20X phase contrast images demonstrated that the cells were not spread at 6 hours post seeding (the time of LPS and IFN-γ stimulation). In fact, BMDMs were very round (Fig.12B); it can be assumed based on morphology that the cells were most likely dead. Thus, despite copious amounts of washing, it seems that the cytotoxicity induced by glutaraldehyde impairs our ability to accurately assess whether or not crosslinking by glutaraldehyde and subsequent changes in matrix stiffness has an effect on BMDM activation and behavior.

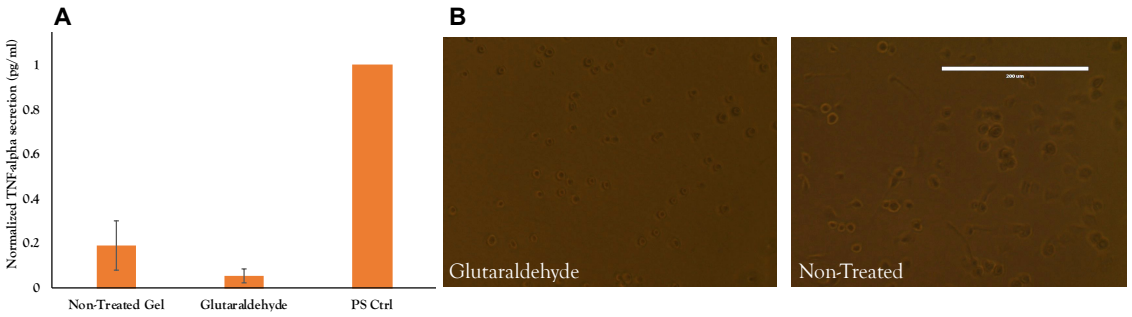

Figure 3.12 Glutaraldehyde crosslinking is cytotoxic. (A) Plot of normalized TNF-α secretion by BMDM cultured on non-treated or glutaraldehyde treated fibrin gels or TCPS. Error bars depict SD of n = 3 biological replicates. No statistics was performed. (B) 20X phase contrast images of BMDMs at 6 hours post seeding on glutaraldehyde treated vs. non-treated gels. Scale bar is 200 μm.

3.3.7 *EDC-NHS Crosslinking Induces Clumping of BMDMs*

Aside from glutaraldehyde, we also explored the use of heterobifunctional carbodiimides, more specifically 1-ethyl-3-(3-dimethylaminopropyl) carbodiimide hydrochloride, also known as

EDC. The benefit of using EDC is that it is a zero-length crosslinker, meaning that it does not become incorporated in the target molecule, thereby decreasing potential cytotoxic effects.[233] We found BMDMs secreted less TNF-α on EDC-NHS treated cells—it should be noted that the MES buffer alone did not alter the inhibitory effects of fibrin. However, one concerning observation was that the BMDMs were bunched up in clusters on the EDC-NHS treated gels. It has been previously suggested that rounded morphology observed in BMDMs results in reduced macrophage inflammatory activation.[163,234] Gels crosslinked by biological agents did not induce a clustering effect, supporting the idea that it is unlikely that this clumping observed with BMDMs on EDC-NHS treated gels should be attributed to increased substrate rigidity.

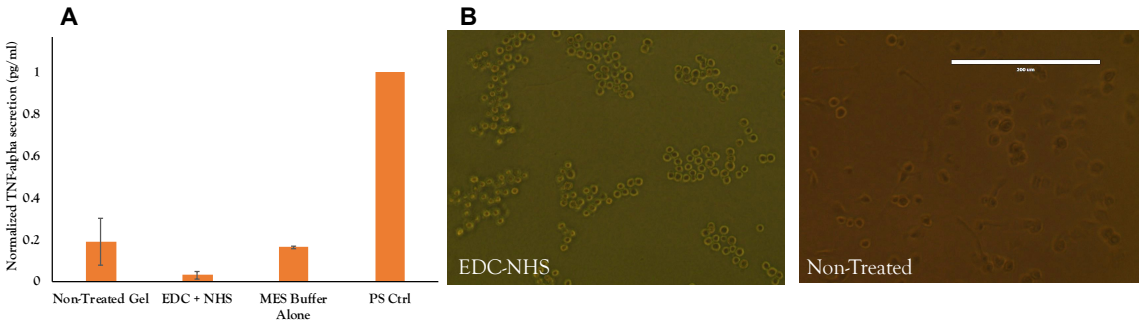

Figure 3.13 EDC-NHS crosslinking induces clumping of BMDMs. (A) Plot of normalized TNF-α secretion by BMDM cultured on non-treated, EDC-NHS treated, or MES alone treated fibrin gels or TCPS. Error bars depict SD of n = 3 biological replicates. No statistics was performed. (B) 20X phase contrast images of BMDMs at 6 hours post seeding on EDC-NHS treated vs. non-treated gels. Scale bar is 200 μm.

3.3.8 *Adsorbed Fibrinogen on TCPS Reduces Inflammatory Cytokine Secretion*

Besides attempting to change the mechanical properties of fibrin gels, we also investigated how to modulate the mechanical properties of fibrinogen by tethering it to surfaces via adsorption or conjugation. Before exploring tethering of the protein onto surfaces of varying stiffnesses, we first did a baseline experiment to see if adsorbed fibrinogen on TCPS had any effect on macrophage activation and function. We did in fact verify that fibrinogen was adsorbed onto TCPS by using biotinylated fibrinogen (data not shown). The limiting factor of this technique was

that the detection and quantification of biotinylated fibrinogen using avidin-HRP of was limited to adsorption concentrations below 3 pg/ml.

Here, we found that BMDMs cultured on TCPS adsorbed with fibrinogen lowered TNF-α secretion by approximately 25% when compared to uncoated TCPS controls (Fig. 3.14B). Regardless of the fibrinogen concentrations in the range of 3-200 μg/ml, we found that the presence of adsorbed fibrinogen reduced the BMDM inflammatory activation in response to LPS and IFN-γ. In particular, the TNF-α level of BMDMs cultured on TCPS with 12.5 μg/ml of fibrinogen adsorbed is statistically significant from the level expressed by cells cultured on bare TCPS. There does not seem to be a fibrinogen dose dependent response.

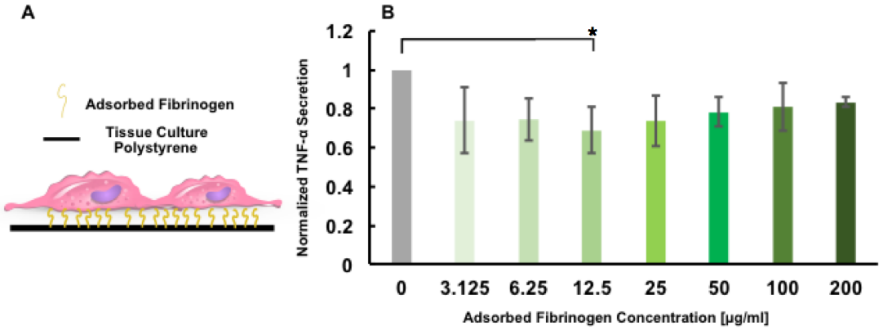

Figure 3.14 Adsorbed fibrinogen lowers TNF-α secretion (A) Schematic for experimental set-up. (B) Plot of normalized TNF-α secretions by macrophages cultured on TCPS with or without adsorbed fibrinogen. Error bars depict SEM of n = 3, and asterisks denote $p < 0.05$ by Student's T-test.

3.3.9 *Tuning Stiffness of Polyacrylamide Gels Does Not Alter Macrophage Behavior*

To investigate the effect of mechanical tethering onto substrates of varying stiffnesses, we first functionalized fibrinogen onto mechanically tunable polyacrylamide substrates. Polyacrylamide gels are materials that have been widely used with many cell types to determine how cells respond to the physical characteristics of their microenvironment.[235] We tuned the stiffness of the polyacrylamide gels by varying the amount of bis-acrylamide cross-linker and total acrylamide monomers (Table 3.1) and fabricated 1 kPa and 40 kPa gels. According to Engler et al.,

tissue elasticity can range from 1kPa for the brain, 4 kPa for adipose tissue, 10kPa for muscle, 30kPa for osteoid, and 100kPa for collagenous bone.[194,236]

The BMDMs, not further stimulated by LPS or cytokines, secreted very minimal TNF-α (Fig. 3.15). In fact, regardless of either substrate stiffness (1kPa or 40 kPa) or the amount of fibrinogen conjugated, the BMDMs behaved similarly overall. However, it should be kept in mind that at the time of this experiment, fibrinogen containing high levels of endotoxin (Sigma) was still being used. Thus, despite eliciting strong inflammatory responses when presented as a soluble protein, it is interesting that minimal activation is observed when this particular fibrinogen is conjugated onto a surface.

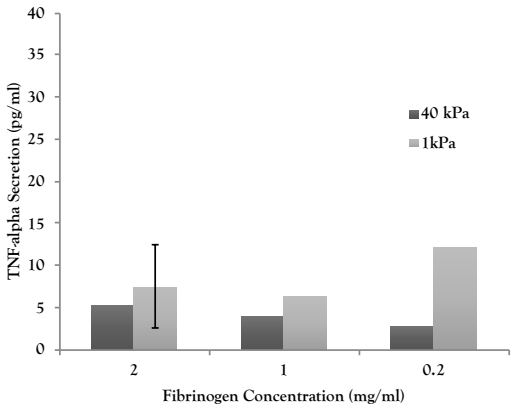

Figure 3.15 Conjugating fibrinogen on polyacrylamide gels of different stiffnesses have minimal effect on macrophage activation. Plot of TNF-α secretions by macrophages cultured on polyacrylamide gels with indicated stiffnesses with or without conjugated fibrinogen of denoted concentrations. Error bars depict SD of 2 technical replicates.

3.3.10 *Effects of Adsorbed Fibrinogen may be Dependent on Substrate Mechanics*

Apart from polyacrylamide, we also utilized PDMS to fabricate synthetic substrates with varying mechanical rigidities. In particular, we examined PDMS surfaces with the following PDMS elastomer to curing agent ratios: (1) 10 to 1, (2) 40 to 1, (3) 80 to 1. These PDMS surfaces have reported values of around (1) 50 kPa based on tensile testing, (2) 128 kPa based on micro-indentation, and (3) 4 kPa based on micro-indentation respectively.[237,238] Despite these values, the

10 to 1 PDMS surface is stiffer than either 40 to 1 or 80 to 1 PDMS surfaces. Although different methods for measuring elasticity exist and are presented in literature, it is generally accepted that the higher elastomer to curing agent ratio, the softer the PDMS substrate.

We found that regardless of the presence of adsorbed fibrinogen, there was a trend associated with substrate rigidity alone (Fig. 3.16B). On surfaces where no fibrinogen was adsorbed, we demonstrated that TNF-α was highest on the 10:1 PDMS substrate and moderate on the two softer substrates. When fibrinogen was adsorbed onto PDMS, although it is apparent that stiffness still influences macrophage inflammatory cytokine secretion, it also appears that there is an effect with regard to fibrinogen concentration. When the adsorption concentration is low at 0.5 μg/ml, TNF-α decreases with decreasing stiffness. However, when the concentration of fibrinogen increases toward 50 μg/ml, there is a biphasic response—the lowest amount of TNF-α is actually observed on the PDMS substrate with the intermediate stiffness.

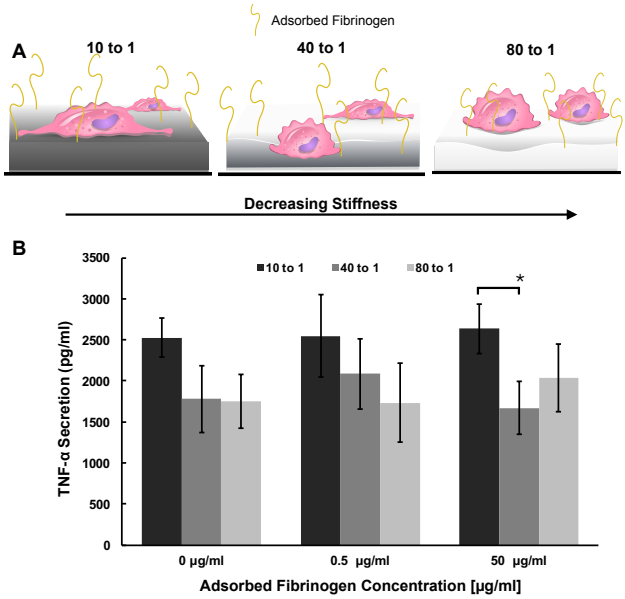

Figure 3.16 Effects of adsorbed fibrinogen is dependent on substrate mechanics. (A) Schematic for experimental set-ups. Numbers indicate PDMS elastomer to curing agent ratios. (B) Plot of TNF-α secretions by macrophages cultured on PDMS surfaces of varying stiffnesses with or without adsorbed fibrinogen. Error bars depict SEM of n = 3, and asterisks denote $p < 0.05$ by Student's T-test

In particular, we further explored varying the amount of adsorbed fibrinogen on the 10 to 1 PDMS surfaces. Compared to the polystyrene control, the levels of TNF-α secreted was inversely proportional to the amount of fibrinogen, at least up to 50 μg/ml. The reduction of TNF-α went from about 25% for 1.5 μg/ml to about 50% for 50 μg/ml. Interestingly, TNF-α went up slightly at 200 μg/ml of adsorbed fibrinogen (Fig. 3.17) In conclusion, between a range from 1.5 μg/ml to 200 μg/ml, we did find that at least for the 10 to 1 substrates, TNF-α secretion inhibition appeared to be maximal at 50 μg/ml.

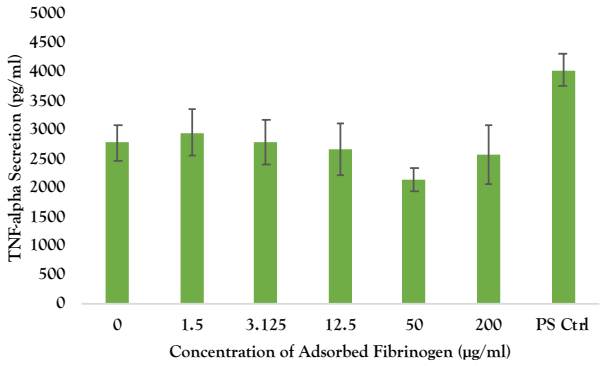

Figure 3.17 Adsorbed fibrinogen on PDMS lowers TNF-α secretion. Plot of TNF-α secretions by macrophages cultured on a 10:1 PDMS surfaces with varying concentrations of adsorbed fibrinogen. Error bars depict SD of n = 2 biological replicates.

3.3.11 *Poly(-ethylene glycol) diacrylate (PEGDA) gels Alone Influence Macrophage Activation*

The last synthetic substrate we tried was poly(-ethylene glycol) diacrylate (PEGDA). PEGDA is a desirable synthetic polymer because it is non-toxic, mechanically tunable, and biocompatible (generates minimal immunogenic response).[239] We first examined if PEGDA gels alone had an effect on macrophage activation—we utilized 3.4 kDa PEGDA and varied the ratio of PEGDA to PBS (5% vs 10% w/v). The results suggested that the culture on PEGDA gels alone are sufficient to bring down TNF-α levels (Fig. 3.18). Although inhibition was observed on both 5% or 10% PEGDA gels, it is interesting that TNF-α secretion was higher on the 10% PEGDA gels.

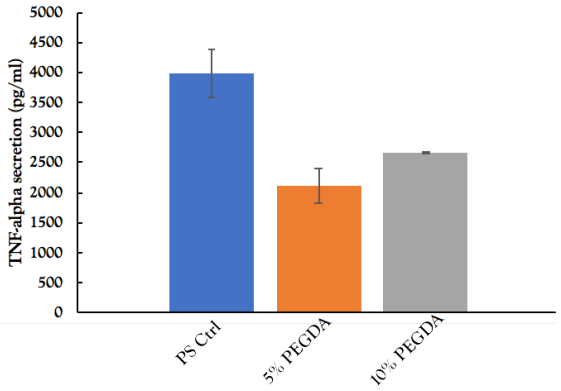

Figure 3.18 PEGDA gels alone lowers TNF-α secretion. Plot of TNF-α secretions by macrophages cultured on TCPS or PEGDA gels with indicated w/v ratios. Error bars depict SD of n = 1 biological replicate.

Next, we examined altering the molecular weight of the PEGDA while maintaining the PEGDA to PBS ratio at 10% w/v. We found that increasing molecular weight decreased TNF-α levels (Fig. 3.19). This is not surprising because in literature, there is a general consensus that as the molecular weight increases, the stiffness of the PDMS substrate decreases albeit mesh size of the gel increases.[240] Compared to 3,000 pg/ml of secreted TNF-α on TCPS, we found that TNF-α decreased to around 1,000 pg/ml for 2 kDa PEGDA surfaces. On 10 kDa PEGDA surfaces, this value went down even more, averaging to be around 200 pg/ml.

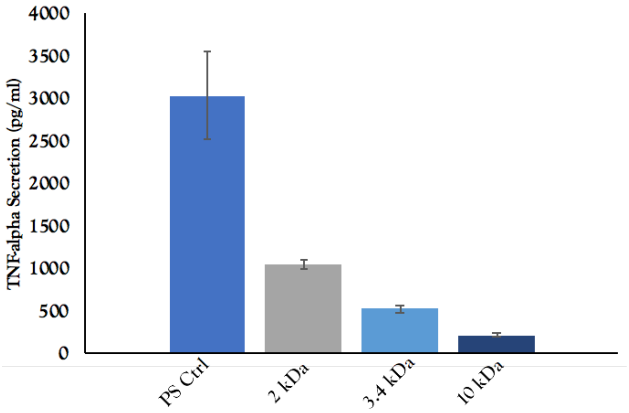

Figure 3.19 Molecular weight of PEGDA modulates TNF-α secretion. Plot of TNF-α secretions to TCPS on PEGDA gels with indicated molecular weights. Error bars depict SD of n = 1 biological replicate.

We proceeded to conjugate fibrinogen onto the PEGDA substrates—PEG by itself is resistant to protein adsorption and thus we utilized acrylate-PEG-NHS linkers to achieve this.[241]

This experiment was repeated four times—only one experiment demonstrated that conjugating fibrinogen, specifically to the 10 kDA PDMS substrate using a 10 kDA acrylate-PEG-NHS linker demonstrated very strong inhibition of TNF-α secretion (Fig. 3.20). From this one successful experiment, it would appear that regardless of the amount of fibrinogen, using a longer linker—that is, tethering a fibrinogen molecule more loosely—decreases TNF-α. However, it is concerning that with the exception of the 10 kDA substrate and 10 kDA linker combination, none of the other PEGDA surfaces demonstrated a decrease in TNF-α secretion. Moreover, the linkers could also be embedded within the gels; we cannot be sure how the linkers are being oriented and presented to both fibrinogen and BMDMs.

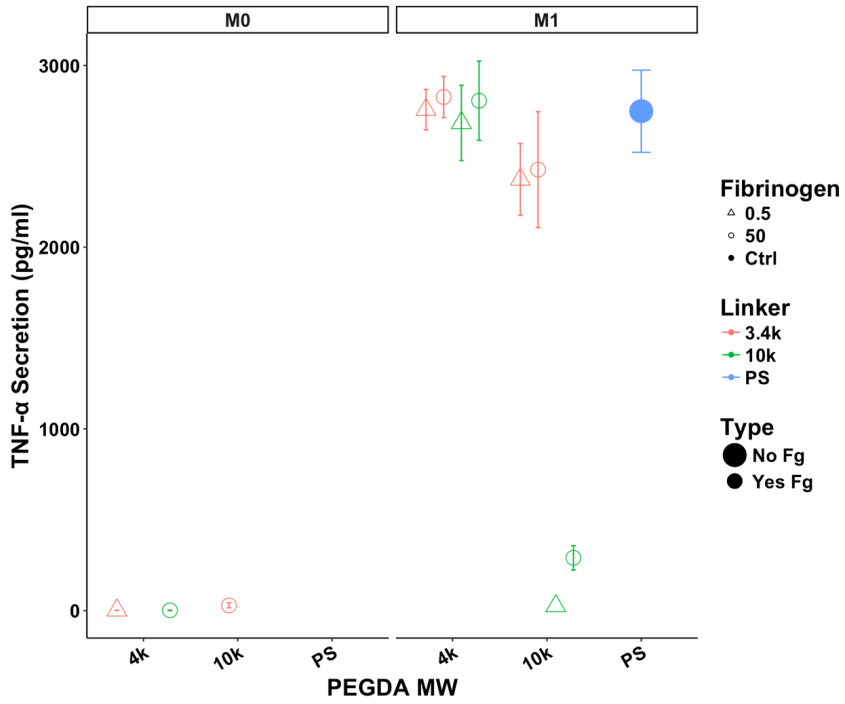

Figure 3.20 Molecular weight of acrylate-PEG-NHS linkers influences TNF-α secretion. Plot of TNF-α secretions to TCPS on PEGDA gels with indicated molecular weights. Error bars depict SD of n = 1 biological replicate.

3.3.12 *Differentiation on Soft PDMS Leads to Decreased CD11b and F4/80*

Finally, we revisited the differentiation experiments discussed in 3.3.1 to examine the effects of matrix rigidity on integrin and cell surface receptor expression. We found that overall,

the softer PDMS substrate, with the 40 to 1 elastomer to curing agent ratio, lowered expression (Fig. 3.21). Almost all examined receptors, with the exception of CD284, demonstrated a 25% reduction. Unlike what was observed on the ECM matrices, we did find that both the integrin and receptor pair, CD11b/CD18 and CD14/CD284 respectively, were all down-regulated in expression. Notably, the differences in CD11b and F4/80 expression were significant between the 10 to 1 and 40 to 1 PDMS surfaces. Together, the data suggests that signals from the matrix may in fact be more potent than cytokines that are recognized as regulators of macrophage integrin expression since these BMDMs were not further activated by cytokines.

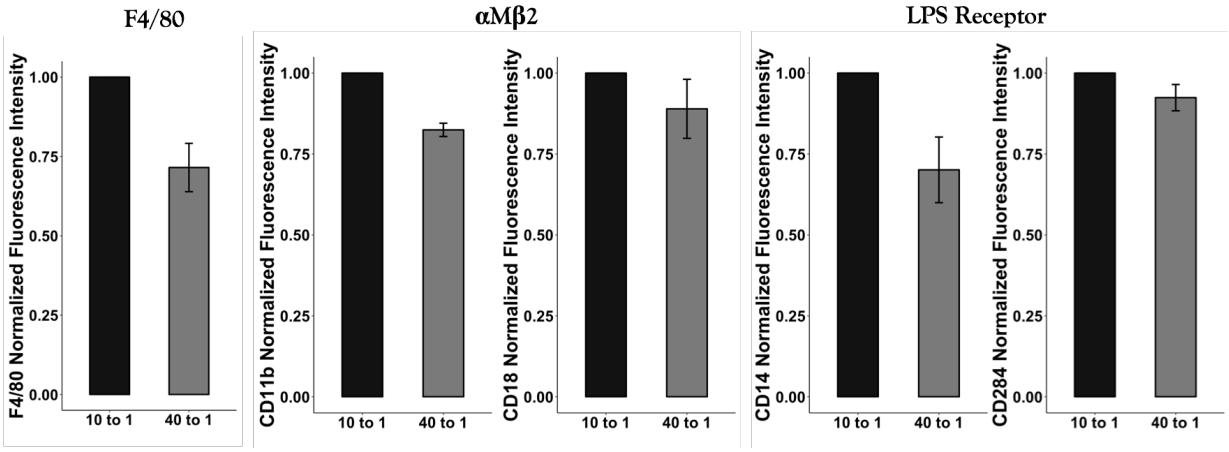

Figure 3.21 Integrin or surface receptor expression is influenced by matrix elasticity. Normalized average fluorescence intensity normalized to 10 to 1 PDMS substrates across three experiments. F4/80, CD11b/CD18, and CD14/CD284 were examined. Statistics were performed using Student's T-test with $p < 0.05$.

3.4 Discussion

3.4.1 Discussion

Differentiation of BMDMs has typically been performed on non-treated Polystyrene Petri dishes. It is well established that a polystyrene Petri dish has a stiffness around 1 GPa, which is six orders of magnitude greater than 1 kPa.[242] We have demonstrated that substrate stiffness can indeed have an effect on macrophage differentiation, in particular with respect to integrin

expression. On both natural and synthetic matrices, CD11b expression decreased on softer substrates. Although there is not a lot of literature suggesting that CD11b is mechanically activated, it is worth noting that CD11b expression is enhanced with increasing stiffness. Interestingly, it is curious that F4/80 is up-regulated on soft collagen and fibrin gels but down-regulated on the softer 40 to 1 PDMS substrates. It may be because the ECM matrices provide native ligands to differentiating monocytes, facilitating their transition to macrophages.

In terms of altering the stiffness of fibrin gels utilizing biological agents—plasmin, FXIII, and ancrod—we have shown that overall, softening fibrin gels does not appear to have much of an influence on fibrin's inhibitory effect. We observed that TNF-α secretion was enhanced on a FXIII crosslinked fibrin gel when compared to the level exhibited on a non-crosslinked fibrin gel. However, it is important to note some of the limitations of using these biological agents to alter fibrin gel mechanical properties. First, using plasmin to soften fibrin gels results in FDPs. We did not further characterize the fibrin gels post plasmin treatment; consequently, the presence of FDPs could have convoluted our results. Moreover, the effects of the solvent on plasmin activity should be considered because it has been previously reported that ions such as calcium can protect degradation of, for example, fragment D.[221]

Second, since bovine fibrinogen is a lyophilized serum protein, it may be possible that there is residual FXIII. In Smith et al., the group characterized commercial human fibrinogen from four different vendors (Calbiochem, Enzyme Research Laboratories, Haematologic Technologies, Sigma-Aldrich).[243] They found that fibrinogen from commercial sources is highly contaminated with FXIII antigen and is capable of crosslinking activity—in fact, only the control (labeled as FXIII-free) from America Diagnostica Inc exhibited very low FXIII content and activity.[243] Consequently,

it was recommended that fibrinogen should be affinity purified via an ammonium sulfate precipitation method or a calcium ion-dependent monoclonal antibody affinity column method.[244,245]

Third, for ancrod polymerized fibrin gels, the structure can again be influenced by ionic strength and/or the presence of calcium ions.[154,246] In addition, the lack of a cleaved fibrinopeptide B should also be considered. It has been postulated that fibrinopeptide B may help enhance contact site orientation for enzymes such as FXIII and plasmin.[247] Moreover, it has been suggested that the physiological relevance of fibrinopeptide B is that it not only helps to stabilize the assembled fibrin matrix but also prevents phagocytic clearance of the fibrin matrix in order to localize deposition.[248]

On the contrary, with the chemical agents, it is apparent that the reagents themselves may have an effect on macrophage viability. First, it has been noted that despite improving tensile strength and pliability to scaffolds, glutaraldehyde induces both toxicity and calcification, limiting their use for scaffolds that may come in contact with cells or used for long-term implantations.[249] Detoxifying strategies such as pretreatment with citric acid or amino acid solutions to remove free aldehyde groups have been suggested.[250] Similarly, EDC has also been noted for its inability to inhibit calcification, thereby limiting its use for crosslinking scaffolds meant for tissue engineering applications.[251] However, EDC has advantages because it leaves low residual toxicity. Furthermore, EDC-crosslinked ECM matrices have been shown to resist enzymatic degradation *in vitro*. [252]

For the synthetic surfaces, there are also certain limitations that should be discussed. First, although polyacrylamide gels have been widely used to examine the effects of substrate rigidity on cell behavior, tuning the ratio of acrylamide monomer and bis-acrylamide crosslinker can also lead

to changes in porosity.[236] Altering the porosity can change the distance between tethering points—consequently and lead to differences in volume and mass swelling ratios.[236] Second, with PDMS substrates, we observed that the culture media did not spread as much on the softer surfaces—this may suggest altering the elastomer to curing agent ratio can also lead to changes in hydrophobicity or surface tension. Moreover, since the fibrinogen was only adsorbed to the surface, this may lead to potential differences in remodeling—other groups suggest rectifying this by conjugating the desired protein using sulfo-SANPAH.[236] Adsorption can also lead to fibrinogen displacement by other plasma proteins and depends on numerous factors such as temperature, surface chemistry, etc. [253] Last, although PEGDA gels are promising for use as tunable scaffolds, PEG-based hydrogels are generally non-degradable and this may be a limitation in its use in tissue engineering applications.[241]

3.4.2 Concluding Remarks

The data presented here, using both natural and synthetic matrices, indicate that substrate rigidity has an effect on macrophage differentiation, activation, and function. More work needs to be done on investigating the tethering of fibrinogen onto synthetic surfaces via adsorption or conjugation. Notably, the data suggest that utilizing biological agents to soften (as opposed to stiffen) fibrin gels does not appear to have much impact on macrophage activation and behavior. Consequently, we will continue exploring the stiffening of fibrin gels and introduce a light-based crosslinking technique in Chapter 4 and discuss its effects on macrophage function.

Chapter 4: Photo-induced Matrix Crosslinking Controls Macrophage Adhesion, Migration, and Inflammatory Activation

4.1 Background

4.1.1 Ruthenium-based Photo-crosslinking

Fibrin has been the subject of chemical cross-linking research—aside from glutaraldehyde and bifunctional carbodiimide, researchers have also used genipin (a plant-derived crosslinking agent) and UV light.[254–256] However, these techniques have their limitations. First, in the previous chapter, we have demonstrated that the use of glutaraldehyde or carbodiimide is not ideal. Second, although genipin has been demonstrated to exhibit relatively low cytotoxicity, it is an expensive reagent. Last, polymerization by UV light has been demonstrated to also have cytotoxic effects on cells.[257] Thus, in this chapter, we turned to a method first proposed by Fancy and Kodadek in 1999 that utilizes a type of protein cross-linking reaction that uses a photogenerated oxidant to mediate rapid and efficient cross-linking to stiffen our fibrin constructs.[258]

Although Fancy and Kodadek proposed this method, Elvin et al. was the first to extend this technique to fibrinogen.[259,260] This particular crosslinking reaction utilizes ruthenium II trisbipyridyl chloride [RuII(bpy3)]2+ and sodium persulfate (SPS). In the presence of SPS, the ruthenium metal complex is activated by blue light, resulting in a reactive tyrosine radical as well as a sulfate radical—the intermediate radicals can react with another tyrosine phenyl group to form a covalent dityrosine bond (Fig. 4.1).[258] Fibrinogen is rich in tyrosine—β-chain = 4.9% tyrosine, γ-chain = 5.6% tyrosine, and α-chain = 0.65% tyrosine—requiring no further modification for this technique to work.[259] While Elvin et al. utilized this strategy to make fibrin into a mechanically stronger surgical tissue sealant, the Tranquillo group used this method to engineer fibrin-based

tissues.[257,261] In particular, Bjork et al. reported that this nontoxic ruthenium-based crosslinking chemistry increased stiffness by around ten-fold as well as enhanced mechanical strength by three-fold.[257] Most importantly, it has been demonstrated by both Elvin et al. and Syedain et al. that minimal cell death occurs after this type of crosslinking.[259,261]

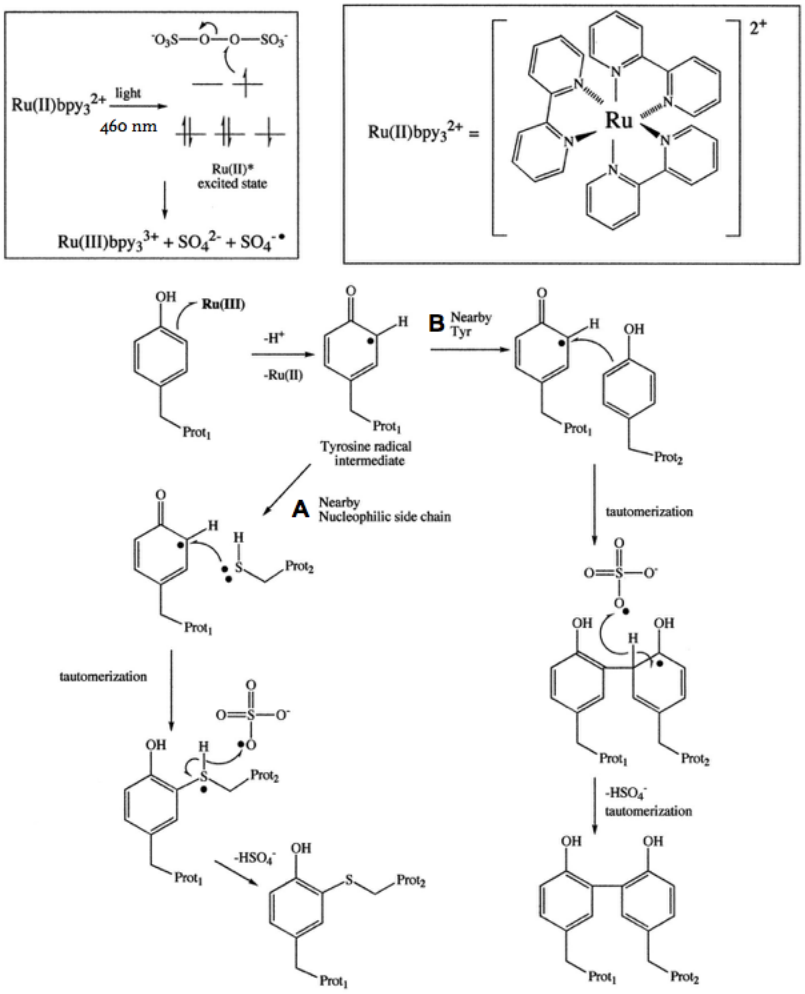

Figure 4.1 Mechanism of ruthenium-based photo-crosslinking. (A) A nearby nucleophilic lysine or cysteine could attack the Ru(III) radical to provide a heteroatom-arene linkage (B) Ru(III) oxidant finds another tyrosine residue nearby and arene coupling occurs. (Adapted and modified from [258])

4.1.2 Microrheology

Material properties can be quantified on the bulk-scale or the micro-scale. In particular, microrheology—a technique that involves embedding probe particles in the desired medium and

monitoring their motion in time—can be utilized to determine micro-scale mechanical properties.[262] Microrheology, if done properly with probes that are sized equally or slightly greater than the pore size of the mesh to avoid Brownian motion, is sensitive to the micro-scaled spatial heterogeneities that are inherent within natural ECM matrices such as fibrin or collagen.[262]

For a viscoelastic gel like fibrin, two techniques exist: (1) passive microrheology (PMR) and (2) active microrheology (AMR).[262] PMR correlates thermal fluctuations of freely diffusing particles to the rheological properties of the surrounding material.[263] This technique is cost-friendly because it just requires tracking probe motion via video or laser.[262] However, this technique is not ideal for ECM systems because PMR measurements are limited to soft gels on the order of a few pascals.[264] Furthermore, PMR underestimates the viscoelastic properties of the ECM if the ECM is not in thermodynamic equilibrium.[265] On the contrary, laser optical tweezers-based AMR does not depend on the equilibrium conditions of the measured medium.[265] Although more expensive to set-up, the AMR technique is advantageous because it can measure materials with stiffnesses up to 1 kPa and is less sensitive to external noise.[262,265]

In particular, optical tweezers-based AMR forces oscillations of microbeads confined within the fibrin gel and determines the beads' positions with a detection laser (Fig. 4.2).[266] Transparent beads are forced to oscillate under the influence of a single-beam gradient radiation pressure laser trap; the local matrix helps to resist the microsphere's movements.[262,267] By determining the amplitude and the phase of the sphere's oscillation, the complex shear modulus, G*, can be calculated for the matrix: G* is comprised of a real component G' or the bulk modulus and an imaginary component G'' or the loss modulus.[262,266]

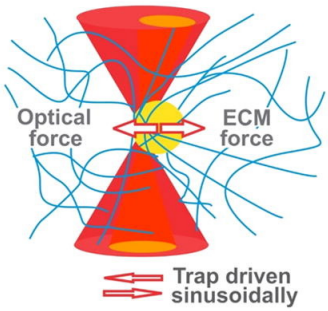

Figure 4.2 Schematic of optical tweezers-based active microrheology (AMR). Microbeam (red) is spatially oscillated to exert forces on a microbead (yellow). Forces are resisted by the ECM (blue). Detection beams (orange) are utilized to compute the complex shear modulus G*. (Adapted from [266])

4.1.3 Macrophage motility & migration

Both transendothelial and interstitial motility are essential for macrophages to move to specific sites upon demand and carry out a variety of roles in immune surveillance and normal tissue development.[268] Monocytes/macrophages do play a role for extravasation and homing to sites of injury. In particular, macrophages can respond rapidly to wound or inflammatory signals and migrate over considerable distances. Compared to fibroblasts and epithelial cells, which have been characterized to move around 0.1 to 0.5 μm per minute, macrophages have been demonstrated to be faster, moving anywhere from 1 μm to 10 μm per minute.[268,269] Yet, when compared to other immune cells, macrophages are slower since neutrophils and lymphocytes can move at speeds up to 25 to 30 μm per minute.[269,270] Notably, with their intermediate migration speed, macrophages are actually capable of both mesenchymal interstitial as well as amoeboid migration—they can actively digest through denser surroundings or propel themselves through loose matrices respectively.[271,272]

Moreover, macrophage migration has been demonstrated to play roles in inflammation and disease progression. For example, it has been shown that macrophages can not only migrate to the sites of injury but can also move to lymph nodes at the resolution of inflammation.[273] With

respect to diseases, macrophages have been implicated to play a role in cancer, atherosclerosis, and arthritis. Wyckoff et al. demonstrated in two different publications that tumor cell intravasation occurs in conjunction with perivascular macrophages in mammary tumors, even in the absence of angiogenesis.[274,275] Moreover, matrix remodeling was observed by tumor-associated macrophages, indicating that macrophages can digest through extracellular matrix during migration.[276] In atherosclerosis, lipid laden macrophages that have very low motility can attribute to necrobiosis in the fatty core of atherosclerotic lesions.[277] In terms of migration studies observing cell-ECM interactions, Hind et al. assessed the random migration of unstimulated macrophages on 2D surfaces as a function of fibronectin density as well as the exerted forces and motility patterns of activated macrophages.[278,279] In this chapter, we extended these studies by examining different migratory behaviors of non-activated macrophages on non-crosslinked or crosslinked fibrin as well as glass surfaces.

4.1.4 CD11b/CD18 Mediated Migration

Integrins play an integral role during macrophage migration. It has been shown that α4β1 and α5β1 integrins play a role in helping macrophage efflux to the lymph nodes—blocking these integrins actually prevents macrophage clearance.[280] This is also the case with αMβ2 or CD11b/CD18; this integrin pair has been shown to play a role in migration for a variety of cell types. Cao et al. found that genetic inactivation of αMβ2 in mice inhibited macrophage efflux from the peritoneal mesothelium to the lymphatics while Shang et al. demonstrated that human monocytes relied on CD11b/CD18 along with other integrins to make their way through the endothelium and connective tissues.[281,282] Moreover, Forsyth et al. showed that αMβ2 facilitates HEK cell migration in the presence of fibrinogen and fibrin.[283] Gao et al. found that

CD11b/CD18 mediates neutrophil migration through synovial and dermal fibroblast barriers.[284] Next, Kavanaugh et al. demonstrated that CD11b/CD18 helped T cells adhere and perform transendothelial migration.[285] Finally, Jia et al. showed that CD11b/CD18 is involved in eotaxin-induced eosinophil transendothelial migration.[286] Thus, these studies suggest that integrins not only transduce or respond to signals but also enable cells to mechanically adhere to their substrates or move to different sites.

In Chapter 2, we found that the culture of BMDMs on a fibrin matrix abrogated inflammatory activation of macrophages even in the presence of LPS and/or IFN-γ.[287] In this chapter, we sought to further elucidate the role of a fibrin matrix by altering its mechanical properties via photo-crosslinking. We investigated the effects of enhancing substrate rigidity of fibrin and observed that non-crosslinked and crosslinked fibrin matrices elicit distinct macrophage responses in terms of morphology, integrin expression, migration, and inflammatory migration.

4.2 Materials & Methods

4.2.1 Ruthenium-based Photo-crosslinking

Fibrin gels were fabricated at 2.0 mg/ml using bovine fibrinogen. 0.4 U of bovine plasma thrombin was used per mg of protein. Gels were held in a humidified, 37°C incubator for 30 minutes prior to the addition of the crosslinker at ambient temperature. The crosslinker solution was composed of 1.5 mg/ml ruthenium II trisbipyridyl chloride and 2.4 mg/ml sodium persulfate (SPS) solution.[257] The active crosslinking components were the dissociated ions of ruthenium and persulfate. Gels were incubated for 10 minutes with the crosslinker prior to the exposure to visible light at wavelengths 465-470 nm using an in-house fabricated LED light apparatus for 20 seconds. Immediately post exposure, the crosslinking solution was removed. Gels were consequently washed

four times with PBS at 37°C on a shaker and then left in PBS overnight for a fifth wash. "Crosslinker only" controls were gels that were incubated with crosslinker solution but never exposed to visible light prior to removal of the crosslinking solution.

4.2.2 Active Microrheology (AMR)

2 mg/ml fibrin gels were polymerized as described in 4.2.1 but with the addition of microbeads that were 2 μm in diameter. 8 μl of beads were added to unpolymerized fibrinogen to make a 1 ml solution prior to mixing with thrombin. We utilized reflection confocal microscopy mentioned in 2.2.3 to confirm that the beads were confined within the fibrin gels. We also utilized the technique to visualize network structure and fiber architecture. The one exception is that instead of using a 488 nm laser, a 559 nm laser was utilized since crosslinked gels were optically more orange than non-crosslinked gels. This work was done in collaboration with Mark T. Keating in Dr. Elliot Botvinick's laboratory.

Around 30 microbeads were chosen at random for active AMR at a depth of 35 μm into the fabricated fibrin gel. The trapping microbeam that oscillated microbeads, steered by a pair of galvanometer mirrors (Thorlabs) was generated by a continuous-wave fiber laser with emission at 1064 nm (IPG Photonics). A low power laser diode with emission at 785 nm (World Star Technologies) served as the detection beam. Sinusoidal oscillations with an amplitude of 100 nm at a frequency of 50 Hz were utilized. G' and G'' were computed from the amplitude-phase response of each microbead relative to the laser. Statistical analysis was performed using a Mann-Whitney Test with $p < 0.05$ followed by Bonferroni correction.

4.2.3 Enzyme-linked immunosorbent assay

Day 6 to 8 BMDMs were seeded at 100,000 cells/cm^2 on TCPS, non-crosslinked, crosslinker only control, or crosslinked fibrin gels. Macrophages were stimulated at 6 hours post seeding with a combination of 5.0 ng/ml of E. coli-derived UltraPure LPS (Invivogen) with 1.0 ng/ml of recombinant murine IFN-γ (R&D Systems). Supernatants of BMDMs cultured on these surfaces were collected at 12 hours after stimulation. Tumor necrosis factor alpha (TNF-α), interleukin-6 (IL-6), and monocyte chemoattract protein-1 (MCP-1) secretion levels were assessed by enzyme-linked immunosorbent assay (ELISA) following manufacturer's protocol (BioLegend). Statistical analysis was performed using Student's T-test followed by false discovery rate corrections on normalized values.

4.2.4 Live imaging of macrophage migration

4.2.4.1 Set-up

8-well chamber slides (Thermo Scientific Lab-Tek®) were used for live imaging. Day 7 BMDMs were seeded at 20,000 cells per well (or 25,000 cells/μm^2) in D10 media. This seeding density was selected after attempts to balance having sufficient number of cells per analysis frame and leaving enough space to prevent overcrowding of cells and inhibition of movement. After BMDMs were seeded for 6 hours, macrophages were stimulated with 5.0 ng/ml of E. coli-derived UltraPure LPS (Invivogen) and 1.0 ng/ml of recombinant murine IFN-γ (R&D Systems), 1.0 ng/ml of E. coli-derived LPS (Sigma) and 1.0 ng/ml of IFN-γ, or 10 ng/ml of IL-4 (BioLegend) and 10 ng/ml IL-13 (BioLegend). Immediately after stimulation, slides were placed on a stage incubator. Chambers were observed with an Olympus IX-83 inverted microscope equipped with a Tokai Hit stage incubator and controlled by Micro-Manager. Incubator settings were chosen to

maintain a 5% CO_2 atmosphere at 37°C; temperatures were periodically measured with a thermosensitive probe. Cells in chambers were imaged at 2 minute intervals for a total of 6 hours using the built-in Multi-Dimensional Acquisition function in Micro-Manager.

4.2.4.2 Integrin Knockdown

Day 7 BMDMs were transformed with Lonza 4D-Nucleofector system using proprietary primary solution 3, supplement 1, and program DS137. siGENOME siRNAs were ordered for each target integrin knockdown gene from Dharmacon. After transformation, cells were maintained in RPMI 1640 media supplemented with 10% recombinant mouse MCSF secreted from Ltk-cells and 10% heat-inactivated FBS. Cells were seeded according to 4.2.4.1. However, cells were seeded for 24 hours prior to stimulation to abate stress potentially induced by the knockdown process. Cells were stimulated at 24 hours with 1.0 ng/ml of E. coli-derived LPS (Sigma) and 1.0 ng/ml of recombinant murine IFN-γ (R&D Systems) or 10 ng/ml of IL-4 (BioLegend) and 10 ng/ml IL-13 (BioLegend). Live imaging was performed according to 4.2.4.1 after an additional 24 hours post stimulation—cells were cultured for 48 hours overall.

4.2.4.3 Data Analysis

No nuclear tracking dye was used for migration studies. We found that nuclear tracking dyes commonly used for live cell imaging, such as Hoechst 33342, DRAQ5, and CyTRAK Orange impeded BMDM migration and could not be used.[288] The centers of cell nuclei were annotated by hand using ImageJ's built-in MTrackJ plug-in (National Institutes of Health).[289] Cells that divided or migrated out of the imaging frame were considered only up to the time point of division or exit. At least 50 cells were dotted for each condition per biological replicate. Velocity and maximum displacement were quantified using an in-house developed Python script by Dr. Tim Smith.

Measurements were further analyzed in R; plots were compiled using the gplots package. Statistical analysis was performed using one-way ANOVA followed by Tukey's HSD post-hoc test.

4.2.5 CD11b Immunofluorescence

After 1, 4, 6, and 24 hours of adhesion, cells were fixed with 4% paraformaldehyde (Electron Microscopy Sciences) and washed with PBS (Lonza). Cells were not permeabilized to localize CD11b on the surface. Samples were blocked with 2% bovine serum albumin in PBS. Samples were incubated with rat anti-CD11b (M1/70 clone, BioLegend) primary antibody, followed by Alexa Fluor-596 donkey anti-rat secondary antibody (Jackson ImmunoResearch). Then, samples were incubated with Alexa Fluor-488 conjugated phalloidin and counterstained with Hoechst 33342 (both from ThermoFisher). Images were acquired with a Zeiss LSM780 confocal microscope using a 63x oil immersion lens and Zen microscope control software. Mean fluorescence intensity was quantified using the ImageJ software.

4.2.5.1 Morphology Analysis

To assess cell morphology, phalloidin confocal images were analyzed. The area and elongation factors were determined by manual tracing. Based on F-actin staining, cell boundaries were manually traced using the ImageJ software. Area, major axis, and minor axis were values that were measured and obtained from the software. The major or long axis was determined as the longest length of each cell while the minor or short axis was defined as the length across the nucleus, in a direction that is perpendicular to the long axis. The ratio of the two axes results in the elongation factor. A total of around 150 cells were analyzed per condition across the three separate biological experiments. Statistical analysis was performed using one-way ANOVA followed by Tukey's HSD post-hoc test.

4.3 Results

4.3.1 Ruthenium Photo-crosslinking Increases Storage Modulus

To characterize the fibrin gels, we first investigated the stiffness by AMR. 2 μm diameter probe microbeads were embedded into the fibrin gels by introducing them first into the unpolymerized fibrinogen solution. First, we found that the presence of the beads did not alter the fibrin network structure via laser confocal scanning microscopy (data not shown). Second, we determined that photo-crosslinking significantly increased the stiffness of the fibrin gel (Fig. 4.3). We found that a non-crosslinked fibrin gel had a G' value of 74.17 ± 39.49 Pa. Similarly, a fibrin gel that was exposed to the crosslinker solution but not to blue light had a G' value of 61.06 ± 39.09 Pa. Finally, a crosslinked gel had a G' value of 251.74 ± 77.67 Pa. Based on these values, we have demonstrated that a ruthenium photo-crosslinked gel is approximately three- to four-fold stiffer in terms of storage modulus compared to those from the non-crosslinked control fibrin gels.

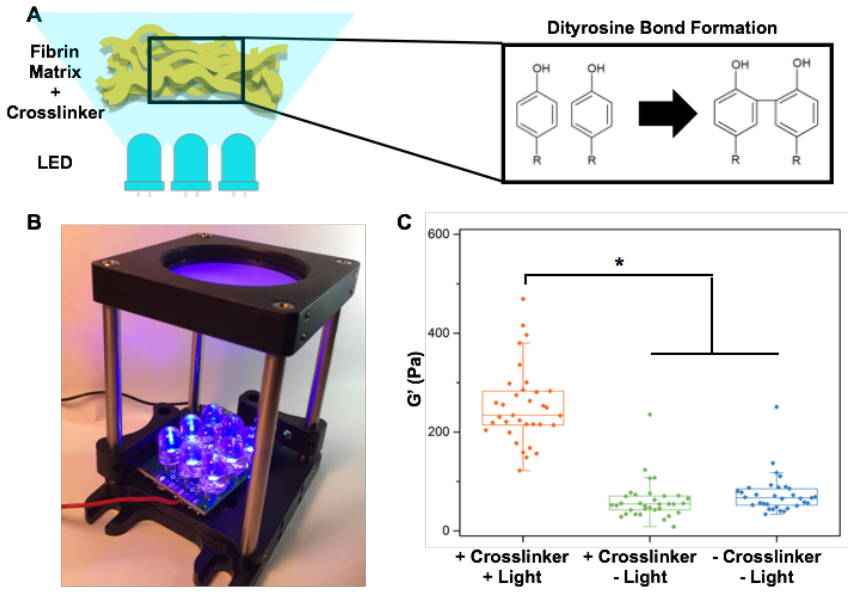

Figure 4.3. Characterization of the stiffness of ruthenium-based photo-crosslinked fibrin gels. (A) Cartoon schematic detailing the photo-crosslinking process. (B) 465 nm blue light is provided by a light rig fabricated in-house. (C) Scatterplot of AMR measurements of G' in 2 mg/ml fibrin gels with the indicated conditions. Asterisk denotes $p < 0.05$ using Mann Whitney test followed by Bonferroni correction.

4.3.2 *Ruthenium Crosslinked Gels Have Denser Network Architecture and Smaller Pores*

We proceeded to examine the fiber architecture in the photo-crosslinked fibrin gel vs. the non-crosslinked fibrin gels via laser scanning confocal microscopy and observed distinct fiber network structures (Fig. 4.4). First, the crosslinking solution by itself, without exposure to blue light, has no effect on altering the network architecture of the fibrin gel. Second, it is obvious that the fibrin network looks the densest in the crosslinked gel. The individual fiber bundles are closer in distance to surrounding fibers—it is likely that the crosslinking caused contraction and resulted in a denser fibrin matrix. Moreover, although there are still similarly sized large pores in the crosslinked gel when compared to the non-crosslinked gels, it is obvious that overall, the size of individual pores decreased in the crosslinked gels. However, it does not appear that fiber architecture necessarily changed: fiber diameter and length appear to be preserved among the three conditions.

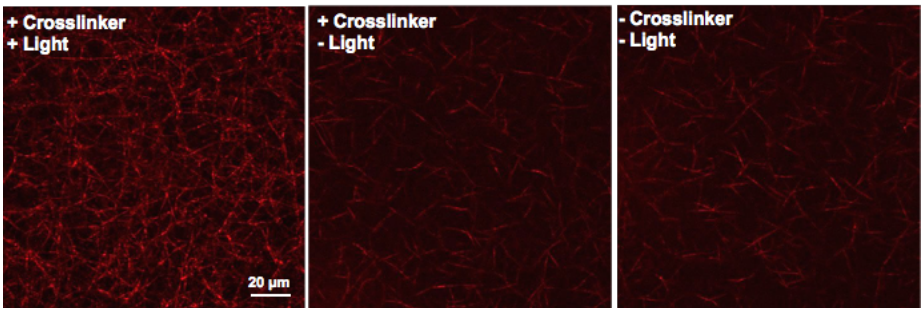

Figure 4.4. Fiber architecture and network structure of photo-crosslinked fibrin gels. Representative backscatter images of 2 mg/ml fibrin gels with indicated conditions. Scale bar: 20 μm.

4.3.3 *Substrate Rigidity Influences TNF-α, MCP-1, but not IL-6 secretions*

As previously mentioned in Chapter 3, it has been suggested that substrate rigidity plays a role in macrophage activation. In particular, enhanced substrate rigidity has been demonstrated to be associated with increased inflammatory cytokine secretions for murine macrophages.[196,198] To specifically examine the effect of increased substrate stiffness on murine BMDMs, we cultured

BMDMs on tissue culture polystyrene (TCPS) or fibrin gels that were crosslinked, exposed to only the crosslinker solution, or non-crosslinked. At 6 hours post seeding, we stimulated the macrophages with LPS, with or without IFN-γ. After 12 more hours of culture, we collected the supernatants to investigate cytokine secretion after a total of 18 hours of culture.

We found that the increased substrate rigidity enhanced secretions of TNF-α and MCP-1 but not that of IL-6 (Fig. 4.5). First, TNF-α secretion was enhanced on the photo-crosslinked gels. While the normalized TNF-α level did not increase for BMDMs seeded on gels that received only the crosslinker solution, normalized TNF-α secretion was significantly different on both crosslinked fibrin and TCPS surfaces from that of the fibrin control. Additionally, this trend was also observed for MCP-1 although not with statistical significance. However, IL-6 secretion did not appear to be sensitive to changes in fibrin stiffness—we were wary that the crosslinker solution alone appears to lower IL-6 secretion although we could not figure out a plausible explanation.

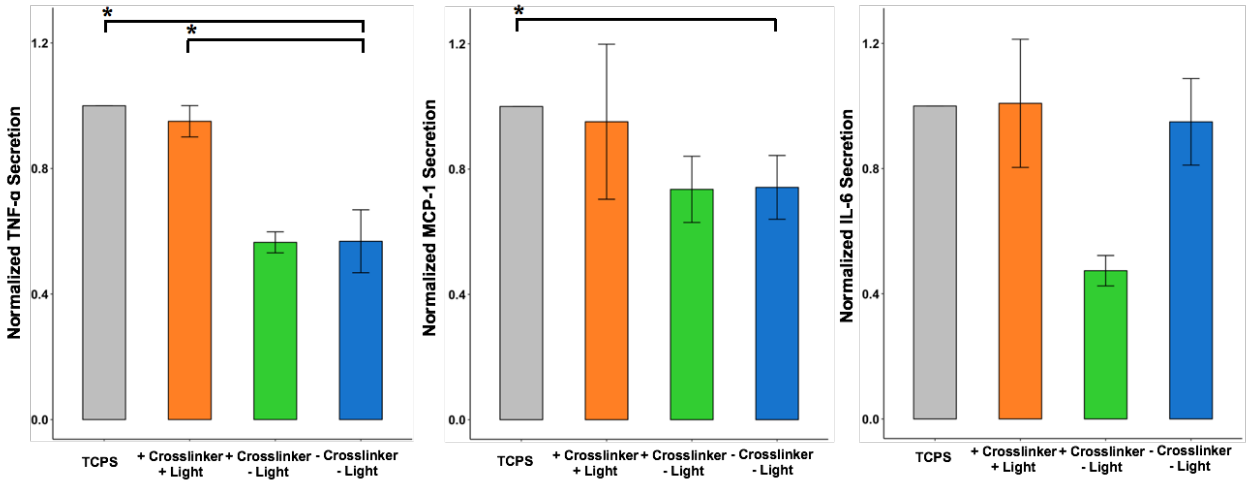

Figure 4.5. Inflammatory cytokine secretions as determined by individual ELISAs. Graph of normalized (A) TNF-α, (B) MCP-1, and (C) IL-6 secretions by macrophages cultured on TCPS or 2 mg/ml fibrin with indicated conditions. BMDMs were stimulated at 6 hours post seeding. Values are mean ± SEM of n = 6 biological replicates for TNF-α, n = 5 biological replicates for MCP-1, and n =3 biological replicates for IL-6. Day 6 to 8 BMDMs were used. Asterisks denote $p < 0.05$ by Student's t-test followed by false discovery rate correction for multiple comparisons for comparisons within each stimulation group.

4.3.4 *Macrophage Motility is Dependent on Activation State*

Prior to examining migration of macrophages on non-crosslinked or crosslinked fibrin surfaces, we first observed how unstimulated and activated macrophages moved in on glass. We seeded BMDMs on glass surfaces and observed their movements for 6 hours. We found that unstimulated macrophages and macrophages stimulated with IL-4 and IL-13 moved with similar velocities although unstimulated macrophages did not displace as far as macrophages simulated with IL-4 and IL-13; this difference though was not statistically significant (Fig. 4.6A and 4.6B). On the contrary, macrophages stimulated with LPS and IFN-γ moved the slowest and stayed closest to their originating positions (Fig. 4.6C). LPS and IFN-γ stimulated macrophages had significantly slower velocities than the other two phenotypes. This data suggested to us that we could not overlook the effects of soluble mediators and cytokines when examining macrophage motility.

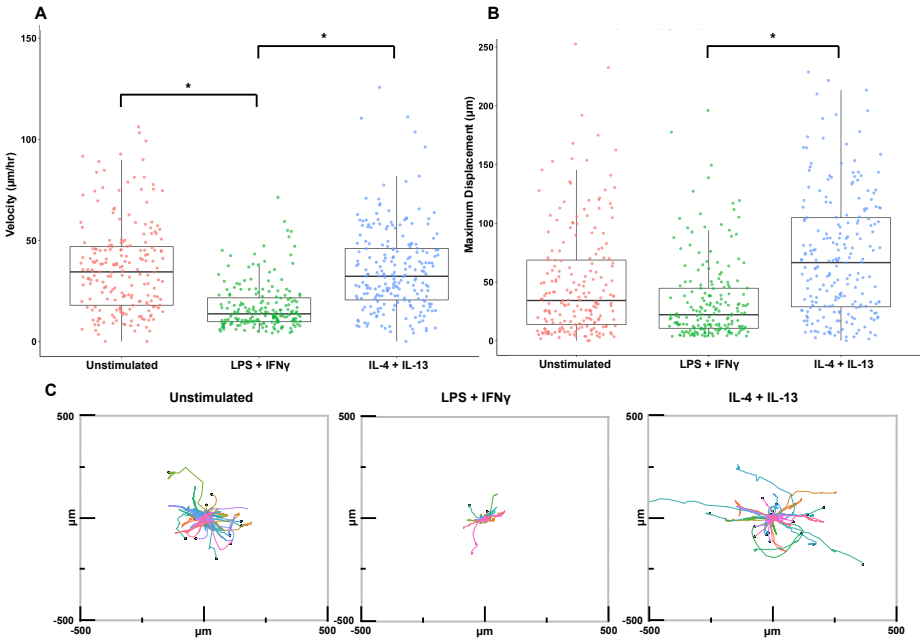

Figure 4.6. Macrophages exhibit different motility patterns dependent on activation. (A) Scatterplot of velocity. (B) Scatterplot of maximum displacement. For both plots, bar and whisker plot values are mean ± SEM of n = 3 biological replicates. Asterisks denote $p < 0.05$ by one-way ANOVA followed by Tukey's HSD post-hoc test. (C) Representative displacement plots of different macrophage phenotypes. Black circles end trajectories that terminate early due to cell division or exit from imaging frame. LPS-containing conditions were stimulated with 1.0 ng/ml of LPS (Sigma).

Table 4.1. Velocity and maximum displacement values of different phenotypes. Values are mean ± SEM of n = 3 biological replicates. For each biological replicate, over 50 cells were individually tracked.

Phenotype	Velocity (μm/hour)	Maximum Displacement (μm)
Unstimulated macrophages	38.67 ± 6.22	53.78 ± 11.67
LPS + IFN-γ stimulated macrophages	17.44 ± 1.75	33.98 ± 3.15
IL-4 + IL-13 stimulated macrophages	35.18 ± 2.97	75.25 ± 3.87

4.3.5 Macrophages with Downregulated CD11b or CD18 Lose Motility

Since integrins are responsible for macrophage-ECM interactions, we sought to investigate the role of integrins in migration by knocking down various integrins. We utilized siRNAs to knockdown specifically αM, β1, β2, and β3. Here, it should be noted that the velocity values increased while the maximum displacement values decreased when compared to what was previously observed in section 4.3.4. We believe this may be due to stock DMEM changes or inherent biological variability since BMDMs used for migration studies are isolated from mice with ages anywhere from 6-12 weeks. Other factors such as temperature or CO_2 levels were maintained across experiments and thus should not have contributed to changes in velocity and maximum displacement values.

We found that individually knocking down αM or β2 decreased velocity and maximum displacement for unstimulated and IL-4 and IL-13 macrophages (Fig. 4.7A and 4.7B). Based on the displacement plots, unstimulated macrophages with αM knocked down stayed closest to their originating positions (Fig. 4.7C). It appears that knocking down either β1 or β3 did not strongly influence macrophage motility. These trends were also observed with the IL-4 and IL-13 stimulated macrophages. Although velocity differences were not as large, maximum displacement values did differ by a similar range as those observed with the unstimulated macrophages. Interestingly, down-regulating β3 actually slightly enhanced the velocity of IL-4 and IL-13 stimulated macrophages. Contrastingly, LPS and IFN-γ macrophages had migratory patterns that were mainly driven by their stimulation conditions. Regardless of the integrin knocked down, these cells had the lowest

velocities and maximum displacements compared to those of their unstimulated and M2 activated counterparts. However, notably, macrophages with β2 had the lowest velocity and maximum displacement overall.

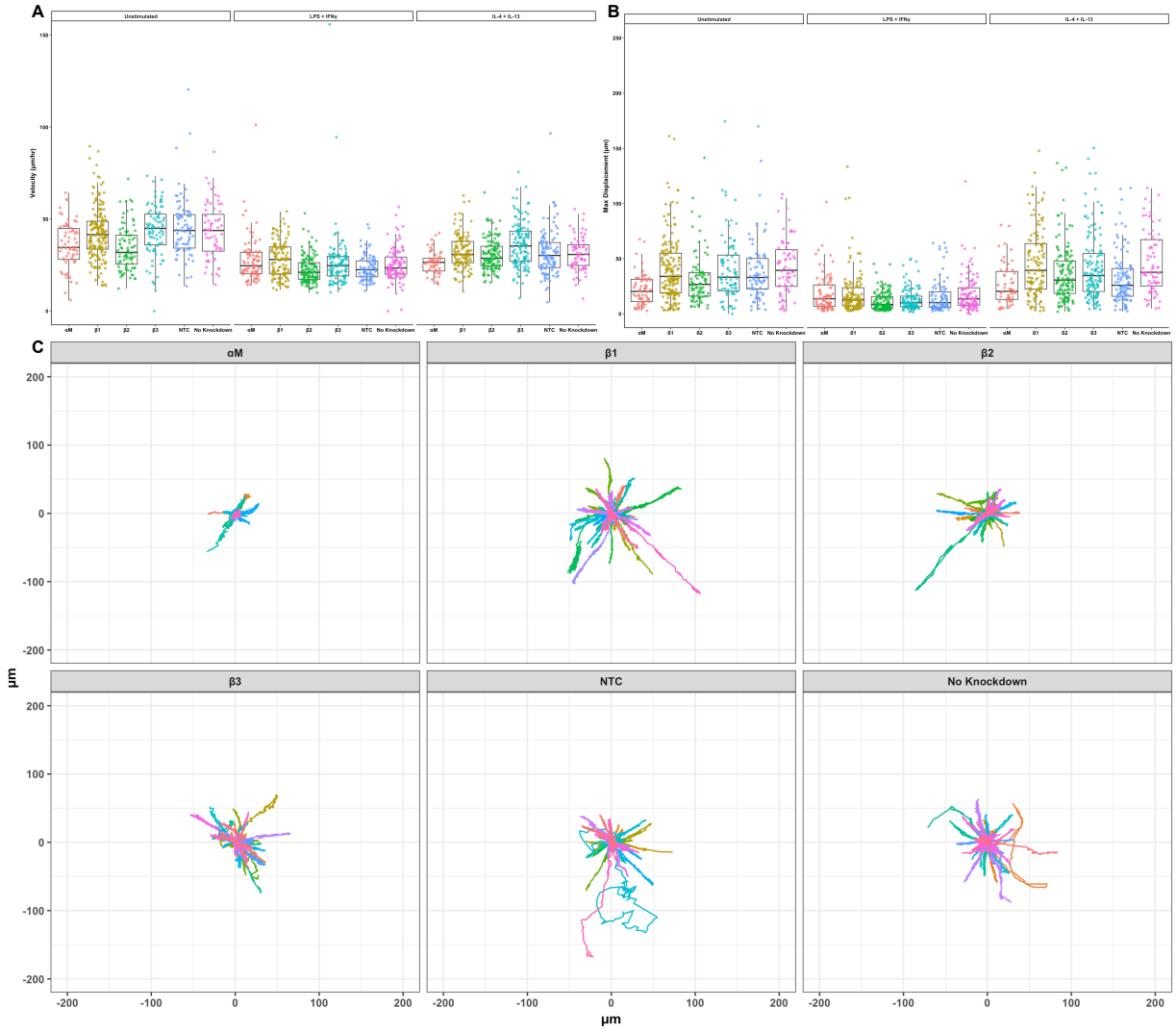

Figure 4.7. Macrophages decreased motility with lowered CD11b or CD18 expression. (A) Scatterplot of velocity (B) Scatterplot of maximum displacement. For both plots, bar and whisker plot values are mean ± SEM of n = 2 biological replicates. (C) Representative displacement plots of unstimulated macrophages with the indicated integrin knocked out. Black circles end trajectories that terminate early due to cell division or exit from imaging frame. LPS-containing conditions were stimulated with 1.0 ng/ml of LPS (Sigma).

Table 4.2. Velocity and maximum displacement values of BMDMs on glass with indicated integrin knocked down. Values are mean ± SEM of n = 2 biological replicates. For each replicate, over 50 cells were individually tracked.

Stimulation	Integrin Knocked Down	Velocity (μm/hour)	Maximum Displacement (μm)
Unstimulated	αM	35.95 ± 1.52	22.10 ± 1.73
Unstimulated	β1	42.21 ± 1.28	40.40 ± 2.08
Unstimulated	β2	34.21 ± 1.28	31.91 ± 2.50
Unstimulated	β3	43.7 ±1.48	40. 57 ± 3.13
Unstimulated	NTC	45.17 ± 1.85	38.94 ± 3.13
Unstimulated	No Knockdown	43.23 ± 1.79	42.88 ± 3.06
LPS + IFNγ	αM	27.71 ± 1.29	18.53 ± 1.76
LPS + IFNγ	β1	28.08 ± 0.86	18.91 ± 1.76
LPS + IFNγ	β2	22.61 ± 0.63	11.43 ± 0.72
LPS + IFNγ	β3	26.45 ± 1.51	13.60 ± 0.94
LPS + IFNγ	NTC	23.43 ± 0.74	16.23 ± 1.66
LPS + IFNγ	No Knockdown	25.14 ± 0.87	18.53 ± 1.62
IL-4 + IL-13	αM	26.36 ± 0.86	26.95 ± 2.59
IL-4 + IL-13	β1	32.34 ± 0.83	46.16 ± 2.73
IL-4 + IL-13	β2	30.54 ± 0.74	36.60 ± 2.26
IL-4 + IL-13	β3	36.12 ± 1.04	42.32 ± 2.58
IL-4 + IL-13	NTC	31.66 ± 1.19	32.30 ± 2.26
IL-4 + IL-13	No Knockdown	31.11 ± 1.05	46.50 ± 3.29

4.3.6 Increased ECM Substrate Rigidity Enhances Macrophage Motility

After examining the motility of different phenotypes on glass, we proceeded to examine macrophage migration on fibrin gels—non-crosslinked or crosslinked. We found that BMDMs activated by LPS and IFN-γ still remained slow and stayed close to their starting positions (data not shown). However, we found that for unstimulated macrophages and IL-4 and IL-13 stimulated macrophages, velocity and maximum displacement values were the greatest on crosslinked fibrin (Fig. 4.8A and 4.8B). The difference was most striking for unstimulated macrophages: (1) velocities increased from 40 μm per hour on glass to 58 μm per hour on non-crosslinked fibrin to 62 μm per hour on crosslinked fibrin while (2) maximum displacements increased from 26 μm to 45 μm to 61 μm respectively.

Regardless of the stimulatory cytokines, macrophages appeared to be more motile on the ECM surfaces compared to on glass. This may not be that surprising considering that there may be

more ligands for cell-ECM interactions on fibrin gels than on glass; although serum proteins from the media can adsorb on glass, the quantity of proteins ultimately adsorbed is probably limited. Moreover, when comparing motility of BMDMs on just non-crosslinked vs. crosslinked fibrin gels, it is apparent that macrophages not only are more motile but also move further from their originating positions on a stiffer ECM substrate (Fig. 4.8C).

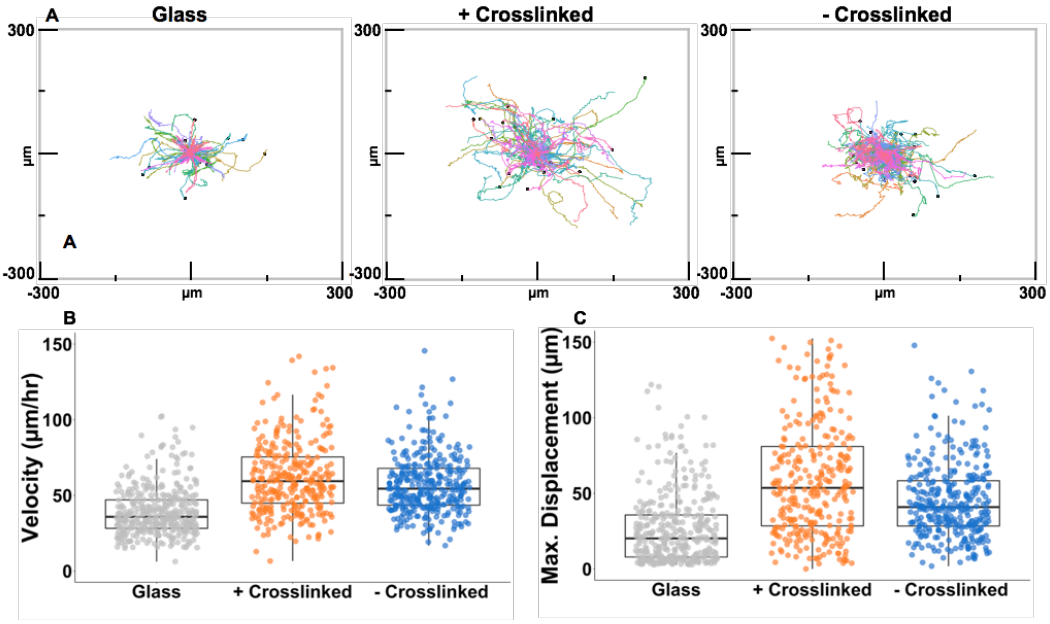

Figure 4.8. Macrophages move fastest and farthest on crosslinked fibrin. (A) Representative displacement plots of unstimulated macrophages on glass, crosslinked, or non-crosslinked surfaces. Black circles end trajectories that terminate early due to cell division or exit from the imaging frame. (B) Scatterplot of velocity (μm/hour). (C) Scatterplot of maximum displacement. Bar and whisker plot values are mean ± SEM of n = 4 biological replicates and over 250 cells were individually tracked per condition.

Table 4.3. Velocity and maximum displacement values of macrophages with indicated simulation conditions on glass and crosslinked or non-crosslinked fibrin gels. Values are mean ± SEM of n =4 biological replicates and over 50 cells were individually tracked per replicate. Due to the physical constraint of the 8 chamber well set-up, the LPS + IFN-γ control on glass was not included.

Stimulation	Surface	Velocity (μm/hour)	Maximum Displacement (μm)
Unstimulated	Glass	39.51	26.40
LPS + IFN-γ	Glass	37.43	33.28
Unstimulated	Crosslinked	61.71	61.02
LPS + IFN-γ	Crosslinked	36.83	36.4
IL-4 + IL-13	Crosslinked	57.97	54.86
Unstimulated	Not Crosslinked	57.71	45.15
LPS + IFN-γ	Not Crosslinked	39.27	33.28
IL-4 + IL-13	Not Crosslinked	61.71	51.48

4.3.7 Substrate Stiffness Alters Temporal CD11b Expression

Aside from investigating the role of CD11b on macrophage migration, we also examined the role it may play in adhesion. We analyzed CD11b on the surface on macrophages by immunostaining at 1 hour, 4 hours, 6 hours, and 24 hours after adhesion on glass surfaces as well as non-crosslinked or crosslinked fibrin matrices (Fig. 4.9). At 1 hour, CD11b is expressed across all surfaces although a more intense level of expression is observed on glass compare to those exhibited on the fibrin surfaces. Most of the CD11b expression is localized on the periphery of the cells across all conditions. However, by 4 hours, CD11b expression decreased dramatically to no expression on the non-crosslinked fibrin surfaces and very low expression on the crosslinked fibrin gels. Contrastingly, macrophages on glass still exhibited high CD11b expression, with the staining localized around the edges of the cells.

At 6 hours, we observed that CD11b expression may not be static but dynamic. Although cells cultured on non-crosslinked fibrin gels still showed no CD11b expression, BMDMs on crosslinked fibrin expressed some CD11b. Even though the intensity of the immunofluorescence was not as bright as that exhibited at 1 hour, we observed that CD11b has once again been localized to the edges of the cells. Interestingly, BMDMs on glass demonstrated decreased CD11b. In fact, CD11b expression on glass that was previously always high was at an intensity level that was comparable to that observed on crosslinked fibrin at 6 hours.

Finally, at 24 hours, we again saw more temporal shifts in CD11b expression. First, macrophages on non-crosslinked fibrin exhibited moderate levels of CD11b. Second, macrophages cultured on crosslinked fibrin demonstrated another decrease in CD11b expression from that at 6

hours. Last, CD11b expression is back up again for cells cultured on glass, increasing its level from that observed at 6 hours.

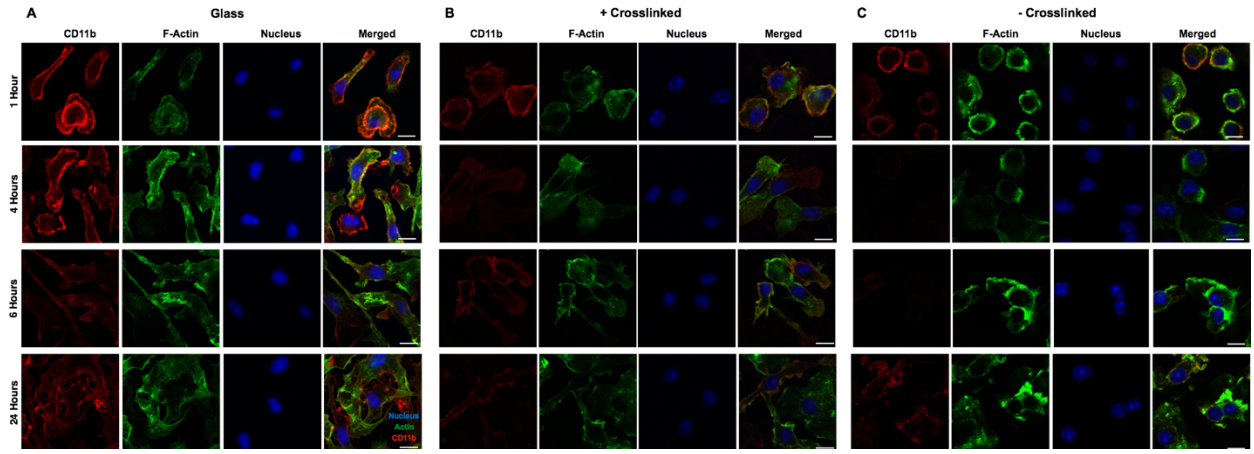

Figure 4.9. CD11b expression and filamentous actin of macrophages on glass and crosslinked or non-crosslinked fibrin. Fluorescent images of CD11b (red; immunostaining), F-actin filaments (green; phalloidin staining), and nucleus (blue; Hoechst staining) of BMDMs cultured on (A) non-crosslinked fibrin gels (B) crosslinked fibrin gels or (C) glass at 1, 2, 4, or 24 hours. Scale bar is 10 μm.

Although there were four different time points, since 6 hours is the time point when we introduced exogenous cytokines and soluble mediators, we proceeded to quantify the CD11b intensity just at this time point. We found that the average CD11b intensity on glass is indeed similar to that observed on crosslinked fibrin (Fig. 4.10). Overall, although individual cells express varying levels of CD11b, BMDMs cultured on stiffer surfaces, either crosslinked fibrin gels or glass, exhibited higher levels of CD11b than cells cultured on non-crosslinked fibrin gels.

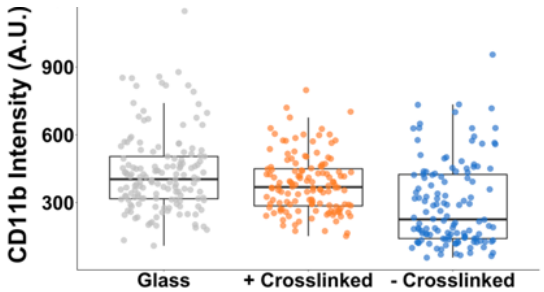

Figure 4.10. CD11b expression is enhanced on crosslinked fibrin. Scatterplot of CD11b intensity (AU). Over 30 cells were analyzed per condition for n =3 biological replicates.

Overall, these results suggest that the regulation is of CD11b is dynamic and linked to substrate rigidity. On a very stiff substrate such as glass, CD11b expression undergoes little perturbation; levels remain moderate to high regardless of the duration of adhesion. However, on a very soft substrate such as that of non-crosslinked fibrin, CD11b expression decreases dramatically and recovers only after many hours of adhesion. On a slightly stiffer, crosslinked fibrin gel, CD11b expression is even more dynamic, decreasing or increasing its expression within a much shorter time frame.

4.3.8 Substrate Rigidity Regulates Macrophage Morphology and Elongation

Aside from differences observed in CD11b expression, F-actin staining via phalloidin binding also indicated variability in macrophage morphology on the different surfaces (Fig. 4.9). At 1 hour, BMDMs seeded on either of the fibrin gels still exhibited a round morphology while cells on fibrin appeared to be more spread. Next, at 4 hours, macrophages still remained round on non-crosslinked fibrin whereas cells started to spread on the crosslinked fibrin. On glass, cells have lost much of their round morphology. Then, at 6 hours, BMDMs on non-crosslinked fibrin still remained small, round, and clustered. Macrophages on crosslinked gels did not differ much in spreading compared to what was observed at 4 hours; however, cells exhibited filopodial extensions that were previously absent. On the contrary, BMDMs seeded on glass were very elongated at 6 hours. Finally, BMDMs appeared to be similarly spread by 24 hours on either non-crosslinked or crosslinked fibrin matrices. Contrastingly, macrophages on glass surfaces were not as elongated by 24 hours but were still similarly well spread.

We proceeded to analyze cell surface area and elongation factor at 6 hours because again, this was the time when we stimulated with LPS and IFN-γ for the inflammatory cytokines ELISA

analyses. Examining at least 50 cells per biological replicate, we found that first, cells cultured on crosslinked fibrin gels were much more spread than those on non-crosslinked fibrin gels (Fig. 4.11A). In fact, cells had average area of 350 μm^2 on non-crosslinked fibrin; this value increased to 523 μm^2 when cells were cultured on crosslinked fibrin. Notably, cell areas on crosslinked fibrin were closer to those of cells cultured on glass, which had a mean cell area of 471 μm^2.

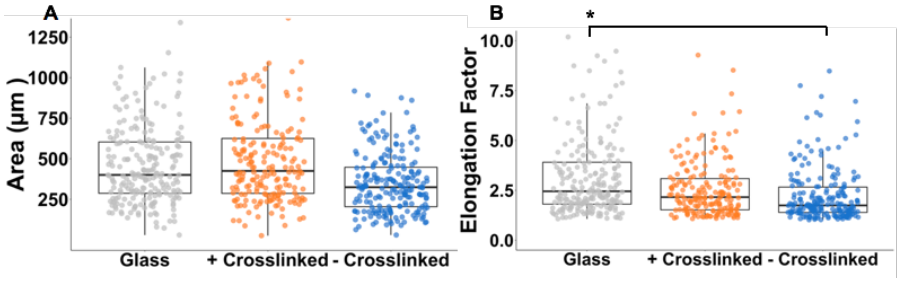

Figure 4.10. Macrophages are more spread on crosslinked fibrin. (A) Scatterplot of cell area (µm). (B) Scatter plot of elongation factor. Over 50 cells were analyzed per condition for n = 3 biological replicates. Asterisk denotes $p < 0.05$ by one-way ANOVA followed by Tukey's HSD post-hoc test.

Second, cells had the largest elongation factor on glass, averaging around a value of 3.5 (Fig. 4.11B) Compared to cells cultured on glass, cells cultured on non-crosslinked fibrin gels had a significantly lower average elongation factor of 2.2. Contrarily, macrophages on crosslinked fibrin gels exhibited an intermediate elongation factor of 2.7. Together, both these values indicate that after 6 hours of adhesion, macrophages are more spread and less round on crosslinked fibrin gels than on non-crosslinked fibrin gels. Moreover, though cells cultured on crosslinked fibrin were not as elongated as those cultured on glass, BMDMs on both surfaces were similarly spread in terms of cell area.

4.4 Discussion

4.5.1 Discussion

Substrate rigidity and its effects on cellular behavior has been a groundbreaking area of work in recent years. Engler et al. and Gilbert et al. have shown that substrate rigidity directs stem cell

lineage commitment and helps to maintain stem cell self-renewal potential.[194,290] For macrophages, there have also been several studies, using either murine or human cells, that have investigated the role of substrate stiffness on macrophage activation and function. Macrophages cultured on synthetic matrices such as PEG or polyacrylamide of varying stiffnesses typically exhibited a more inflammatory behavior when the substrate is stiffer.[196,198] However, the effects of changing the rigidity of ECM matrices, specifically the provisional wound healing matrix fibrin, on macrophage behavior has still not been clearly elucidated.

Here, we utilized a ruthenium-based photo-crosslinking method to alter the mechanical stiffness of fibrin matrices. From reflection confocal images, it is apparent that although fiber length and diameter did not change significantly, the resulting crosslinked matrix is dense and has smaller pores than its non-crosslinked counterpart. AMR indicated that along with a change in matrix network structure, there was also an increase in local matrix stiffness. Future work can focus on exploring this stiffness change in depth by using atomic force microscopy to gauge the stiffness at the surface of the fibrin gels.

After demonstrating changes in local stiffness, we found that murine BMDMs cultured on a stiffer, crosslinked fibrin gel secreted more inflammatory cytokines, namely TNF-α and MCP-1, than those cultured on a softer, non-crosslinked fibrin matrix. On the contrary, IL-6 secretion was not altered by changes in substrate rigidity. It has been suggested that IL-6 is a mechanosensitive cytokine and responds to changes in compressive strength—it may be possible that the stiffness regime we are operating in is too narrow to observe changes in IL-6 secretion.[291] Future studies should examine a panel of inflammatory cytokines to determine which ones are sensitive to changes in the pascal regime. Nonetheless, based on the data presented, it is likely that murine BMDMs are

mechanosensitive. In particular, enhanced matrix stiffness modulate macrophages to increase their inflammatory activation in the presence of LPS and IFN-γ.

We also demonstrated that the migratory behaviors of macrophages differ among crosslinked or non-crosslinked fibrin and glass surfaces. First, we found that unstimulated macrophages and IL-4 and IL-13 stimulated macrophages are more motile than LPS and IFN-γ stimulated macrophages. This may not be surprising taking into consideration that LPS and IFN-γ stimulated macrophages are pro-inflammatory macrophages present during the early stages of wound healing—they may stay at the site of injury, clearing away pathogens.[278] It has also been observed that in disease pathogenesis, pro-inflammatory macrophages tend to accumulate in diseased regions, such as atherosclerotic plaques or obese adipose tissues.[292,293] In a different manner, IL-4 and IL-13 macrophages are anti-inflammatory macrophages that tend to be present during the resolution of an immune response—they may require increased motility to migrate away from the site of infection. Interestingly, the enhanced migratory capability of IL-4 and IL-13 stimulated macrophages has been suggested to play a role during cancer metastasis.[294]

Second, we found that knocking down CD11b or CD18 impaired motility of macrophages. LPS and IFN-γ stimulated macrophages did not alter their migratory behaviors greatly when these integrins were knocked down. However, unstimulated macrophages and IL-4 and IL-13 stimulated macrophages both exhibited decreased velocities and maximum displacements upon down-regulation of CD11b or CD18. It is possible that a double knockdown of CD11b/CD18 would further impede macrophage motility and is worth considering for future migration experiments.

Third, we demonstrated that culture of macrophages on non-crosslinked or crosslinked fibrin matrices led to differences in migratory behavior. Ciano et al. was one of the first groups to

explore macrophage migration in fibrin-impregnated nitrocellulose filters: they found that macrophage migration in fibrin gels depended on both fibrin and thrombin concentrations as well as the nature of crosslinking.[58] In particular, motility was decreased as fibrinogen concentration or degree of crosslinking increased. Lanir et al. refined this migration assay by investigating migration of peritoneal macrophages in three-dimensional fibrin-fibronectin matrices: when the gels were further crosslinked with Factor XIII, the group found that both the number of migrating cells and the distance of migration were reduced.[59] Our findings were different in that macrophages were actually the most motile, in terms of both velocity and maximum displacement, on crosslinked fibrin gels. However, since our investigation focused on characterizing two-dimensional migratory patterns, we will need to extend our studies to three dimensions in order to compare with previous studies.

Aside from changes in migratory behaviors, we also found that the expression of CD11b on BMDMs was dynamic except for those cultured on glass. Over the course of 24 hours, CD11b expression remained relatively stable and high on BMDMs adhered to glass surfaces. Contrastingly, CD11b expression was down-regulated on both non-crosslinked and crosslinked fibrin matrices, demonstrating temporal expression patterns dependent on hours of adhesion. The observation that CD11b expression altered with adhesion time is noteworthy because CD11b is often used as a marker for identifying macrophages from other immune cells such as neutrophils and dendritic cells in both mice and human.[295–297] Understanding the shifts in CD11b expression may help reveal insights on macrophage inflammatory activation. It will be worthwhile in future studies to further examine the temporal regulation of CD11b at the gene level with qPCR and again at the protein level with Western blots.

Although CD11b expression was influenced by adhesion time, overall, CD11b was lower on either of the fibrin matrices than on glass. This is in accordance with our findings in 3.3.1 and 3.3.12—CD11b expression was lower on softer surfaces, either natural or synthetic substrates. CD11b's role in immunity is still being debated; it has been shown to both negatively and positively regulate inflammation in varying disease models. For example, in murine models of chronic obstructive lung disease, heightened alveolar macrophage CD11b expression was associated with acute lung exacerbations.[298] Conversely, in murine models of lung *Bordetella bronchiseptica* infection, $CD11b^{-/-}$ mice succumbed to the respiratory infection much faster than mice with intact CD11b.[299] In murine models of transient focal ischemia, microglial CD11b gene expression was elevated from day 3 until at least day 14 in ischemic animals.[300] Last, Faridi et al. demonstrated that reduced CD11b activity is directly associated with chronically increased inflammatory status in systemic lupus erythematosus.[301] Although more work needs to be done delving into the signaling pathways associated with CD11b expression, we postulate that low expression of CD11b on the non-crosslinked fibrin gels led to an inhibition of inflammatory activation of macrophages.

Last, culturing macrophages on fibrin gels of different stiffnesses also resulted in changes in cell morphology and elongation. We found that macrophages cultured on stiffer substrates tended to be more spread over a bigger surface area. Other studies investigating the effects of substrate rigidity have shown that macrophages are more spread and flattened on stiffer substrates and more rounded on softer surfaces.[196,199,302] Additionally, we have also demonstrated that macrophages tend to be more elongated on stiffer substrates—in the case of crosslinked fibrin, we also observed some filopodial extensions after 6 hours of adhesion. This is in accordance with findings from other

groups who have also shown that stiffer substrates encourage the formation of long protrusive actin structures. [302,303]

The ability to photo-crosslink ECM matrices containing tyrosine can be leveraged to study macrophage activation and behavior in response to changes in matrix rigidity. It should be noted though that this photo-crosslinking technique results in substrates with stiffnesses that are within pascals to kilopascals. It still remains unclear if macrophages will respond differently depending on the stiffness regimes. Consequently, it is likely that in order to get a more complete understanding of how macrophages respond to changes in substrate rigidity, a bigger range of stiffnesses will need to be explored. Gaining this more comprehensive knowledge will help the design of new biomaterials for wound healing because the mechanical properties of the substrate and their effects on macrophage activation and function can be considered.

4.5.2 Concluding Remarks

We demonstrated that non-crosslinked and crosslinked fibrin matrices elicited distinct macrophage responses in terms of inflammatory activation, migration, CD11b expression, and morphology. Culture of macrophages on crosslinked fibrin enhanced inflammatory cytokines that were inhibited on non-crosslinked fibrin. Furthermore, culture of macrophages on crosslinked fibrin increased cell motility; BMDMs traversed faster and further than cells on non-crosslinked fibrin. Last, macrophages cultured on a stiffer substrate were observed to have larger areas as well as more elongated morphologies. These findings contribute to our understanding of how the rigidity of the extracellular matrix regulates macrophages during wound healing.

Chapter 5: Discussion, Future Directions, and Concluding Remarks

5.1 Summary & Discussion

In this dissertation, we have explored in depth the interactions between fibrin(ogen) and murine BMDMs. First, in Chapter 2, we investigated the individual effects of composite fibrin-collagen gels, thrombin, fibrinogen, and fibrin on macrophage inflammatory activation and behavior. In particular, we found that fibrinogen and fibrin differentially modulate macrophage function in terms of inflammatory cytokine secretion as well as cytoskeletal organization and morphology. Notably, fibrin inhibits inflammatory activation of macrophages that are induced by LPS and IFN-γ. In particular, our results demonstrated that a single protein, fibrin(ogen), either presented in its soluble form or incorporated within an insoluble matrix, can be an activation switch for modulating macrophage inflammatory activation.

This ability to control macrophage inflammatory versus anti-inflammatory activation is highly desirable for the design of biomaterials to be used for tissue regeneration. Most biomaterials elicit a significant host immune reaction and fibrosis after implantation, although a few recent studies suggest that modulation of the immune response and reduction of fibrosis can be achieved.[304,305] However, it still remains unclear how much inflammatory versus anti-inflammatory activation of macrophages is necessary to achieve the optimal host response, since both functions are needed for proper wound healing. It is likely that a tightly controlled dynamic activation pattern will be required. Since fibrinogen and fibrin appear to shift macrophage activation from pro- to anti-inflammatory, engineering biomaterials that utilize this activation switch may help to develop a better understanding of the foreign body response. More importantly, designing new

materials that dynamically present fibrinogen or fibrin may ultimately help control the response to minimize fibrosis and promote proper tissue regeneration.

Next, in Chapter 3, we examined the role of matrix rigidity as a cue for macrophage inflammatory activation. We not only modulated the rigidity of fibrin matrices via biological and chemical agents but also altered the mechanical properties of synthetic surfaces such as polyacrylamide, PEG, and PDMS. First, data from the ancrod polymerization and plasmin degradation experiments suggested that softening of fibrin gels does not impinge on fibrin's ability to inhibit inflammatory activation. Second, we also explored the effects of adsorbing or tethering fibrinogen to matrices of varying stiffnesses. The data from the PDMS and PEG substrate experiments indicated that substrate rigidity alone has an effect on controlling macrophage inflammatory activation. Moreover, the presence of fibrinogen, either adsorbed or conjugated, does not seem to play an impactful role. Last, flow cytometry data of BMDMs differentiated on PDMS substrates of different stiffnesses suggested that substrate rigidity has an effect on not only inflammatory activation but also differentiation.

Macrophages mature from monocytes in the blood; thus, it is important to consider how substrates these cells may encounter during this maturation process may influence their differentiation. Furthermore, macrophages are master regulators in wound healing; they again experience ECM changes during the healing process when many proteins are being simultaneously deposited or degraded. It is pertinent for us to consider how mechanical cues may alter their inflammatory activation and impact wound healing. Finally, understanding how substrate rigidity influences macrophage inflammatory activation can have far-reaching impact beyond wound healing. For one, dynamic changes to ECM stiffnesses can also occur in many disease pathologies,

such as atherosclerosis. Macrophages play a role in the development of many diseases. Hence, understanding how both local and global stiffness of the environment influence macrophages can help us leverage these immune cells to impede disease progression.

Finally, in Chapter 4, we introduced a ruthenium-based crosslinking method. We characterized the effects of this crosslinking on a fibrin matrix by examining structural and stiffness changes via reflection confocal microscopy and AMR respectively. The crosslinked fibrin gel is more densely structured and has an increased storage modulus value compared to its non-crosslinked counterpart. Moreover, we saw similar results as those mentioned in Chapter 3—namely, increased substrate rigidity enhances inflammatory activation. In this chapter, we also introduced studies involving macrophage migration and motility. We found that migratory behaviors are dependent on not only phenotypes but also mechanical properties of the adhesive substrate. Moreover, we implicated potential roles the integrin CD11b may play in adhesion, migration, and possibly, inflammatory regulation.

Chapter 4 thoroughly examined the effects of altering the provisional wound healing matrix's mechanical properties on murine BMDM behavior via a non-cytotoxic crosslinking method. The advantage of the photo-crosslinking method is that it is inexpensive and facile, facilitating an ease of adoption by other laboratories who may want to explore the effects of substrate rigidity on cells. One caveat though is that the resulting ECM substrates have a stiffness in the range of pascals to low kilopascals which may or may not offer a suitable range to tease apart mechanical effects for specific cell types.

Technique aside, this work has added to the body of knowledge regarding macrophage migration. It is obvious that cell morphology, cytoskeletal organization, and integrin expression all

play a role in not only macrophage inflammatory activation but also migration. A fundamental understanding of how these macrophage phenotypes migrate to and behave at any injury or pathologic site will help design better strategies to specifically modulate the local immune response. Moreover, macrophages need to move to many locations throughout the body, whether during wound healing, disease development, or even homeostasis.

From our data, we observed a biphasic response that suggested that both cell-ECM interactions and substrate rigidity are at play. When the matrix was very stiff with no natural adhesion sites, macrophages seemed to be sticking to the glass substrate, thereby having limited motility. Yet when natural ECM ligands were being presented, the stiffer, crosslinked fibrin substrates were postulated to enable cells to generate more tension, allowing them to propel through the matrix and migrate. This interesting balance between integrin-ECM interactions and substrate stiffness still needs to be further elucidated because it is essential to investigate how substrate stiffness can alter macrophages' migratory capacities.

5.2 Future Directions

These studies thus far have all be done with murine BMDMs and in two-dimensional, *in vitro* environments. First, it would be wise to explore the effects of the mechanochemical regulation of fibrin(ogen) on other types of macrophages, whether they are cells from a different source other than mice, or from a different tissue. In our lab, we have already begun conducting studies that examine fibrin(ogen)'s interactions with primary human macrophages and primary murine peritoneal cells. Results from both these cell types would provide further insight to this current work because it is possible that certain trends are specific to primary murine BMDMs.

Alternatively, observing similar behaviors even despite the noise introduced by the biological variabilities inherent in primary cells would bolster the findings in this work.

Second, it is pertinent to extend these current studies to a more complex, three-dimensional environment as macrophages do not interact solely with each other and with one primary protein. It would be ideal to introduce other cell types that may be responsible for laying down or breaking down fibrin during wound healing. Furthermore, composite gels involving collagen should again be explored because collagen is deposited toward the end of wound resolution. Finally, it would be relevant to explore and optimize a methodology for encapsulating macrophages into fibrin gels and observe macrophage behavior in a truly three-dimensional environment. In particular, in terms of migration studies, it would be necessary to examine the migratory patterns in not only x and y planes, but also the z plane. A three-dimensional gel migration study would provide insight as to how macrophages move relative to a specific location, for example, toward the center or to the periphery of a gel construct.

Third, it will be useful to investigate macrophage-fibrinogen interactions in *in vivo* studies. We have preliminary evidence indicating that for mouse full thickness skin wound models, when we delivered either saline or fibrin into the wound pockets of animals, fibrin abrogated the expression of iNOS, whereas saline did not. It will be pertinent to perform more histological staining with other markers before we can conclude the effects of fibrin *in vivo*.

Finally, it is vital to elucidate the intracellular molecular signaling pathways underlying the responses observed in this work. Notably, our lab has been focused on understanding the role of the Yes-associated protein, also known as YAP. This protein is a transcriptional factor downstream of the Hippo signaling pathway that has been demonstrated to play roles for maintaining normal

homeostasis, promoting tissue repair, and participating in oncogenic signaling; interestingly, YAP expression has also been shown to positively correlate with ECM stiffness.[306] We have preliminary evidence suggesting that YAP is differentially localized dependent on substrate rigidity. In particular, we found that YAP is present in the nucleus on the stiffer, glass surface while it is outside the nucleus and in the cytoplasm on the softer, fibrin matrix.

5.3 Concluding Remarks

This body of work contributes new knowledge to the specific interactions between fibrin(ogen) and macrophages. Previous to this work, there was limited understanding about the potential role the extracellular matrix plays in wound healing. Specifically, this work has brought more understanding as to how the first provisional extracellular matrix regulates macrophage behavior. The fibrin matrix not only provides adhesive cues through ligand binding sites but also mechanical cues via mechanical stiffness to macrophages. We have contributed more knowledge to how substrate stiffness alters macrophage morphology, differentiation, activation, and motility. All of these findings will help offer new insights for designing biomaterials that can mitigate undesirable immune responses and promote proper wound healing.

REFERENCES

1. Martin, P. & Leibovich, S. J. Inflammatory cells during wound repair: The good, the bad and the ugly. *Trends in Cell Biology* **15,** 599–607 (2005).
2. Anderson, J. M., Rodriguez, A. & Chang, D. T. Foreign body reaction to biomaterials. *Seminars in Immunology* (2008). doi:10.1016/j.smim.2007.11.004
3. Bryers, J. D., Giachelli, C. M. & Ratner, B. D. Engineering biomaterials to integrate and heal: the biocompatibility paradigm shifts. *Biotechnol. Bioeng.* **109,** 1898–911 (2012).
4. Gurtner, G. C., Werner, S., Barrandon, Y. & Longaker, M. T. Wound repair and regeneration. *Nature* **453,** 314–21 (2008).
5. Eming, S. a, Krieg, T. & Davidson, J. M. Inflammation in wound repair: molecular and cellular mechanisms. *J. Invest. Dermatol.* **127,** 514–25 (2007).
6. Martin, P. Wound healing--aiming for perfect skin regeneration. *Science* **276,** 75–81 (1997).
7. Laurens, N., Koolwijk, P. & de Maat, M. P. Fibrin structure and wound healing. *Journal of thrombosis and haemostasis : JTH* **4,** 932–939 (2006).
8. Stout, R. D. *et al.* Macrophages Sequentially Change Their Functional Phenotype in Response to Changes in Microenvironmental Influences. *J. Immunol.* (2005). doi:10.4049/jimmunol.175.1.342
9. Duque, G. A. & Descoteaux, A. Macrophage cytokines: Involvement in immunity and infectious diseases. *Frontiers in Immunology* (2014). doi:10.3389/fimmu.2014.00491
10. Turner, M. D., Nedjai, B., Hurst, T. & Pennington, D. J. Cytokines and chemokines: At the crossroads of cell signalling and inflammatory disease. *Biochimica et Biophysica Acta - Molecular Cell Research* (2014). doi:10.1016/j.bbamcr.2014.05.014
11. McWhorter, F. Y., Davis, C. T. & Liu, W. F. Physical and mechanical regulation of macrophage phenotype and function. *Cellular and Molecular Life Sciences* (2014).
12. Wynn, T. A., Chawla, A. & Pollard, J. W. Macrophage biology in development, homeostasis and disease. *Nature* (2013). doi:10.1038/nature12034
13. Guilliams, M. *et al.* Dendritic cells, monocytes and macrophages: A unified nomenclature based on ontogeny. *Nature Reviews Immunology* (2014). doi:10.1038/nri3712
14. Epelman, S. *et al.* Origin and functions of tissue macrophages. *Immunity* (2014). doi:10.1016/j.immuni.2014.06.013
15. Sieweke, M. H. *et al.* Beyond stem cells: self-renewal of differentiated macrophages. *Science* (2013). doi:10.1126/science.1242974
16. Schulz, C. *et al.* A Lineage of Myeloid Cells Independent of Myb and Hematopoietic Stem Cells. *Science (80-.).* (2012). doi:10.1126/science.1219179
17. Gordon, S. & Taylor, P. R. Monocyte and macrophage heterogeneity. *Nature Reviews Immunology* (2005). doi:10.1038/nri1733
18. Mosser, D. M. & Edwards, J. P. Exploring the full spectrum of macrophage activation. *Nat. Rev. Immunol.* **8,** 958–69 (2008).
19. Janeway, C. J., Travers, P. & Walport, M. Immunobiology: The Immune System in Health and Disease. 5th edition. *Garl. Sci.* (2001). doi:10.1016/S0944-7113(96)80081-X
20. Stout, R. D. *et al.* Macrophages sequentially change their functional phenotype in response to changes in microenvironmental influences. *J. Immunol.* **175,** 342–349 (2005).
21. Martinez, F. O., Gordon, S., Locati, M. & Mantovani, A. Transcriptional Profiling of the

Human Monocyte-to-Macrophage Differentiation and Polarization: New Molecules and Patterns of Gene Expression. *J. Immunol.* (2006). doi:10.4049/jimmunol.177.10.7303
22. Xue, J. *et al.* Transcriptome-Based Network Analysis Reveals a Spectrum Model of Human Macrophage Activation. *Immunity* **40,** 274–288 (2014).
23. Martinez, F. O. & Gordon, S. The M1 and M2 paradigm of macrophage activation: time for reassessment. *F1000Prime Rep.* (2014). doi:10.12703/P6-13
24. Murray, P. J. *et al.* Macrophage Activation and Polarization: Nomenclature and Experimental Guidelines. *Immunity* (2014). doi:10.1016/j.immuni.2014.06.008
25. Sica, A. & Mantovani, A. Macrophage plasticity and polarization: In vivo veritas. *Journal of Clinical Investigation* (2012). doi:10.1172/JCI59643
26. Mantovani, A. *et al.* The chemokine system in diverse forms of macrophage activation and polarization. *Trends in Immunology* **25,** 677–686 (2004).
27. Stein, M., Keshav, S., Harris, N. & Gordon, S. Interleukin-4 Potently Enhances Murine Macrophage Mannose Receptor Activity - a Marker of Alternative Immunological Macrophage Activation. *J Exp Med* (1992). doi:DOI 10.1084/jem.176.1.287
28. Martinez, F. (Fernando) O., Sica, A., Mantovani, A. & Locati, M. Macrophage activation and polarization. *Front. Biosci.* (2008). doi:10.2741/2692
29. Lang, R., Patel, D., Morris, J. J., Rutschman, R. L. & Murray, P. J. Shaping Gene Expression in Activated and Resting Primary Macrophages by IL-10. *J. Immunol.* (2002). doi:10.4049/jimmunol.169.5.2253
30. Rath, M., Müller, I., Kropf, P., Closs, E. I. & Munder, M. Metabolism via arginase or nitric oxide synthase: Two competing arginine pathways in macrophages. *Frontiers in Immunology* (2014). doi:10.3389/fimmu.2014.00532
31. Thomas, A. C. & Mattila, J. T. 'Of mice and men': Arginine metabolism in macrophages. *Frontiers in Immunology* (2014). doi:10.3389/fimmu.2014.00479
32. Raes, G. *et al.* Arginase-1 and Ym1 Are Markers for Murine, but Not Human, Alternatively Activated Myeloid Cells. *J. Immunol.* (2005). doi:10.4049/jimmunol.174.11.6561
33. Mantovani, Sica & Locati, M. Macrophage Polarization Comes of Age. *Immunity* (2005). doi:10.1016/j.immuni.2005.10.001
34. Roszer, T. Understanding the mysterious M2 macrophage through activation markers and effector mechanisms. *Mediators of Inflammation* (2015). doi:10.1155/2015/816460
35. Ferrante, C. J. *et al.* The adenosine-dependent angiogenic switch of macrophages to an M2-like phenotype is independent of interleukin-4 receptor alpha (IL-4Rα) signaling. *Inflammation* (2013). doi:10.1007/s10753-013-9621-3
36. Brundu S, F. A. Polarization and Repolarization of Macrophages. *J. Clin. Cell. Immunol.* (2015). doi:10.4172/2155-9899.1000319
37. Mantovani, A., Biswas, S. K., Galdiero, M. R., Sica, A. & Locati, M. Macrophage plasticity and polarization in tissue repair and remodelling. *Journal of Pathology* **229,** 176–185 (2013).
38. Mirza, R., DiPietro, L. A. & Koh, T. J. Selective and specific macrophage ablation is detrimental to wound healing in mice. *Am. J. Pathol.* **175,** 2454–62 (2009).
39. Brancato, S. K. & Albina, J. E. Wound macrophages as key regulators of repair: Origin, phenotype, and function. *American Journal of Pathology* **178,** 19–25 (2011).
40. Daley, J. M., Brancato, S. K., Thomay, A. A., Reichner, J. S. & Albina, J. E. The phenotype of murine wound macrophages. *J. Leukoc. Biol.* **87,** 59–67 (2010).

41. Koh, T. J. & DiPietro, L. A. Inflammation and wound healing: the role of the macrophage. *Expert Rev. Mol. Med.* **13,** e23 (2011).
42. Nizet, V. & Johnson, R. S. Interdependence of hypoxic and innate immune responses. *Nature Reviews Immunology* (2009). doi:10.1038/nri2607
43. Vats, D. *et al.* Oxidative metabolism and PGC-1β attenuate macrophage-mediated inflammation. *Cell Metab.* (2006). doi:10.1016/j.cmet.2006.05.011
44. Lucas, T. *et al.* Differential roles of macrophages in diverse phases of skin repair. *J. Immunol.* **184,** 3964–3977 (2010).
45. Sindrilaru, A. *et al.* An unrestrained proinflammatory M1 macrophage population induced by iron impairs wound healing in humans and mice. *J. Clin. Invest.* (2011). doi:10.1172/JCI44490
46. Zhu, Z., Ding, J., Ma, Z., Iwashina, T. & Tredget, E. E. Systemic depletion of macrophages in the subacute phase of wound healing reduces hypertrophic scar formation. *Wound Repair Regen.* (2016). doi:10.1111/wrr.12442
47. Xue, M. & Jackson, C. J. Extracellular Matrix Reorganization During Wound Healing and Its Impact on Abnormal Scarring. *Adv. Wound Care* (2015). doi:10.1089/wound.2013.0485
48. Clark, R. A. F. *et al.* Fibronectin and fibrin provide a provisional matrix for epidermal cell migration during wound reepithelialization. *J. Invest. Dermatol.* (1982). doi:10.1111/1523-1747.ep12500075
49. Barker, T. H. & Engler, A. J. The provisional matrix: setting the stage for tissue repair outcomes. *Matrix Biology* (2017). doi:10.1016/j.matbio.2017.04.003
50. Sottile, J. Fibronectin Polymerization Regulates the Composition and Stability of Extracellular Matrix Fibrils and Cell-Matrix Adhesions. *Mol. Biol. Cell* (2002). doi:10.1091/mbc.E02-01-0048
51. Li, J., Chen, J. & Kirsner, R. Pathophysiology of acute wound healing. *Clin. Dermatol.* (2007). doi:10.1016/j.clindermatol.2006.09.007
52. O'Toole, E. A. Extracellular matrix and keratinocyte migration. *Clinical and Experimental Dermatology* (2001). doi:10.1046/j.1365-2230.2001.00891.x
53. Reinke, J. M. & Sorg, H. Wound repair and regeneration. *European Surgical Research* (2012). doi:10.1159/000339613
54. Allison, A. C. *Biochemistry of Blood Clotting Factors:* (1974).
55. Coughlin, S. R. Thrombin signalling and protease-activated receptors. *Nature* **407,** 258–264 (2000).
56. Clark, R. a. Fibrin and wound healing. *Ann. N. Y. Acad. Sci.* **936,** 355–367 (2001).
57. Weisel, J. W. Fibrinogen and fibrin. *Advances in Protein Chemistry* **70,** 247–299 (2005).
58. Ciano, P. S., Colvin, R. B., Dvorak, A. M., McDonagh, J. & Dvorak, H. F. Macrophage migration in fibrin gel matrices. *Lab. Invest.* **54,** 62–70 (1986).
59. Lanir, N. *et al.* Macrophage migration in fibrin gel matrices. II. Effects of clotting factor XIII, fibronectin, and glycosaminoglycan content on cell migration. *J. Immunol.* **140,** 2340–2349 (1988).
60. Brown, L. F. *et al.* Fibroblast migration in fibrin gel matrices. *Am. J. Pathol.* (1993).
61. Drew, A. F., Liu, H., Davidson, J. M., Daugherty, C. C. & Degen, J. L. Wound-healing defects in mice lacking fibrinogen. *Blood* (2001). doi:10.1182/blood.V97.12.3691
62. Flick, M. J., Du, X. & Degen, J. L. Fibrin(ogen)-alpha M beta 2 interactions regulate

leukocyte function and innate immunity in vivo. *Exp. Biol. Med. (Maywood).* (2004). doi:229/11/1105 [pii]
63. Mosesson, M. W. Fibrinogen and fibrin structure and functions. in *Journal of Thrombosis and Haemostasis* **3,** 1894–1904 (2005).
64. Brown, A. C. & Barker, T. H. Fibrin-based biomaterials: Modulation of macroscopic properties through rational design at the molecular level. *Acta Biomaterialia* **10,** 1502–1514 (2014).
65. Janmey, P. A., Winer, J. P. & Weisel, J. W. Fibrin gels and their clinical and bioengineering applications. *J. R. Soc. Interface* **6,** 1–10 (2009).
66. Weisel, J. W. & Litvinov, R. I. Mechanisms of fibrin polymerization and clinical implications. *Blood* **121,** 1712–1719 (2013).
67. Weisel, J. W. & Medved, L. The structure and function of the alpha C domains of fibrinogen. *Ann. N. Y. Acad. Sci.* **936,** 312–327 (2001).
68. Mosesson, M. W., Siebenlist, K. R. & Meh, D. A. The structure and biological features of fibrinogen and fibrin. *Ann. N. Y. Acad. Sci.* (2001). doi:10.1111/j.1749-6632.2001.tb03491.x
69. Collen, D. On the regulation and control of fibrinolysis. Edward Kowalski Memorial Lecture. *Thrombosis and Haemostasis* (1980).
70. Levin, E. G. Latent tissue plasminogen activator produced by human endothelial cells in culture: evidence for an enzyme-inhibitor complex. *Proc. Natl. Acad. Sci. U. S. A.* **80,** 6804–8 (1983).
71. Mosesson, M. W., Siebenlist, K. R., Voskuilen, M. & Nieuwenhuizen, W. Evaluation of the factors contributing to fibrin-dependent plasminogen activation. *Thromb Haemost* (1998).
72. Hoylaerts, M., Rijken, D. C., Lijnen, H. R. & Collen, D. Kinetics of the activation of plasminogen by human tissue plasminogen activator. Role of fibrin. *J. Biol. Chem.* (1982). doi:10.1016/0268-9499(88)90464-x
73. Sakata, Y. & Aoki, N. Significance of cross-linking of α2-plasmin inhibitor to fibrin in inhibition of fibrinolysis and in hemostasis. *J. Clin. Invest.* (1982). doi:10.1172/JCI110479
74. Jennewein, C. *et al.* Novel aspects of fibrin(ogen) fragments during inflammation. *Mol. Med.* **17,** 568–73 (2011).
75. Medcalf, R. L. Fibrinolysis, inflammation, and regulation of the plasminogen activating system. *Journal of Thrombosis and Haemostasis* **5,** 132–142 (2007).
76. Levi, M., Van Der Poll, T. & Büller, H. R. Bidirectional relation between inflammation and coagulation. *Circulation* (2004). doi:10.1161/01.CIR.0000131660.51520.9A
77. Robson, S. C., Shephard, E. G. & Kirsch, R. E. Fibrin degradation product D-dimer induces the synthesis and release of biologically active IL-1 beta, IL-6 and plasminogen activator inhibitors from monocytes in vitro. *Br. J. Haematol.* **86,** 322–6 (1994).
78. Lee, M. E., Rhee, K. J. & Nham, S. U. Fragment E derived from both fibrin and fibrinogen stimulates interleukin-6 production in rat peritoneal macrophages. *Mol. Cells* **9,** 7–13 (1999).
79. Lee, M. E., Kweon, S. M., Ha, K. S. & Nham, S. U. Fibrin stimulates microfilament reorganization and IL-1beta production in human monocytic THP-1 cells. *Mol. Cells* **11,** 13–20 (2001).
80. Zhou, D., Yang, P. Y., Zhou, B. & Rui, Y. C. Fibrin D-dimer fragments enhance

inflammatory responses in macrophages: Role in advancing atherosclerosis. *Clin. Exp. Pharmacol. Physiol.* **34,** 185–190 (2007).
81. Naito, M., Stirk, C. M., Smith, E. B. & Thompson, W. D. Smooth muscle cell outgrowth stimulated by fibrin degradation products: The potential role of fibrin fragment E in restenosis and atherogenesis. *Thromb. Res.* **98,** 165–174 (2000).
82. Thompson, W. D. *et al.* Angiogenic activity of fibrin degradation products is located in fibrin fragment E. *J. Pathol.* **168,** 47–53 (1992).
83. Litvinov, R. & Weisel, J. What Is the Biological and Clinical Relevance of Fibrin? *Semin. Thromb. Hemost.* (2016). doi:10.1055/s-0036-1571342
84. Prasad, J. M. *et al.* Mice expressing a mutant form of fibrinogen that cannot support fibrin formation exhibit compromised antimicrobial host defense. *Blood* (2015). doi:10.1182/blood-2015-04-639849
85. Stalker, T. J. *et al.* Hierarchical organization in the hemostatic response and its relationship to the platelet-signaling network. *Blood* (2013). doi:10.1182/blood-2012-09-457739
86. Muthard, R. W. & Diamond, S. L. Blood clots are rapidly assembled hemodynamic sensors: Flow arrest triggers intraluminal thrombus contraction. *Arterioscler. Thromb. Vasc. Biol.* (2012). doi:10.1161/ATVBAHA.112.300312
87. Johnson, L. L., Berggren, K. N., Szaba, F. M., Chen, W. & Smiley, S. T. Fibrin-mediated Protection Against Infection-stimulated Immunopathology. *J. Exp. Med.* (2003). doi:10.1084/jem.20021493
88. Cruz-Topete, D., Iwaki, T., Ploplis, V. A. & Castellino, F. J. Delayed inflammatory responses to endotoxin in fibrinogen-deficient mice. *J. Pathol.* (2006). doi:10.1002/path.2060
89. Ko, Y. P. & Flick, M. J. Fibrinogen Is at the Interface of Host Defense and Pathogen Virulence in Staphylococcus aureus Infection. *Semin. Thromb. Hemost.* (2016). doi:10.1055/s-0036-1579635
90. Fries, D. & Martini, W. Z. Role of fibrinogen in trauma-induced coagulopathy. *British Journal of Anaesthesia* (2010). doi:10.1093/bja/aeq161
91. Martini, J., Cabrales, P., Fries, D., Intaglietta, M. & Tsai, A. G. Effects of fibrinogen concentrate after shock/resuscitation: A comparison between in vivo microvascular clot formation and thromboelastometry. *Crit. Care Med.* (2013). doi:10.1097/CCM.0b013e31828a4520
92. Haas, T. *et al.* The in vitro effects of fibrinogen concentrate, factor XIII and fresh frozen plasma on impaired clot formation after 60% dilution. *Anesth. Analg.* (2008). doi:10.1213/01.ane.0b013e3181684339
93. Innerhofer, P. *et al.* The exclusive use of coagulation factor concentrates enables reversal of coagulopathy and decreases transfusion rates in patients with major blunt trauma. *Injury* (2013). doi:10.1016/j.injury.2012.08.047
94. Thompson, D. F., Letassy, N. A. & Thompson, G. D. Fibrin glue: a review of its preparation, efficacy, and adverse effects as a topical hemostat. *Ann Pharmacother* **22,** 946–952 (1988).
95. Spotnitz, W. D. Fibrin sealant: past, present, and future: a brief review. *World Journal of Surgery* **34,** 632–634 (2010).
96. Spotnitz, W. D. & Burks, S. Hemostats, sealants, and adhesives III: A new update as well as

cost and regulatory considerations for components of the surgical toolbox. *Transfusion* **52,** 2243–2255 (2012).
97. Currie, L. J., Sharpe, J. R. & Martin, R. The use of fibrin glue in skin grafts and tissue-engineered skin replacements: a review. *Plastic and Reconstructive Surgery* **108,** 1713–1726 (2001).
98. Spicer, P. P. & Mikos, A. G. Fibrin glue as a drug delivery system. *J. Control. Release* **148,** 49–55 (2010).
99. De la Puente, P. & Ludeña, D. Cell culture in autologous fibrin scaffolds for applications in tissue engineering. *Experimental Cell Research* **322,** 1–11 (2014).
100. Ahmed, T. A. E., Dare, E. V & Hincke, M. Fibrin: a versatile scaffold for tissue engineering applications. *Tissue Eng. Part B. Rev.* **14,** 199–215 (2008).
101. Whelan, D., Caplice, N. M. & Clover, A. J. P. Fibrin as a delivery system in wound healing tissue engineering applications. *Journal of Controlled Release* **196,** 1–8 (2014).
102. Allen, P., Melero-Martin, J. & Bischoff, J. Type I collagen, fibrin and PuraMatrix matrices provide permissive environments for human endothelial and mesenchymal progenitor cells to form neovascular networks. *J. Tissue Eng. Regen. Med.* (2011). doi:10.1002/term.389
103. Davalos, D. & Akassoglou, K. Fibrinogen as a key regulator of inflammation in disease. *Seminars in Immunopathology* **34,** 43–62 (2012).
104. de Maat, M. P., Pietersma, A., Kofflard, M., Sluiter, W. & Kluft, C. Association of plasma fibrinogen levels with coronary artery disease, smoking and inflammatory markers. *Atherosclerosis* **121,** 185–91 (1996).
105. Bini, A., Fenoglio, J. J., Mesa-Tejada, R., Kudryk, B. & Kaplan, K. L. Identification and distribution of fibrinogen, fibrin, and fibrin(ogen) degradation products in atherosclerosis. Use of monoclonal antibodies. *Arterioscler. Thromb. Vasc. Biol.* **9,** 109–121 (1989).
106. Cushman, M. *et al.* Fibrin fragment D-dimer and the risk of future venous thrombosis. *Blood* **101,** 1243–1248 (2003).
107. Iwaki, T., Sandoval-Cooper, M. J., Brechmann, M., Ploplis, V. A. & Castellino, F. J. A fibrinogen deficiency accelerates the initiation of LDL cholesterol-driven atherosclerosis via thrombin generation and platelet activation in genetically predisposed mice. *Blood* **107,** 3883–3891 (2006).
108. Wiedemann, D. *et al.* The fibrin-derived peptide Bbeta(15-42) significantly attenuates ischemia-reperfusion injury in a cardiac transplant model. *Transplantation* **89,** 824–829 (2010).
109. Roesner, J. P. *et al.* The fibrin-derived peptide B beta(15-42) is cardioprotective in a pig model of myocardial ischemia-reperfusion injury. *Crit. Care Med.* **35,** 1730–1735 (2007).
110. Petzelbauer, P. *et al.* The fibrin-derived peptide Bβ15–42 protects the myocardium against ischemia-reperfusion injury. *Nat. Med.* **11,** 298–304 (2005).
111. Dvorak, H. F. Tumors: Wounds That Do Not Heal - Redux. *Cancer Immunol. Res.* (2015). doi:10.1056/NEJM198612253152606
112. Brown, L. F., Asch, B., Harvey, V. S., Buchinski, B. & Dvorak, H. F. Fibrinogen influx and accumulation of cross-linked fibrin in mouse carcinomas. *Cancer Res.* (1988).
113. Palumbo, J. S. *et al.* Fibrinogen is an important determinant of the metastatic potential of circulating tumor cells Focus on hematology. *Blood* **96,** 3302–3309 (2000).
114. Lipinski, B. & Egyud, L. G. Resistance of cancer cells to immune recognition and killing.

Med. Hypotheses **54,** 456–460 (2000).
115. Paul, J., Strickland, S. & Melchor, J. P. Fibrin deposition accelerates neurovascular damage and neuroinflammation in mouse models of Alzheimer's disease. *J. Exp. Med.* **204,** 1999–2008 (2007).
116. Davalos, D. *et al.* Fibrinogen-induced perivascular microglial clustering is required for the development of axonal damage in neuroinflammation. *Nat. Commun.* **3,** 1227 (2012).
117. Kofoed, S. C., Wittrup, H. H., Sillesen, H. & Nordestgaard, B. G. Fibrinogen predicts ischaemic stroke and advanced atherosclerosis but not echolucent, rupture-prone carotid plaques the Copenhagen City Heart Study. *Eur. Heart J.* **24,** 567–576 (2003).
118. van Oijen, M., Witteman, J. C., Hofman, A., Koudstaal, P. J. & Breteler, M. M. B. Fibrinogen is associated with an increased risk of Alzheimer disease and vascular dementia. *Stroke.* **36,** 2637–41 (2005).
119. Schachtrup, C. *et al.* Fibrinogen triggers astrocyte scar formation by promoting the availability of active TGF-beta after vascular damage. *J. Neurosci.* **30,** 5843–54 (2010).
120. Adams, R. A. *et al.* The fibrin-derived gamma377-395 peptide inhibits microglia activation and suppresses relapsing paralysis in central nervous system autoimmune disease. *J. Exp. Med.* **204,** 571–82 (2007).
121. Berton, G. & Lowell, C. A. Integrin signalling in neutrophils and macrophages. *Cellular Signalling* (1999). doi:10.1016/S0898-6568(99)00003-0
122. Brown, E. J. Integrins of Macrophages and Macrophage-Like Cells. in *The Macrophage as Therapeutic Target* (ed. Gordon, S.) 111–130 (Springer Berlin Heidelberg, 2003). doi:10.1007/978-3-642-55742-2_7
123. Wright, S. D. *et al.* Complement receptor type three (CD11b/CD18) of human polymorphonuclear leukocytes recognizes fibrinogen. *Proc. Natl. Acad. Sci. U. S. A.* **85,** 7734–7738 (1988).
124. Altieri, D. C. *et al.* A unique recognition site mediates the interaction of fibrinogen with the leukocyte integrin Mac-1 (CD11b/CD18). *J. Biol. Chem.* **265,** 12119–12122 (1990).
125. Loike, J. D. *et al.* CD11c/CD18 on neutrophils recognizes a domain at the N terminus of the A alpha chain of fibrinogen. *Proc. Natl. Acad. Sci. U. S. A.* **88,** 1044–1048 (1991).
126. Nham, S. Characteristics of Fibrinogen Binding to the Domain of CD11c , an alpha Subunit of p150 , 95. *Biochem. Biophys. Res. Commun.* **634,** 630–634 (1999).
127. Zhou, L., Lee, D. H. S., Plescia, J., Lau, C. Y. & Altieri, D. C. Differential ligand binding specificities of recombinant CD11b/CD18 integrin I-domain. *J. Biol. Chem.* **269,** 17075–17079 (1994).
128. Motley, M. P. *et al.* A CCR2 macrophage endocytic pathway mediates extravascular fibrin clearance in vivo. *Blood* (2016). doi:10.1182/blood-2015-05-644260
129. Sahni, a, Odrljin, T. & Francis, C. W. Binding of basic fibroblast growth factor to fibrinogen and fibrin. *J Biol Chem* **273,** 7554–9 (1998).
130. Campbell, P. G., Durham, S. K., Hayes, J. D., Suwanichkul, A. & Powell, D. R. Insulin-like growth factor-binding protein-3 binds fibrinogen and fibrin. *J. Biol. Chem.* **274,** 30215–30221 (1999).
131. Makogonenko, E., Tsurupa, G., Ingham, K. & Medved, L. Interaction of fibrin(ogen) with fibronectin: Further characterization and localization of the fibronectin-binding site. *Biochemistry* **41,** 7907–7913 (2002).

132. Fan, S. T. & Edgington, T. S. Integrin regulation of leukocyte inflammatory functions. CD11b/CD18 enhancement of the tumor necrosis factor-alpha responses of monocytes. *J. Immunol.* **150,** 2972–2980 (1993).
133. Perez, R. L. & Roman, J. Fibrin enhances the expression of IL-1 beta by human peripheral blood mononuclear cells. Implications in pulmonary inflammation. *J Immunol* **154,** 1879–1887 (1995).
134. Wang, L. *et al.* Indirect Inhibition of Toll-like Receptor and Type I Interferon Responses by ITAM-Coupled Receptors and Integrins. *Immunity* **32,** 518–530 (2010).
135. Tang, L. & Eaton, J. W. Fibrin(ogen) mediates acute inflammatory responses to biomaterials. *J. Exp. Med.* **178,** 2147–2156 (1993).
136. Tang, L., Ugarova, T. P., Plow, E. F. & Eaton, J. W. Molecular determinants of acute inflammatory responses to biomaterials. *J. Clin. Invest.* **97,** 1329–34 (1996).
137. Altieri, D. C., Plescia, J. & Plow, E. F. The structural motif glycine 190-valine 202 of the fibrinogen gamma chain interacts with CD11b/CD18 integrin (alphaMbeta 2, Mac-1) and promotes leukocyte adhesion. *J. Biol. Chem.* **268,** 1847–1853 (1993).
138. Hu, W. J., Eaton, J. W. & Tang, L. Molecular basis of biomaterial-mediated foreign body reactions. *Blood* **98,** 1231–1238 (2001).
139. Ahn, G. O. *et al.* Inhibition of Mac-1 (CD11b/CD18) enhances tumor response to radiation by reducing myeloid cell recruitment. *Proc. Natl. Acad. Sci.* (2010). doi:10.1073/pnas.0911378107
140. Rogers, C., Edelman, E. R. & Simon, D. I. A mAb to the beta2-leukocyte integrin Mac-1 (CD11b/CD18) reduces intimal thickening after angioplasty or stent implantation in rabbits. *Proc. Natl. Acad. Sci. U. S. A.* (1998). doi:10.1073/pnas.95.17.10134
141. Gefen, A. Introduction to Cell Mechanics and Mechanobiology. *Comput. Methods Biomech. Biomed. Engin.* (2015). doi:10.1080/10255842.2013.780048
142. Carey, S. P., Kraning-Rush, C. M., Williams, R. M. & Reinhart-King, C. A. Biophysical control of invasive tumor cell behavior by extracellular matrix microarchitecture. *Biomaterials* (2012). doi:10.1016/j.biomaterials.2012.02.029
143. Pedersen, J. A. & Swartz, M. A. Mechanobiology in the third dimension. *Ann. Biomed. Eng.* (2005). doi:10.1007/s10439-005-8159-4
144. Ryan, E. A., Mockros, L. F., Weisel, J. W. & Lorand, L. Structural origins of fibrin clot rheology. *Biophys. J.* **77,** 2813–2826 (1999).
145. Gelse, K., Pöschl, E. & Aigner, T. Collagens - Structure, function, and biosynthesis. *Advanced Drug Delivery Reviews* (2003). doi:10.1016/j.addr.2003.08.002
146. Elsdale, T. & Bard, J. Collagen substrata for studies on cell behavior. *J. Cell Biol.* (1972). doi:10.1083/jcb.54.3.626
147. Kahn, L. D., Carroll, R. J. & Witnauer, L. P. Some effects of electrolytes on collagen in solution. *BBA - Biochim. Biophys. Acta* (1962). doi:10.1016/0006-3002(62)90678-9
148. Williams, B. R., Gelman, R. A., Poppke, D. C. & Piez, K. Collagen fibril formation. Optimal in vitro conditions and preliminary kinetic results. *J. Biol. Chem.* (1978).
149. Roeder, B. A., Kokini, K., Sturgis, J. E., Robinson, J. P. & Voytik-Harbin, S. L. Tensile Mechanical Properties of Three-Dimensional Type I Collagen Extracellular Matrices With Varied Microstructure. *J. Biomech. Eng.* (2002). doi:10.1115/1.1449904
150. Raub, C. B. *et al.* Image correlation spectroscopy of multiphoton images correlates with

collagen mechanical properties. *Biophys. J.* (2008). doi:10.1529/biophysj.107.120006
151. Raub, C. B. *et al.* Noninvasive assessment of collagen gel microstructure and mechanics using multiphoton microscopy. *Biophys. J.* (2007). doi:10.1529/biophysj.106.097998
152. Gobeaux, F. *et al.* Fibrillogenesis in Dense Collagen Solutions: A Physicochemical Study. *J. Mol. Biol.* (2008). doi:10.1016/j.jmb.2007.12.047
153. Rowe, S. L., Lee, S. Y. & Stegemann, J. P. Influence of thrombin concentration on the mechanical and morphological properties of cell-seeded fibrin hydrogels. *Acta Biomater.* (2007). doi:10.1016/j.actbio.2006.08.006
154. Carr, M. E., Gabriel, D. a & McDonagh, J. Influence of Ca2+ on the structure of reptilase-derived and thrombin-derived fibrin gels. *Biochem. J.* (1986). doi:10.1042/bj2390513
155. Henderson, S. J. *et al.* Zinc promotes clot stability by accelerating clot formation and modifying fibrin structure. *Thromb. Haemost.* (2016). doi:10.1160/TH15-06-0462
156. Di Stasio, E., Nagaswami, C., Weisel, J. W. & Di Cera, E. Cl- regulates the structure of the fibrin clot. *Biophys. J.* **75,** 1973–1979 (1998).
157. Allen, T. D., Schor, S. L. & Schor, A. M. An ultrastructural review of collagen gels, a model system for cell-matrix, cell-basement membrane and cell-cell interactions. *Scan. Electron Microsc.* (1984).
158. Brightman, A. O. *et al.* Time-lapse confocal reflection microscopy of collagen fibrillogenesis and extracellular matrix assembly in vitro. *Biopolymers* (2000). doi:10.1002/1097-0282(200009)54:3<222::AID-BIP80>3.0.CO;2-K
159. Takahashi, A., Kita, R., Shinozaki, T., Kubota, K. & Kaibara, M. Real space observation of three-dimensional network structure of hydrated fibrin gel. *Colloid Polym. Sci.* (2003). doi:10.1007/s00396-002-0839-0
160. Anand, S., Wu, J. -H & Diamond, S. L. Enzyme-mediated proteolysis of fibrous biopolymers: Dissolution front movement in fibrin or collagen under conditions of diffusive or convective transport. *Biotechnol. Bioeng.* (1995). doi:10.1002/bit.260480203
161. Blombäck, B. *et al.* Native fibrin gel networks observed by 3D microscopy, permeation and turbidity. *Biochim. Biophys. Acta (BBA)/Protein Struct. Mol.* (1989). doi:10.1016/0167-4838(89)90140-4
162. Saltzman, W. M., Radomsky, M. L., Whaley, K. J. & Cone, R. A. Antibody diffusion in human cervical mucus. *Biophys. J.* (1994). doi:10.1016/S0006-3495(94)80802-1
163. Kim, Y. K., Que, R., Wang, S. W. & Liu, W. F. Modification of Biomaterials with a Self-Protein Inhibits the Macrophage Response. *Adv. Healthc. Mater.* **3,** 989–994 (2014).
164. Laurell, H. *et al.* Correction of RT-qPCR data for genomic DNA-derived signals with ValidPrime. *Nucleic Acids Res.* **40,** (2012).
165. Pattyn, F., Speleman, F., De Paepe, A. & Vandesompele, J. RTPrimerDB: The real-time PCR primer and probe database. *Nucleic Acids Research* **31,** 122–123 (2003).
166. Edelstein, A. D. *et al.* Advanced methods of microscope control using μManager software. *J. Biol. Methods* (2014). doi:10.14440/jbm.2014.36
167. Jones, a & Geczy, C. L. Thrombin and factor Xa enhance the production of interleukin-1. *Immunology* (1990).
168. Bizios, R., Lai, L., Fenton, J. W. & Malik, A. B. Thrombin-induced chemotaxis and aggregation of neutrophils. *J. Cell. Physiol.* (1986). doi:10.1002/jcp.1041280318
169. Rowand, J. K., Marucha, P. & Berliner, L. J. Hirudin C-terminal fragments inhibit

thrombin induced neutrophil chemotaxis. *Thromb. Haemost.* (1992).
170. Cirino, G. *et al.* Thrombin functions as an inflammatory mediator through activation of its receptor. *J Exp Med* (1996). doi:10.1084/jem.183.3.821
171. Chambers, R. C. *et al.* Thrombin stimulates fibroblast procollagen production via proteolytic activation of protease-activated receptor 1. *Biochem. J.* (1998). doi:10.1042/bj3330121
172. Dawes, K. E., Gray, A. J. & Laurent, G. J. Thrombin stimulates fibroblast chemotaxis and replication. *Eur. J. Cell Biol.* (1993).
173. Pilcher, B. K., Kim, D. W., Carney, D. H. & Tomasek, J. J. Thrombin stimulates fibroblast-mediated collagen lattice contraction by its proteolytically activated receptor. *Exp. Cell Res.* (1994). doi:10.1006/excr.1994.1100
174. White, M. J. V. & Gomer, R. H. Trypsin, tryptase, and thrombin polarize macrophages towards a pro-fibrotic M2a phenotype. *PLoS One* (2015). doi:10.1371/journal.pone.0138748
175. Shao, D. D., Suresh, R., Vakil, V., Gomer, R. H. & Pilling, D. Pivotal Advance: Th-1 cytokines inhibit, and Th-2 cytokines promote fibrocyte differentiation. *J. Leukoc. Biol.* (2008). doi:10.1189/jlb.1107782
176. McGaha, T. L. *et al.* Molecular mechanisms of interleukin-4-induced up-regulation of type I collagen gene expression in murine fibroblasts. *Arthritis Rheum.* (2003). doi:10.1002/art.11089
177. Smiley, S. T., King, J. a & Hancock, W. W. Fibrinogen stimulates macrophage chemokine secretion through toll-like receptor 4. *J. Immunol.* **167,** 2887–2894 (2001).
178. McWhorter, F. Y., Wang, T., Nguyen, P., Chung, T. & Liu, W. F. Modulation of macrophage phenotype by cell shape. *Proc. Natl. Acad. Sci.* **2013,** 1308887110- (2013).
179. Weinstein, J. R., Swarts, S., Bishop, C., Hanisch, U. K. & Möller, T. Lipopolysaccharide is a frequent and significant contaminant in microglia-activating factors. *Glia* (2008). doi:10.1002/glia.20585
180. Gorbet, M. B. & Sefton, M. V. Endotoxin: The uninvited guest. *Biomaterials* (2005). doi:10.1016/j.biomaterials.2005.04.063
181. US Department of Health and Human Services/Public Health Services/Food and Drug Administration. *Guidance for Industry-Pyrogen and Endotoxins Testing: Questions and Answers.* (2012).
182. Rowe, S. L. & Stegemann, J. P. Interpenetrating collagen-fibrin composite matrices with varying protein contents and ratios. *Biomacromolecules* **7,** 2942–2948 (2006).
183. Colotta, F. *et al.* Expression of monocyte chemotactic protein-1 by monocytes and endothelial cells exposed to thrombin. *Am J Pathol* (1994).
184. Boneberg, E. M. & Hartung, T. Molecular aspects of anti-inflammatory action of G-CSF. *Inflamm. Res.* **51,** 119–28 (2002).
185. Han, C. *et al.* Integrin CD11b negatively regulates TLR-triggered inflammatory responses by activating Syk and promoting degradation of MyD88 and TRIF via Cbl-b. *Nat. Immunol.* **11,** 734–742 (2010).
186. Ugarova, T. P. *et al.* Sequence gamma 377-395(P2), but not gamma 190-202(P1), is the binding site for the alpha MI-domain of integrin alpha M beta 2 in the gamma C-domain of fibrinogen. *Biochemistry* **42,** 9365–9373 (2003).

187. Lishko, V. K., Kudryk, B., Yakubenko, V. P., Yee, V. C. & Ugarova, T. P. Regulated unmasking of the cryptic binding site for integrin alphaMbeta2 in the gammaC-domain of fibrinogen. *Biochemistry* **41,** 12942–12951 (2002).
188. Lishko, V. K. *et al.* Multiple binding sites in fibrinogen for integrin alphaMbeta2 (Mac-1). *J. Biol. Chem.* **279,** 44897–906 (2004).
189. Ryu, J. K. *et al.* Blood coagulation protein fibrinogen promotes autoimmunity and demyelination via chemokine release and antigen presentation. *Nat. Commun.* **6,** 8164 (2015).
190. Iyer, S. S., Ghaffari, A. A. & Cheng, G. Lipopolysaccharide-Mediated IL-10 Transcriptional Regulation Requires Sequential Induction of Type I IFNs and IL-27 in Macrophages. *J. Immunol.* (2010). doi:10.4049/jimmunol.1002041
191. Jaalouk, D. E. & Lammerding, J. Mechanotransduction gone awry. *Nature Reviews Molecular Cell Biology* (2009). doi:10.1038/nrm2597
192. Yeung, T. *et al.* Effects of substrate stiffness on cell morphology, cytoskeletal structure, and adhesion. *Cell Motil. Cytoskeleton* (2005). doi:10.1002/cm.20041
193. Lo, C. M., Wang, H. B., Dembo, M. & Wang, Y. L. Cell movement is guided by the rigidity of the substrate. *Biophys. J.* (2000). doi:10.1016/S0006-3495(00)76279-5
194. Engler, A. J., Sen, S., Sweeney, H. L. & Discher, D. E. Matrix Elasticity Directs Stem Cell Lineage Specification. *Cell* (2006). doi:10.1016/j.cell.2006.06.044
195. Nemir, S., Hayenga, H. N. & West, J. L. PEGDA hydrogels with patterned elasticity: Novel tools for the study of cell response to substrate rigidity. *Biotechnol. Bioeng.* (2010). doi:10.1002/bit.22574
196. Blakney, A. K., Swartzlander, M. D. & Bryant, S. J. The effects of substrate stiffness on the in vitro activation of macrophages and in vivo host response to poly(ethylene glycol)-based hydrogels. *J. Biomed. Mater. Res. - Part A* (2012). doi:10.1002/jbm.a.34104
197. Anselmo, A. C. *et al.* Elasticity of nanoparticles influences their blood circulation, phagocytosis, endocytosis, and targeting. *ACS Nano* (2015). doi:10.1021/acsnano.5b00147
198. Previtera, M. L. & Sengupta, A. Substrate stiffness regulates proinflammatory mediator production through TLR4 activity in macrophages. *PLoS One* (2015). doi:10.1371/journal.pone.0145813
199. Irwin, E. F. *et al.* Modulus-dependent macrophage adhesion and behavior. *J. Biomater. Sci. Polym. Ed.* (2008). doi:10.1163/156856208786052407
200. Okamoto, T. *et al.* Reduced substrate stiffness promotes M2-like macrophage activation and enhances peroxisome proliferator-activated receptor γ expression. *Exp. Cell Res.* (2018). doi:10.1016/j.yexcr.2018.04.005
201. Patel, N. R. *et al.* Cell Elasticity Determines Macrophage Function. *PLoS One* (2012). doi:10.1371/journal.pone.0041024
202. He, X. T. *et al.* Macrophage involvement affects matrix stiffness-related influences on cell osteogenesis under three-dimensional culture conditions. *Acta Biomater.* (2018). doi:10.1016/j.actbio.2018.02.015
203. Weisel, J. W. The mechanical properties of fibrin for basic scientists and clinicians. *Biophysical Chemistry* **112,** 267–276 (2004).
204. Kang, H. *et al.* Nonlinear elasticity of stiff filament networks: Strain stiffening, negative normal stress, and filament alignment in fibrin gels. *J. Phys. Chem. B* **113,** 3799–3805

(2009).
205. Nelb, G. W., Kamykowski, G. W. & Ferry, J. D. Rheology of fibrin clots. v. shear modulus, creep, and creep recovery of fine unligated clots. *Biophys. Chem.* **13,** 15–23 (1981).
206. Chandran, P. L. & Barocas, V. H. Microstructural Mechanics of Collagen Gels in Confined Compression: Poroelasticity, Viscoelasticity, and Collapse. *J. Biomech. Eng.* (2004). doi:10.1115/1.1688774
207. Chapman, G. E., Danyluk, S. S. & McLauchlan, K. a. A Model for Collagen Hydration. *Proc. R. Soc. B Biol. Sci.* (1971). doi:10.1098/rspb.1971.0076
208. Xu, B., Li, H. & Zhang, Y. Understanding the viscoelastic behavior of collagen matrices through relaxation time distribution spectrum. *Biomatter* (2013). doi:10.4161/biom.24651
209. Knapp, D. M. *et al.* Rheology of reconstituted type I collagen gel in confined compression. *J. Rheol. (N. Y. N. Y).* (1997). doi:10.1122/1.550817
210. Kurniawan, N. A., Grimbergen, J., Koopman, J. & Koenderink, G. H. Factor XIII stiffens fibrin clots by causing fiber compaction. *J. Thromb. Haemost.* **12,** 1687–1696 (2014).
211. Siebenlist, K. R., Meh, D. A. & Mosesson, M. W. Protransglutaminase (factor XIII) mediated crosslinking of fibrinogen and fibrin. *Thromb. Haemost.* **86,** 1221–1228 (2001).
212. Bagoly, Z., Koncz, Z., Hársfalvi, J. & Muszbek, L. Factor XIII, clot structure, thrombosis. *Thrombosis Research* **129,** 382–387 (2012).
213. Veklich, Y., Ang, E. K., Lorand, L. & Weisel, J. W. The complementary aggregation sites of fibrin investigated through examination of polymers of fibrinogen with fragment E. *Proc. Natl. Acad. Sci. U. S. A.* **95,** 1438–1442 (1998).
214. Mosesson, M. W., Siebenlist, K. R., Hernandez, I., Wall, J. S. & Hainfeld, J. F. Fibrinogen assembly and crosslinking on a fibrin fragment E template. *Thromb. Haemost.* **87,** 651–658 (2002).
215. Janmey, P. a. Rheology of Fibrin Clots. VI. Stress Relaxation, Creep, and Differential Dynamic Modulus of Fine Clots in Large Shearing Deformations. *J. Rheol. (N. Y. N. Y).* **27,** 135 (1983).
216. Ryan, E. a, Mockros, L. F., Stern, a M. & Lorand, L. Influence of a natural and a synthetic inhibitor of factor XIIIa on fibrin clot rheology. *Biophys. J.* **77,** 2827–2836 (1999).
217. Glover, C. J., McIntire, L. V, Brown, C. H. & Natelson, E. A. Rheological properties of fibrin clots. Effects of fibrinogen concentration, Factor XIII deficiency, and Factor XIII inhibition. *J. Lab. Clin. Med.* (1975).
218. Venzin CM, Jacot V, Berdichevsky A, Karol AA, Seliktar D, von Rechenberg B, Nuss, K. Biocompatibility of Pegylated Fibrinogen and Its Effect on Healing of Full- Thickness Skin Defects: A Preliminary Study in Rats. *J. Biotechnol. Biomater.* **6,** (2016).
219. Santos, S. G. *et al.* Adsorbed fibrinogen leads to improved bone regeneration and correlates with differences in the systemic immune response. *Acta Biomater.* (2013). doi:10.1016/j.actbio.2013.04.008
220. Peled, E., Boss, J., Bejar, J., Zinman, C. & Seliktar, D. A novel poly(ethylene glycol)-fibrinogen hydrogel for tibial segmental defect repair in a rat model. *J. Biomed. Mater. Res. - Part A* (2007). doi:10.1002/jbm.a.30928
221. Haverkate, F. & Timan, G. Protective effect of calcium in the plasmin degradation of fibrinogen and fibrin fragments D. *Thromb. Res.* (1977). doi:10.1016/0049-3848(77)90137-2
222. Rowe, S. L. & Stegemann, J. P. Microstructure and Mechanics of Collagen-Fibrin Matrices

Polymerized Using Ancrod Snake Venom Enzyme. *J. Biomech. Eng.* (2009). doi:10.1115/1.3128673
223. Illig KA, O. K. Ancrod: understanding the agent. *Semin Vasc Surg.* **9,** 303–314 (1996).
224. Johnson, T. J. A. Glutaraldehyde Cross-Linking Fast and Slow Modes. in 283–295 (1993).
225. Richards, F. M. & Knowles, J. R. Glutaraldehyde as a protein cross-linking reagent. *J. Mol. Biol.* (1968). doi:10.1016/0022-2836(68)90086-7
226. Chen, E. Y., Liu Loreto Megido, W. F. & Díez, P. Understanding and utilizing the biomolecule/nanosystems interface. *Nanotechnologies in Preventive and Regenerative Medicine* (2018). doi:10.1016/B978-0-323-48063-5/00003-4
227. Riedel, T., Brynda, E., Dyr, J. E. & Houska, M. Controlled preparation of thin fibrin films immobilized at solid surfaces. *J. Biomed. Mater. Res. - Part A* (2009). doi:10.1002/jbm.a.31755
228. Tse, J. R. & Engler, A. J. Preparation of hydrogel substrates with tunable mechanical properties. *Current Protocols in Cell Biology* (2010). doi:10.1002/0471143030.cb1016s47
229. Ziegler-Heitbrock, H. W. L. & Ulevitch, R. J. CD14: Cell surface receptor and differentiation marker. *Immunol. Today* (1993). doi:10.1016/0167-5699(93)90212-4
230. Akira, S., Takeda, K. & Kaisho, T. Toll-like receptors: Critical proteins linking innate and acquired immunity. *Nature Immunology* (2001). doi:10.1038/90609
231. Sell, S. A. *et al.* Cross-linking methods of electrospun fibrinogen scaffolds for tissue engineering applications. in *Biomedical Materials* (2008). doi:10.1088/1748-6041/3/4/045001
232. van Luyn, M.J.A, van Wachem, P.B, Dijkstra P.J., Olde Damink L.H.H., F. J. Calcification of subcutaneously implanted collagen in relation to cytotoxicity, cellular interactions and crosslinking. *J Mater Sci Mater Med* **6,** 288–296 (1995).
233. Sung, H. W., Chang, W. H., Ma, C. Y. & Lee, M. H. Crosslinking of biological tissues using genipin and/or carbodiimide. *J. Biomed. Mater. Res. - Part A* (2003). doi:10.1002/jbm.a.10346
234. Lee, H. S. *et al.* Correlating macrophage morphology and cytokine production resulting from biomaterial contact. *J. Biomed. Mater. Res. - Part A* **101 A,** 203–212 (2013).
235. Denisin, A. K. & Pruitt, B. L. Tuning the Range of Polyacrylamide Gel Stiffness for Mechanobiology Applications. *ACS Applied Materials and Interfaces* (2016). doi:10.1021/acsami.5b09344
236. Wen, J. H. *et al.* Interplay of matrix stiffness and protein tethering in stem cell differentiation. *Nat. Mater.* (2014). doi:10.1038/nmat4051
237. Gutekunst, S. B., Grabosch, C., Kovalev, A., Gorb, S. N. & Selhuber-Unkel, C. Influence of the PDMS substrate stiffness on the adhesion of Acanthamoeba castellanii. *Beilstein J. Nanotechnol.* (2014). doi:10.3762/bjnano.5.152
238. Palchesko, R. N., Zhang, L., Sun, Y. & Feinberg, A. W. Development of Polydimethylsiloxane Substrates with Tunable Elastic Modulus to Study Cell Mechanobiology in Muscle and Nerve. *PLoS One* (2012). doi:10.1371/journal.pone.0051499
239. Zellander, A., Kadakia-Bhasin, a, Mahksous, M. & Cho, M. Mechanical Diversity of Porous Poly (Ethylene Glycol) Diacrylate. *Adv. Biomed. Eng. Res.* (2013).
240. Lee, S., Tong, X. & Yang, F. The effects of varying poly(ethylene glycol) hydrogel

crosslinking density and the crosslinking mechanism on protein accumulation in three-dimensional hydrogels. *Acta Biomater.* (2014). doi:10.1016/j.actbio.2014.05.023
241. Swartzlander, M. D., Lynn, A. D., Blakney, A. K., Kyriakides, T. R. & Bryant, S. J. Understanding the host response to cell-laden poly(ethylene glycol)-based hydrogels. *Biomaterials* (2013). doi:10.1016/j.biomaterials.2012.10.037
242. Kolahi, K. S. *et al.* Effect of substrate stiffness on early mouse embryo development. *PLoS One* (2012). doi:10.1371/journal.pone.0041717
243. Smith, E. L., Cardinali, B., Ping, L., Ariëns, R. A. S. & Philippou, H. Elimination of coagulation factor XIII from fibrinogen preparations. *Journal of Thrombosis and Haemostasis* (2013). doi:10.1111/jth.12174
244. Ariëns, R. a *et al.* The factor XIII V34L polymorphism accelerates thrombin activation of factor XIII and affects cross-linked fibrin structure. *Blood* (2000). doi:10.1182/blood.v100.1.148
245. Takebe, M., Soe, G., Kohno, I., Sugo, T. & Matsuda, M. Calcium ion-dependent monoclonal antibody against human fibrinogen: Preparation, characterization, and application to fibrinogen purification. *Thromb. Haemost.* (1995).
246. Shen, L. L., Hermans, J., McDonagh, J. & McDonagh, R. P. Role of fibrinopeptide B release: comparison of fibrins produced by thrombin and Ancrod. *Am. J. Physiol. - Hear. Circ. Physiol.* (1977). doi:10.1152/ajpheart.1977.232.6.H629
247. Furlan, M., Seelich, T. & Beck, E. A. Clottability and cross linking reactivity of fibrin(ogen) following differential release of fibrinopeptides A and B. *Thromb. Haemost.* (1976).
248. Shainoff, J. R. & Dardik, B. N. Fibrinopeptide B in fibrin assembly and metabolism: physiologic significance in delayed release of the peptide. *Ann. N. Y. Acad. Sci.* (1983). doi:10.1111/j.1749-6632.1983.tb23249.x
249. Ma, B., Wang, X., Wu, C. & Chang, J. Crosslinking strategies for preparation of extracellular matrix-derived cardiovascular scaffolds. *Regen. Biomater.* (2014). doi:10.1093/rb/rbu009
250. Jorge-Herrero, E., Fernández, P., Escudero, C., García-Páez, J. M. & Castillo-Olivares, J. L. Calcification of pericardial tissue pretreated with different amino acids. *Biomaterials* (1996). doi:10.1016/0142-9612(96)88707-2
251. Jorge-Herrero, E. *et al.* Influence of different chemical cross-linking treatments on the properties of bovine pericardium and collagen. *Biomaterials* (1999). doi:10.1016/S0142-9612(98)90205-8
252. Olde Damink, L. H. H. *et al.* Cross-linking of dermal sheep collagen using a water-soluble carbodiimide. *Biomaterials* (1996). doi:10.1016/0142-9612(96)81413-X
253. Jung, S. Y. *et al.* The Vroman Effect: A Molecular Level Description of Fibrinogen Displacement. *J. Am. Chem. Soc.* (2003). doi:10.1021/ja037263o
254. Dare, E. V. *et al.* Genipin cross-linked fibrin hydrogels for in vitro human articular cartilage tissue-engineered regeneration. *Cells Tissues Organs* (2009). doi:10.1159/000209230
255. Schek, R. M., Michalek, A. J. & Iatridis, J. C. Genipin-crosslinked fibrin hydrogels as a potential adhesive to augment intervertebral disc annulus repair. *Eur. Cells Mater.* (2011). doi:10.22203/eCM.v021a28
256. Cornwell, K. G. & Pins, G. D. Discrete crosslinked fibrin microthread scaffolds for tissue regeneration. *J. Biomed. Mater. Res. - Part A* (2007). doi:10.1002/jbm.a.31057

257. Bjork, J. W., Johnson, S. L. & Tranquillo, R. T. Ruthenium-catalyzed photo cross-linking of fibrin-based engineered tissue. *Biomaterials* **32,** 2479–2488 (2011).
258. Fancy, D. A. & Kodadek, T. Chemistry for the analysis of protein–protein interactions: Rapid and efficient cross-linking triggered by long wavelength light. *Chem. Biochem.* (1999). doi:10.1073/pnas.96.11.6020
259. Elvin, C. M. *et al.* The development of photochemically crosslinked native fibrinogen as a rapidly formed and mechanically strong surgical tissue sealant. *Biomaterials* (2009). doi:10.1016/j.biomaterials.2008.12.059
260. Elvin, C. M. *et al.* Evaluation of photo-crosslinked fibrinogen as a rapid and strong tissue adhesive. *J. Biomed. Mater. Res. - Part A* (2010). doi:10.1002/jbm.a.32572
261. Syedain, Z. H., Bjork, J., Sando, L. & Tranquillo, R. T. Controlled compaction with ruthenium-catalyzed photochemical cross-linking of fibrin-based engineered connective tissue. *Biomaterials* (2009). doi:10.1016/j.biomaterials.2009.08.039
262. Kurup, A. Spatial Awareness: How Cells Respond and Control Extracellular Matrix Stiffness Topography. (University of California, Irvine, 2015).
263. Squires, T. M. & Mason, T. G. Fluid Mechanics of Microrheology. *Annu. Rev. Fluid Mech.* (2010). doi:10.1146/annurev-fluid-121108-145608
264. Nijenhuis, N., Mizuno, D., Spaan, J. A. E. & Schmidt, C. F. High-resolution microrheology in the pericellular matrix of prostate cancer cells. *J. R. Soc. Interface* (2012). doi:10.1098/rsif.2011.0825
265. Mizuno, D., Head, D. A., MacKintosh, F. C. & Schmidt, C. F. Active and passive microrheology in equilibrium and nonequilibrium systems. *Macromolecules* (2008). doi:10.1021/ma801218z
266. Keating, M., Kurup, A., Alvarez-Elizondo, M., Levine, A. J. & Botvinick, E. Spatial distributions of pericellular stiffness in natural extracellular matrices are dependent on cell-mediated proteolysis and contractility. *Acta Biomater.* (2017). doi:10.1016/j.actbio.2017.05.008
267. Ashkin, A. Forces of a single-beam gradient laser trap on a dielectric sphere in the ray optics regime. *Biophys. J.* (1992). doi:10.1016/S0006-3495(92)81860-X
268. Pixley, F. J. Macrophage migration and its regulation by CSF-1. *International Journal of Cell Biology* (2012). doi:10.1155/2012/501962
269. Friedl, P., Zänker, K. S. & Bröcker, E. B. Cell migration strategies in 3-D extracellular matrix: Differences in morphology, cell matrix interactions, and integrin function. *Microscopy Research and Technique* (1998). doi:10.1002/(SICI)1097-0029(19981201)43:5<369::AID-JEMT3>3.0.CO;2-6
270. Friedl, P. & Weigelin, B. Interstitial leukocyte migration and immune function. *Nature Immunology* (2008). doi:10.1038/ni.f.212
271. Van Goethem, E. *et al.* Macrophage podosomes go 3D. *Eur. J. Cell Biol.* (2011). doi:10.1016/j.ejcb.2010.07.011
272. Van Goethem, E., Poincloux, R., Gauffre, F., Maridonneau-Parini, I. & Le Cabec, V. Matrix Architecture Dictates Three-Dimensional Migration Modes of Human Macrophages: Differential Involvement of Proteases and Podosome-Like Structures. *J. Immunol.* (2010). doi:10.4049/jimmunol.0902223
273. Bellingan, G. J., Caldwell, H., Howie, S. E., Dransfield, I. & Haslett, C. In vivo fate of the

inflammatory macrophage during the resolution of inflammation: inflammatory macrophages do not die locally, but emigrate to the draining lymph nodes. *J. Immunol.* (1996).
274. Wyckoff, J. B. *et al.* Direct visualization of macrophage-assisted tumor cell intravasation in mammary tumors. *Cancer Res.* (2007). doi:10.1158/0008-5472.CAN-06-1823
275. Wyckoff, J. *et al.* A paracrine loop between tumor cells and macrophages is required for tumor cell migration in mammary tumors. *Cancer Res.* (2004). doi:10.1158/0008-5472.CAN-04-1449
276. Guiet, R. *et al.* The Process of Macrophage Migration Promotes Matrix Metalloproteinase-Independent Invasion by Tumor Cells. *J. Immunol.* (2011). doi:10.4049/jimmunol.1101245
277. Libby, P. Inflammation in atherosclerosis. *Arterioscler. Thromb. Vasc. Biol.* (2012). doi:10.1161/ATVBAHA.108.179705
278. Hind, L. E., Lurier, E. B., Dembo, M., Spiller, K. L. & Hammer, D. A. Effect of M1–M2 Polarization on the Motility and Traction Stresses of Primary Human Macrophages. *Cell. Mol. Bioeng.* (2016). doi:10.1007/s12195-016-0435-x
279. Hind, L. E., Mackay, J. L., Cox, D. & Hammer, D. A. Two-dimensional motility of a macrophage cell line on microcontact-printed fibronectin. *Cytoskeleton* (2014). doi:10.1002/cm.21191
280. Bellingan, G. J. *et al.* Adhesion Molecule–dependent Mechanisms Regulate the Rate of Macrophage Clearance During the Resolution of Peritoneal Inflammation. *J. Exp. Med.* (2002). doi:10.1084/jem.20011794
281. Cao, C., Lawrence, D. A., Strickland, D. K. & Zhang, L. A specific role of integrin Mac-1 in accelerated macrophage efflux to the lymphatics. *Blood* (2005). doi:10.1182/blood-2005-03-1288
282. Shang, X. Z. & Issekutz, A. C. Contribution of CD11a/CD18, CD11b/CD18, ICAM-1 (CD54) and -2 (CD102) to human monocyte migration through endothelium and connective tissue fibroblast barriers. *Eur. J. Immunol.* (1998). doi:10.1002/(SICI)1521-4141(199806)28:06<1970::AID-IMMU1970>3.0.CO;2-H
283. Forsyth, C. B., Solovjov, D. a, Ugarova, T. P. & Plow, E. F. Integrin alpha(M)beta(2)-mediated cell migration to fibrinogen and its recognition peptides. *J. Exp. Med.* (2001). doi:10.1084/jem.193.10.1123
284. Gao, J. X. & Issekutz, A. C. Mac-1 (CD11b/CD18) is the predominant β2(CD18) integrin mediating human neutrophil migration through synovial and dermal fibroblast barrier. *Immunology* (1996). doi:10.1046/j.1365-2567.1996.d01-662.x
285. Kavanaugh, A. F., Lightfoot, E., Lipsky, P. E. & Oppenheimer-Marks, N. Role of CD11/CD18 in adhesion and transendothelial migration of T cells. Analysis utilizing CD18-deficient T cell clones. *J. Immunol.* (1991).
286. Jia, G. Q. *et al.* Selective eosinophil transendothelial migration triggered by eotaxin via modulation of Mac-1/ICAM-1 and VLA-4/VCAM-1 interactions. *Int. Immunol.* (1999). doi:10.1093/intimm/11.1.1
287. Hsieh, J. Y. *et al.* Differential regulation of macrophage inflammatory activation by fibrin and fibrinogen. *Acta Biomater.* **47,** 14–24 (2017).
288. Smith, T. D. Control of Macrophage Function by the Microenvironment. (UC Irvine, 2017).

289. Meijering, E., Dzyubachyk, O. & Smal, I. Methods for cell and particle tracking. *Methods Enzymol.* (2012). doi:10.1016/B978-0-12-391857-4.00009-4
290. Gilbert, P. M. *et al.* Substrate elasticity regulates skeletal muscle stem cell self-renewal in culture. *Science (80-.).* (2010). doi:10.1126/science.1191035
291. Sanchez, C., Gabay, O., Salvat, C., Henrotin, Y. E. & Berenbaum, F. Mechanical loading highly increases IL-6 production and decreases OPG expression by osteoblasts. *Osteoarthr. Cartil.* (2009). doi:10.1016/j.joca.2008.09.007
292. Kraakman, M. J., Murphy, A. J., Jandeleit-Dahm, K. & Kammoun, H. L. Macrophage polarization in obesity and type 2 diabetes: Weighing down our understanding of macrophage function? *Front. Immunol.* (2014). doi:10.3389/fimmu.2014.00470
293. Moore, K. J., Sheedy, F. J. & Fisher, E. A. Macrophages in atherosclerosis: a dynamic balance. *Nat. Rev. Immunol.* **13,** 709–21 (2013).
294. Mantovani, A., Sozzani, S., Locati, M., Allavena, P. & Sica, A. Macrophage polarization: Tumor-associated macrophages as a paradigm for polarized M2 mononuclear phagocytes. *Trends in Immunology* (2002). doi:10.1016/S1471-4906(02)02302-5
295. Jablonski, K. A. *et al.* Novel markers to delineate murine M1 and M2 macrophages. *PLoS One* (2015). doi:10.1371/journal.pone.0145342
296. Beyer, M. *et al.* High-Resolution Transcriptome of Human Macrophages. *PLoS One* (2012). doi:10.1371/journal.pone.0045466
297. Perego, C. *et al.* Temporal pattern of expression and colocalization of microglia/macrophage phenotype markers following brain ischemic injury in mice. *J. Neuroinflammation* (2011). doi:10.1186/1742-2094-8-174
298. Duan, M. *et al.* CD11b immunophenotyping identifies inflammatory profiles in the mouse and human lungs. *Mucosal Immunol.* (2016). doi:10.1038/mi.2015.84
299. Pilione, M. R., Agosto, L. M., Kennett, M. J. & Harvill, E. T. CD11b is required for the resolution of inflammation induced by Bordetella bronchiseptica respiratory infection. *Cell. Microbiol.* (2006). doi:10.1111/j.1462-5822.2005.00663.x
300. Hu, X. *et al.* Microglia/macrophage polarization dynamics reveal novel mechanism of injury expansion after focal cerebral ischemia. *Stroke* (2012). doi:10.1161/STROKEAHA.112.659656
301. Faridi, M. H. *et al.* CD11b activation suppresses TLR-dependent inflammation and autoimmunity in systemic lupus erythematosus. *J. Clin. Invest.* (2017). doi:10.1172/JCI88442
302. Féréol, S. *et al.* Sensitivity of alveolar macrophages to substrate mechanical and adhesive properties. *Cell Motil. Cytoskeleton* (2006). doi:10.1002/cm.20130
303. Discher, D. E., Janmey, P. & Wang, Y. L. Tissue cells feel and respond to the stiffness of their substrate. *Science* (2005). doi:10.1126/science.1116995
304. Zhang, L. *et al.* Zwitterionic hydrogels implanted in mice resist the foreign-body reaction. *Nat. Biotechnol.* **31,** 553–6 (2013).
305. Vegas, A. J. *et al.* Combinatorial hydrogel library enables identification of materials that mitigate the foreign body response in primates. *Nat. Biotechnol.* **34,** 345–352 (2016).
306. Zanconato, F., Cordenonsi, M. & Piccolo, S. YAP/TAZ at the Roots of Cancer. *Cancer Cell* (2016). doi:10.1016/j.ccell.2016.05.005